

# **MORPHOLOGICAL PROCESSES IN LOWLAND STREAMS**

IMPLICATIONS FOR STREAM RESTORATION



**JORIS P.C. EEKHOUT**



# Morphological Processes in Lowland Streams

## Implications for Stream Restoration

Joris P.C. Eekhout

## **Thesis committee**

### **Promotors**

Prof. Dr R. Uijlenhoet

Professor of Hydrology and Quantitative Water Management  
Wageningen University

Prof. Dr P.F.M. Verdonschot

Senior researcher, Freshwater Ecology

Alterra, Wageningen UR

Professor of Wetland Restoration Ecology

University of Amsterdam

### **Co-promotor**

Dr A.J.F. Hoitink

Associate professor, Hydrology and Quantitative Water Management Group  
Wageningen University

### **Other members**

Prof. Dr J. Wallinga, Wageningen University

Prof. Dr W.S.J. Uijttewaal, Delft University of Technology

Prof. Dr A.M. Gurnell, Queen Mary University of London, United Kingdom

Dr H. Piégay, Centre National de la Recherche Scientifique, Lyon, France

This research was conducted under the auspices of the Graduate School SENSE

# Morphological Processes in Lowland Streams

## Implications for Stream Restoration

Joris Petrus Cornelis Eekhout

### **Thesis**

submitted in fulfilment of the requirements for the degree of doctor  
at Wageningen University  
by the authority of the Rector Magnificus  
Prof. Dr M.J. Kropff,  
in the presence of the  
Thesis Committee appointed by the Academic Board  
to be defended in public  
on Friday 9 May 2014  
at 4 p.m. in the Aula.

J.P.C. Eekhout  
Morphological Processes in Lowland Streams - Implications for Stream Restoration,  
178 pages.

PhD thesis, Wageningen University, Wageningen, NL (2014)  
With references, with summaries in Dutch and English

ISBN 978-90-6173-911-7

*als de Waal  
uit het zicht is  
stroomt  
de verbeelding*

Twan Niesten (2012)



# Contents

<b>1 General Introduction</b>	<b>1</b>
1.1 Motivation	2
1.2 Stream Restoration and Meandering	6
1.3 Meander Processes	7
1.4 Objective & Research Questions	10
1.5 Thesis Outline	12
1.6 Study Areas	13
<b>2 Lowland Stream Restoration</b>	<b>17</b>
2.1 Introduction	18
2.2 Study Areas	20
2.3 Material & Methods	22
2.4 Results	25
2.5 Discussion	31
2.6 Conclusions	36
<b>3 Alternate Bars</b>	<b>37</b>
3.1 Introduction	38
3.2 Study Area	41
3.3 Materials & Methods	41
3.4 Experimental Results	47
3.5 Predictive Capacity of Bar Theory	49
3.6 Discussion	55
3.7 Conclusions	59
<b>4 Initiation of Meandering</b>	<b>61</b>
4.1 Introduction	62
4.2 Study Area	64
4.3 Materials & Methods	71
4.4 Results	74

4.5 Conclusions	80
<b>5 Chute Cutoff</b>	<b>81</b>
5.1 Introduction	82
5.2 Study Area	85
5.3 Material & Methods	85
5.4 Results	92
5.5 Discussion	98
5.6 Conclusions	103
<b>6 Riparian Vegetation</b>	<b>105</b>
6.1 Introduction	106
6.2 Study Area	108
6.3 Material & Methods	109
6.4 Results	112
6.5 Discussion	120
6.6 Conclusions	124
<b>7 Synthesis</b>	<b>127</b>
7.1 Meander Processes in Lowland Streams	129
7.2 Implications for Lowland Stream Restoration	131
7.3 Outlook	136
<b>Bibliography</b>	<b>139</b>
<b>Summary</b>	<b>155</b>
<b>Samenvatting</b>	<b>159</b>
<b>Dankwoord</b>	<b>163</b>
<b>Publications</b>	<b>167</b>
<b>About the Author</b>	<b>169</b>

# 1 | General Introduction



## 1.1 Motivation

### 1.1.1 Lowland Streams

Lowland streams can be defined as low-energy rivers with a channel slope smaller than  $\sim 1 \text{ m km}^{-1}$ , a channel width smaller than  $\sim 20 \text{ m}$ , and a channel bed consisting of sand or peat (Van der Molen *et al.*, 2012). Lowland streams in Europe can be found in the North-western European Plain, which covers The Netherlands, the northern part of Belgium, Denmark, the northern part of Germany, the southern part of Sweden and the north-western and central parts of Poland. Lowland streams in the Netherlands date from the last glacial period (12,000 years ago). In lowland areas, modification and channelisation of water courses have been severe, and today less than 10% of the lowland streams in the Netherlands, the UK, Germany, and Denmark still feature a natural physical state (Brookes & Long, 1990; Iversen *et al.*, 1993; Verdonschot & Nijboer, 2002; Lorenz *et al.*, 2004). Over the past 200 years, there have been three stages of modification to the morphology of lowland streams in the Netherlands: (1) a period of inundation, (2) a period of drainage, and (3) a period of restoration.

The first stream modifications reported in literature occurred in the 18th and 19th century (Baaijens & Dauvellier, 2011). In this period, nutrient-rich stream water has been used to fertilize agricultural fields. Farmers constructed hydraulic structures, with the purpose to stimulate inundation. The nutrient-rich stream water was periodically directed to the agricultural fields to let nutrients be deposited, serving as a natural fertilizer to increase crop yields. Baaijens & Dauvellier (2011) suggest that part of the lowland streams in the Netherlands have been constructed for this purpose. In the beginning of the 20th century, inundation systems disappeared after the introduction of industrialized fertilizers. From this time onwards, the lowland catchments were adjusted for purposes of drainage.

Halfway the 20th century, changing groundwater management practice in agricultural areas led to channelisation of the majority of lowland streams in the Netherlands. The design of the channelised streams aimed at reducing flood risk and meeting the hydrological requirements for the adjacent agricultural fields. The small sinuous streams were redesigned to become straight, to obtain an increased cross-sectional area, and to become controlled by weirs (Iversen *et al.*, 1993; Verdonschot & Nijboer, 2002). In this period, the drainage density within catchments also increased, through the construction of ditches. All these measures were aiming at a quick discharge response during high flows, whereas weirs were in control of ground water levels during low flows. These measures seriously affected the hydro-

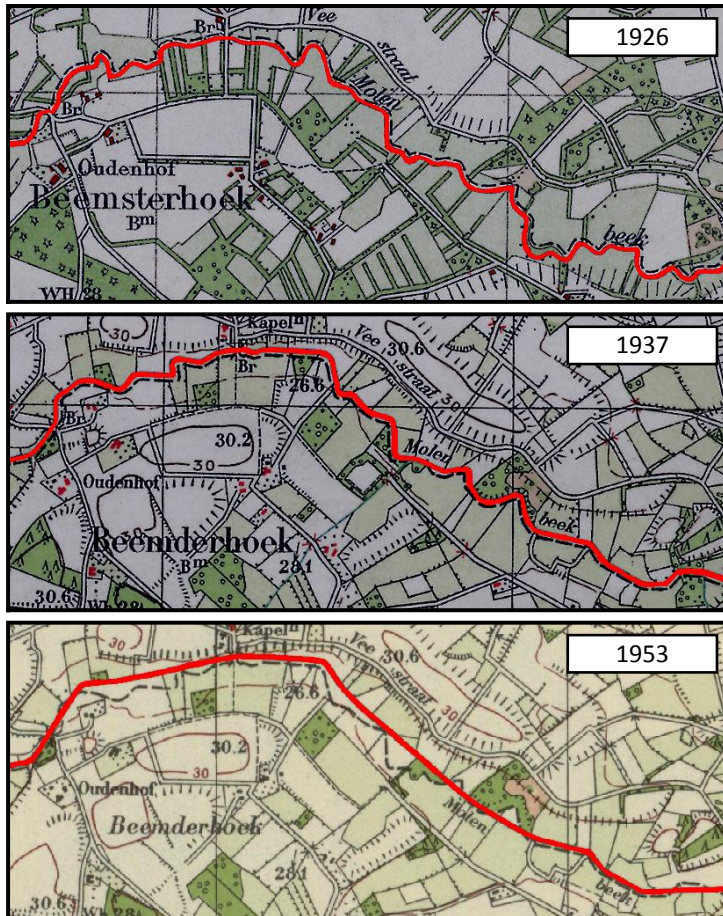


**Figure 1.1** Historical maps showing the process of stepwise channelisation of the Tungelroyse beek. Figure 1.3 shows the location of the Tungelroyse beek in the Netherlands.

logical conditions in the catchments (Meijles & Williams, 2012). Figure 1.1 shows an example of the process of channelisation based on three historical topographic maps of a lowland stream (the Tungelroyse beek). Channelisation occurred in a first phase between 1926 and 1937 and a second phase between 1937 and 1953. Re-meandering measures were implemented in 2011 in this example. Similar channelisation measures of lowland streams were implemented in Denmark (Brookes, 1987; Iversen *et al.*, 1993; Baattrup-Pedersen *et al.*, 2000), Germany (Lorenz *et al.*, 2009), Japan (Nakano & Nakamura, 2008), and the UK (Vivash *et al.*, 1998).

Channelisation had destructive consequences for the abiotic conditions of the benthic ecology in the majority of lowland streams in the Netherlands (Verdonschot

## 1. General Introduction

& Nijboer, 2002). The construction of straight channelised streams resulted in homogeneous in-channel habitat patterns, often solely consisting of bare sand. In an extensive survey, Verdonschot *et al.* (1995) conclude that the measures (channelisation, increase of channel dimensions and increase of drainage density) had major consequences for flow velocity, being the key variable of the abiotic environment relevant for benthic ecology (Fonseca & Hart, 2001). During low flows, weirs were closed to increase ground water levels. This caused flow velocities to drop to nearly zero and fine sediment (e.g. silt) to be deposited on the channel bed. Eventually, this has caused the disappearance of heterogeneous in-stream habitat. In particular, coarse substrates such as large woody debris and gravel were lost (Brookes & Gregory, 1988). During high flows, weirs were lowered and flow velocities increased dramatically. The combination of a channel bed consisting of fine sediment and high flow velocities during high flows were detrimental for the existing benthic ecology. Also, the ground water management had detrimental effects on the terrestrial ecology surrounding the streams.

### 1.1.2 Stream Restoration

The vast majority (96%) of lowland streams in the Netherlands are severely impacted by anthropogenic influences (Nienhuis *et al.*, 2002; Verdonschot & Nijboer, 2002). This reflects the need for stream restoration in the Netherlands. Wohl *et al.* (2005) defines stream restoration as: “assisting the establishment of improved hydrologic, geomorphic, and ecological processes in a degraded watershed system and replacing lost, damaged, or compromised elements of the natural system”. An important element of this definition is the focus on the catchment scale. Recently, several stream restoration concepts have been presented focussing on catchment scale measures, such as the ‘*erodible corridor*’ (Piégay *et al.*, 2005) and ‘*espace de liberté*’ (Kondolf, 2012). Until now, stream restoration has mainly focussed on reach scale measures (Sudduth *et al.*, 2007; McMillan & Vidon, 2014). Common practice in the Netherlands is no exception to this.

Stream restoration in the Netherlands has largely been triggered by the Water Framework Directive (WFD; Council of the European Communities, 2000), in which it is stated that all water bodies should achieve a good qualitative and quantitative status by 2015, with extensions until 2027. The main objective of stream restoration in the Netherlands is to achieve a good ecological status. The second objective is to increase the retention of water within the catchment, which follows from the National Water Act (Waterbeleid voor de 21ste eeuw (WB21); Ministerie van Verkeer en Waterstaat, 2000). Other objectives are related to hydrological conditions (to prevent groundwater damage to crops on agricultural fields and to assure wetland

conditions of natural areas) and recreation (to combine measures with an increase of recreational facilities).

Several approaches are used in stream restoration design, including river classification schemes (e.g., Rosgen, 1994), based on reference reaches (e.g., Newbury & Gaboury, 1993), and process-based approaches (e.g., Copeland *et al.*, 2001; Shields *et al.*, 2003). The design procedures typically adopted in the Netherlands follow a process-based approach. The new channel dimensions should satisfy the following requirements: (1) flood risk reduction, (2) optimal groundwater conditions for adjacent agricultural fields and (3) improvement of the conditions beneficial for benthic ecology. The first requirement is related to the National Water Act (WB21), which aims at reducing flood risk in downstream areas. Water authorities are supposed to take measures to retain water within the catchment during high flows. For stream restoration projects, this means the construction of lowered floodplain areas surrounding the streams. The construction of a lowered floodplain also aims at restoring the natural floodplain processes related to the terrestrial ecology. The second requirement only applies to lowland streams within agricultural areas (the majority of the catchments in the Netherlands), and aims at maintaining the existing ground water levels for adjacent agricultural fields. The third requirement follows from the Water Framework Directive, which aims at increasing the ecological status of the streams.

Stream restoration in the Netherlands involves the construction of sinuous channels (re-meandering), mimicking the channel planform characteristics before channelisation. The sinuous planform is often based on historical sources (such as Figure 1.1). Re-meandering has been widely used as a stream restoration measure (e.g., Sear *et al.*, 1998; Kondolf, 2006; Lorenz *et al.*, 2009). Positive effects on the habitat diversity have been reported after re-meandering measures were implemented (Lorenz *et al.*, 2009). Re-meandering or other channel reconfiguration measures are often applied at local scale, in isolated channel reaches. At local scale, these measures may be successful in improving the habitat conditions, however, recovering the typical benthic ecological communities may only be successful when taking measures at the catchment (Jähnig *et al.*, 2010).

In practice, a 1D-flow model (e.g. SOBEK Channel flow; Deltares, 2011) is typically used in the design of the cross-sectional shape of the new channel. The design procedure focusses on the three main requirements of the new channel design. The channel bed level is adjusted such that existing ground water levels are maintained. The cross-sectional shape is adjusted to achieve conditions of water depth and flow velocity that best suit the needs of specific lowland ecosystems (Verdonschot *et al.*, 1995). Finally, the floodplain level is adjusted to meet the legal

## 1. General Introduction

requirements of flood risk. The measures taken to improve the abiotic conditions for benthic ecology and the construction of a floodplain aims at restoring the natural processes in the streams. Although it has been widely used in stream restoration design, 1D-flow modelling may not capture small scale processes related to the benthic ecology appearing in natural lowland streams.

## 1.2 Stream Restoration and Meandering

There seems to be a cultural preference for meandering planforms within stream restoration projects (Kondolf, 2006). This cultural preference was already acknowledged in the 18th century by Hogarth (1753), who identified the importance of serpentine lines in the perception of beauty. The construction of a sinuous planform is the most common stream restoration practice in the Netherlands. Historical maps (e.g. Figure 1.1) show meandering/sinuous channel planforms in the period before channelisation. These historical maps provide inspiration to construct a meandering planform in lowland areas.

Stream restoration projects are valuable research objects for studying meandering processes (Güneralp *et al.*, 2012). Lowland stream restoration does not involve the construction of hydraulic structures, as often happens in other geographical regions (e.g. Buchanan *et al.*, 2014). Restored lowland streams are allowed to develop laterally, within the boundaries of the floodplain. On the other hand, longitudinal development is often influenced by weirs at the boundaries of the restored channel reaches and bridges, which constrain the width of the floodplain. These influences should be considered when evaluating restoration projects. Compared to river meanders, studying meander processes in lowland streams has the benefit of relatively small physical dimensions. Due to the small water depths, lowland streams are wadeable during the majority of the year. This allows to obtain bathymetrical data using conventional techniques, such as GPS-equipment (Bangen *et al.*, 2014). One individual can perform a high resolution bathymetrical survey of the channel and floodplain at the reach scale (i.e. a series of bends) within one day. A high temporal resolution can be obtained relatively easily. It is likely that morphological processes occur within months to years, since the dimensions of lowland streams are in between those of laboratory experiments and rivers, where morphological processes occur within hours/days and decades/centuries, respectively.

## 1.3 Meander Processes

Traditionally, a simplified distinction has been made between three types of channel planforms, viz. straight, meandering and braided (Leopold & Wolman, 1957). In this classification, straight and meandering planforms consist of a single channel, whereas braided planforms consist of multiple channels. A distinction between meandering and other planforms has been made using empirical relations, applying representative values for discharge, channel slope and bed material (Leopold & Wolman, 1957; Hey & Thorne, 1986; Eaton *et al.*, 2004; Kleinhans & van den Berg, 2011). These empirical relations offer order-of-magnitude threshold values to distinguish channel patterns, but yield limited physical understanding of morphological processes in rivers.

Morphological processes in meandering rivers have been studied with mathematical models and observed in the field and under laboratory conditions, and occur on varying spatial and temporal scales (Table 1.1). Analytical and numerical meander models typically focus on the largest spatial and temporal scales. These meander models are widely used to study the initiation of meandering. Initiation of meandering has been attributed to two types of instability responses, unified by Blondeaux & Seminara (1985). The first to emerge was the so-called *bar theory*, which considers the stability of the alluvial bed and shows that small perturbations in the channel bed may develop into an alternate bar pattern (e.g., Hansen, 1967; Callander, 1969; Blondeaux & Seminara, 1985; Struiksma *et al.*, 1985). The vast majority of the experimental support for the existing alternate bar theory relies on laboratory experiments (e.g., Tubino, 1991; Lanzoni, 2000; Crosato *et al.*, 2011; Venditti *et al.*, 2012). Field studies are rare (Lewin, 1976; Welford, 1994; Rodrigues *et al.*, 2012; Venditti *et al.*, 2012) and reveal complexity of river systems featuring alternate bars, by showing discharge variation, irregular channel width variation, sediment heterogeneity, vegetation development and changes in the longitudinal stream profile due to reach-scale erosion and sedimentation. Until now, Welford (1994) remains the only field study that actually tested the applicability of the existing alternate bar theory.

The second type of instability response to emerge was the so-called *bend theory* (Ikeda *et al.*, 1981), which considers the planform instability of a straight channel and shows that a small perturbation of the channel centerline may lead to the development of meanders. Blondeaux & Seminara (1985) and Struiksma *et al.* (1985) showed the importance of coupling the hydrodynamic equations with the equation of sediment conservation. This has led to meander migration models based on the full Saint Venant equations (e.g., Crosato, 1987; Johannesson & Parker, 1989;

## 1. General Introduction

**Table 1.1** Spatial and temporal scales in meandering rivers (Güneralp *et al.*, 2012).

Main scales	Sub-scales	Definition
Spatial scale	Width	Cross-section or channel-width
	Bend	One meander bend or a few meander bends, including meander wavelength scale
	Reach	Meander train (series of bends)
	Floodplain	Several reaches, including meander belt scale
Temporal scale	Equilibrium	Flow-bed topography is at equilibrium with a given planform geometry - a time scale longer than that of turbulent eddies and shorter than that of bed and planform evolution
	Event	One or a few events causing change in bed morphology
	Engineering	Time scale of planform evolution before cutoffs occur - generally, decades for rivers and a few hours in laboratory flumes
	Geological	Planform evolution including multiple cutoffs

Howard, 1996; Stølum, 1996; Sun *et al.*, 1996, 2001; Zolezzi & Seminara, 2001). Observations of meander initiation have been restricted to laboratory experiments (e.g., Friedkin, 1945; Schumm & Khan, 1971; Smith, 1998; Peakall *et al.*, 2007; Van Dijk *et al.*, 2012), focussing on the role of floodplain material in the process of meander initiation. Due to the long time-scales involved in meander migration, field observations are rare and mainly rely on historical topographic maps.

Several stages are distinguished in the processes related to meander development, which act at multiple spatial and temporal scales. Bank erosion causes an outward migration of the channel centerline, at the smallest spatial and temporal scale, and is often considered as a driver of meander development. Four distinct types of bank erosion failure mechanisms have been identified (ASCE, 1998): planar failures, rotational failures, cantilever failures, and piping and sapping failures. The banks of lowland streams are often steep and covered with vegetation. In that setting, the upper layer may serve as a cohesive layer, whereas the lower layer, consisting solely of sand, may be subject to fluvial erosion. Considering these characteristics, planar and cantilever failures are likely to be the most common failure mechanisms in lowland streams.

Channel migration occurs when the outer bank of a meander bend is subject to bank erosion. At the opposing side of the channel, a point bar emerges and extends in lateral direction towards the eroding bank, keeping the channel width more or less constant over longer time-scales. In most meander models, bank erosion is

parametrised based on the near-bank flow velocity in excess of the mean velocity, and a dimensionless erosion coefficient (Ikeda *et al.*, 1981). The bank accretion rate is assumed constant to the bank erosion rate, by imposing a constant channel width.

Recently, the attention in meander research has shifted from the autogenous processes towards exogenous influences on meander dynamics. Special attention is paid to the role of floodplain heterogeneity and riparian vegetation on meander dynamics. Floodplain heterogeneity causes variation of bank erosion resistance, which cannot be parametrised with solely one erosion coefficient. Based on that consciousness, Motta *et al.* (2012b) coupled a physics-based bank erosion module with the Ikeda *et al.* (1981) meander model. They concluded that the complexity of the meander planform may be represented well with their model, especially for the case of a heterogeneous floodplain. Whereas a constant width is assumed in previous meander models, it has been acknowledged that the processes and time scales of bank erosion and bank accretion are dissimilar (Parker *et al.*, 2011). In existing laboratory experiments, a constant channel width can only been maintained by the addition of cohesive material (Schumm *et al.*, 1972; Smith, 1998) and/or vegetation (Gran & Paola, 2001; Tal & Paola, 2007; Braudrick *et al.*, 2009). In a new framework presented by Parker *et al.* (2011), point bars are supposed to be stabilized by vegetation, and thereby are able to keep up with the eroding outer bank. The new framework has been applied successfully in a numerical meander model, which was capable of producing a variety of meander planform patterns, consistent with those observed in natural rivers (Asahi *et al.*, 2013).

Vegetation also stabilises the outer banks. The importance of riparian vegetation in contributing to channel bank stability has been widely recognized (Simon & Collison, 2002; Pollen-Bankhead & Simon, 2009). Recently, laboratory experiments have shown how riparian vegetation may stabilize floodplain material, causing a morphological regime change from an initially braided channel pattern towards a single-thread (meandering) channel pattern (Gran & Paola, 2001; Braudrick *et al.*, 2009; Tal & Paola, 2010). Riparian vegetation is potentially responsible for changes in meander planform characteristics, including wavelength and skewness (Perucca *et al.*, 2007). Floodplain heterogeneity may have a similar effect on a meander planform, by inducing differences in erodibility of the outer banks (Güneralp & Rhoads, 2011; Motta *et al.*, 2012b). Considering the relatively small spatial scales of streams as compared to rivers (channel width < 20 m), riparian vegetation and floodplain heterogeneity may have a comparatively larger influence.

The process of erosion at the outer bank and the associated accretion at the inner bank, gradually increases channel sinuosity. Sudden decreases of sinuosity are

## 1. General Introduction

caused by meander cutoffs. Two main types of meander cutoffs have been identified. Neck cutoffs can develop by the progressive migration of an elongated bend into itself (Erskine *et al.*, 1992; Hooke, 1995). Chute cutoffs are shortcuts developing over a point bar or across a meander bend (Lewis & Lewin, 1983; Erskine *et al.*, 1992). Neck cutoffs are likely to occur in high-sinuosity meander bends and under low channel gradients. Chute cutoffs are more likely to occur in moderate to low-sinuosity meander bends, and under high channel gradients (Lewis & Lewin, 1983). There is a lack of process-based field studies, which is the main reason why the physical controls on processes of chute cutoff formation remain poorly understood (Micheli & Larsen, 2011; Grenfell *et al.*, 2012).

## 1.4 Objective & Research Questions

In the mid-nineties, when stream restoration was in its infancy, it was already recognized that monitoring of restored channel reaches could potentially reveal the success of restoration efforts (Osborne *et al.*, 1993; Sear, 1994). Until now, post-project monitoring is still rare (England *et al.*, 2008) and little knowledge exists on the success of stream restoration projects (McMillan & Vidon, 2014). It has also been acknowledged that a knowledge gap exists regarding the natural processes that are relevant for stream restoration (Wohl *et al.*, 2005). This is why stream restoration projects create ideal field sites to study both the success of stream restoration (Kondolf, 2006) and the natural processes that are involved in rivers and streams (Hooke *et al.*, 2011; Güneralp *et al.*, 2012). The latter is especially true for the processes related to meandering rivers, since studies on the temporal evolution of meandering rivers are rare (Güneralp *et al.*, 2012).

Only a few studies have been presented focussing on morphological monitoring in lowland areas. Wolfert (2001) presented the most extensive morphological study on lowland stream restoration in the Netherlands to date. Three restored streams, located in the southern part of the Netherlands, were monitored over a period of 2 years. Wolfert (2001) showed that the largest sediment production rates were associated with the first bankfull discharge event, which occurred in the first year after realization. Adjustment of the channel bed included local scouring of pools, undercutting of banks, coarsening of bed material and the formation of depositional bedforms. Following the initial morphological response, rates of sediment production declined and the balance of sediment input and output was restored. Similar observations have been made in lowland stream restoration projects in the U.K. (Sear *et al.*, 1998) and the U.S. (Lindow *et al.*, 2007). These findings confirm the study by Kuenen (1944), who studied the meandering dynamics of several lowland

streams in the northern part of the Netherlands. Kuenen (1944) concluded that the majority of streams did not show signs of lateral migration.

The channel bed of lowland streams mainly consists of sand. In natural streams, a mosaic of substrate patterns has been observed covering the sand bed (Tolkamp, 1980). The variety of substrate patterns include gravel, leaves, branches, large woody debris and organic detritus. Tolkamp (1980) showed that the substrate pattern is dynamic over time, with distinct differences between the four seasons. Macrophytes are frequently observed in lowland streams (Pedersen *et al.*, 2006). Macrophytes may have a strong control over the dynamics of the substrate pattern, by capturing fine sediments (Wolfert, 2001; Lorenz *et al.*, 2009) and by reducing the active channel width (Lindow *et al.*, 2007).

Until recently, morphological developments were rarely being considered in the design process of stream restoration projects in the Netherlands. This is partly caused by the lack of post-project appraisals focussing on morphological developments and, hence, a lack of understanding of the dominant morphological processes. Due to this knowledge gap, water authorities fear morphological developments, including channel migration, large sediment loads and channel incision or aggradation. To bridge the knowledge gap, this thesis aims to *identify, quantify and understand morphological processes in lowland streams*.

Specific research questions are formulated based on this objective. These research questions are divided into two groups. The first group is related to morphological processes in lowland streams, and are fundamental in nature. The second group is related to the implications for lowland stream restoration.

1. Morphological processes in lowland streams:
  - a) How can the archetypical channel planform of a lowland stream be characterized?
  - b) Can post-project appraisals in lowland stream restoration bridge the gap between laboratory studies and rivers with a mild slope?

2. Implications for lowland stream restoration:
  - a) How do the morphological developments relate to the needs to improve the ecological status?
  - b) What is the role of longitudinal connectivity in the morphological development of restored lowland streams?
  - c) Which are the main controls on the lateral development in restored lowland streams?

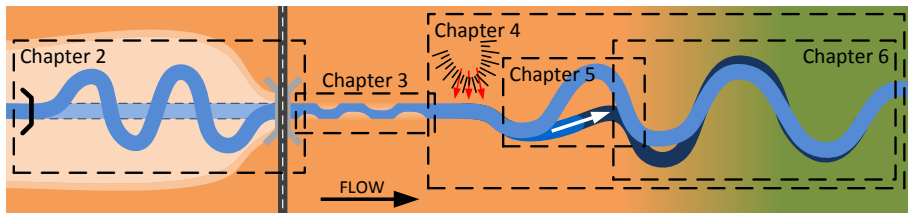


**Figure 1.2** Morphological focus areas of each of the five chapters.

## 1.5 Thesis Outline

The results from this thesis will be presented in five chapters (Chapter 2-6). Figure 1.2 visualizes the main morphological processes studied in each of the five chapters. In Chapter 2 three stream restoration projects are evaluated, focussing on the role of structures and floodplain heterogeneity on longitudinal and lateral channel adjustments, at varying spatial scales. Chapter 3 studies the dynamics of alternate bars in a lowland setting, which are considered a natural means to create stream flow variations. Chapter 4 reveals insight into initiation of meandering in a lowland setting, and subsequent meander development, including bend cutoff and channel incision. Chapter 5 focusses on a chute cutoff event that happened within three months after the construction of a stream restoration project. Chapter 6 sheds light on the morphological developments following the chute cutoff event and focusses on the impact of riparian vegetation and discharge dynamics on channel and floodplain morphodynamics.

The five chapters will assist in answering the five research questions (Section 1.4) as follows. Each of the five chapters will contribute to the knowledge on topics related to planform characteristics of lowland streams (Question 1a), including initiation of meandering (Chapters 3 and 4), floodplain heterogeneity (Chapters 4 and 6), long-term planform development (Chapters 2 and 4), and short-term and small-scale morphodynamics (Chapters 2, 3 and 5). Chapters 3, 5 and 6 present the results of two stream restoration projects, which have been subject to a detailed morphological survey program. From the outcomes of these chapters it will be determined if lowland stream restoration projects can be combined with the study of meander processes of natural systems (Question 1b).

Implications for lowland stream restoration are mainly discussed in Chapter 2. The main objective of stream restoration in the Netherlands is to achieve a good ecological status. In-channel morphological processes influence the benthic ecology

**Table 1.2** Characteristics of the five study areas.

	Gelderns-Nierskanaal	Hagmolenbeek	Hooge Raam	Lunterse beek	Tungelroyse beek
Channel width (m)	8.8	2.0	7.5	6.5	12.9
Channel depth (m)	1.2	0.4	0.4	0.4	1.4
Channel slope ( $m\ km^{-1}$ )	<b>0.48-3.8</b>	0.5	<b>1.8</b>	0.96	0.08
Sinuosity (-)	1.19	1.20	1.00	1.24	1.32
Median grain size ( $\mu m$ )	<b>800-18100</b>	188	218	258	141
Avg. daily discharge ( $m^3 s^{-1}$ )	0.71	0.15	0.22	0.32	1.01
Yearly peak discharge ( $m^3 s^{-1}$ )	4.07	0.99	2.03	7.67	4.77
Ann. coeff. of flow var. <sup>a</sup> (-)	91.5 <sup>b</sup>	123.2 <sup>c</sup>	119.5 <sup>c</sup>	138.5 <sup>c</sup>	77.4 <sup>b</sup>

<sup>a</sup>annual coefficient of flow variation: standard deviation of the discharge divided by the average discharge (Poff & Ward, 1989)

<sup>b</sup>between intermittent flashy and intermittent runoff (Poff & Ward, 1989)

<sup>c</sup>between harsh intermittent and intermittent flashy (Poff & Ward, 1989)

at the smallest spatial scale (Question 2a). These morphological processes include the formation of habitat (Chapter 2) and the dynamics of channel banks and bars (Chapters 3 and 6). Longitudinal and lateral channel bed adjustments may pose a threat to structures (e.g. roads and bridges) and adjacent agricultural fields. These morphological adjustments are one of the main concerns of water authorities in the Netherlands (Questions 2b and 2c). The causes and consequences of longitudinal channel bed adjustments are discussed in Chapters 2, 3 and 5. Lateral channel bed adjustments are discussed in Chapters 2 and 6. Chapter 7 synthesizes the main results of this thesis, in an attempt to reconcile the present-day view on stream restoration in The Netherlands with fundamental insights into morphological processes, gained in this thesis.

## 1.6 Study Areas

Five field locations were selected to study the morphological processes in lowland streams (Figure 1.3). Table 1.2 shows site specific characteristics of each of the five study areas. The table emphasizes in bold font the field characteristics that differ from the characteristics typical for lowland streams, viz. the channel slope of the downstream part of the Gelderns-Nierskanaal and the Hooge Raam, which are relatively steep, and the median grain size of the Gelderns-Nierskanaal, being relatively large.

The field campaigns have focussed on four stream restoration projects, including three traditional re-meandering projects (Hagmolenbeek, Lunterse beek and Tungelroyse beek) and one experimental study reach (Hooge Raam). The three traditional stream restoration projects have been evaluated over a period of 2 years.

## 1. General Introduction

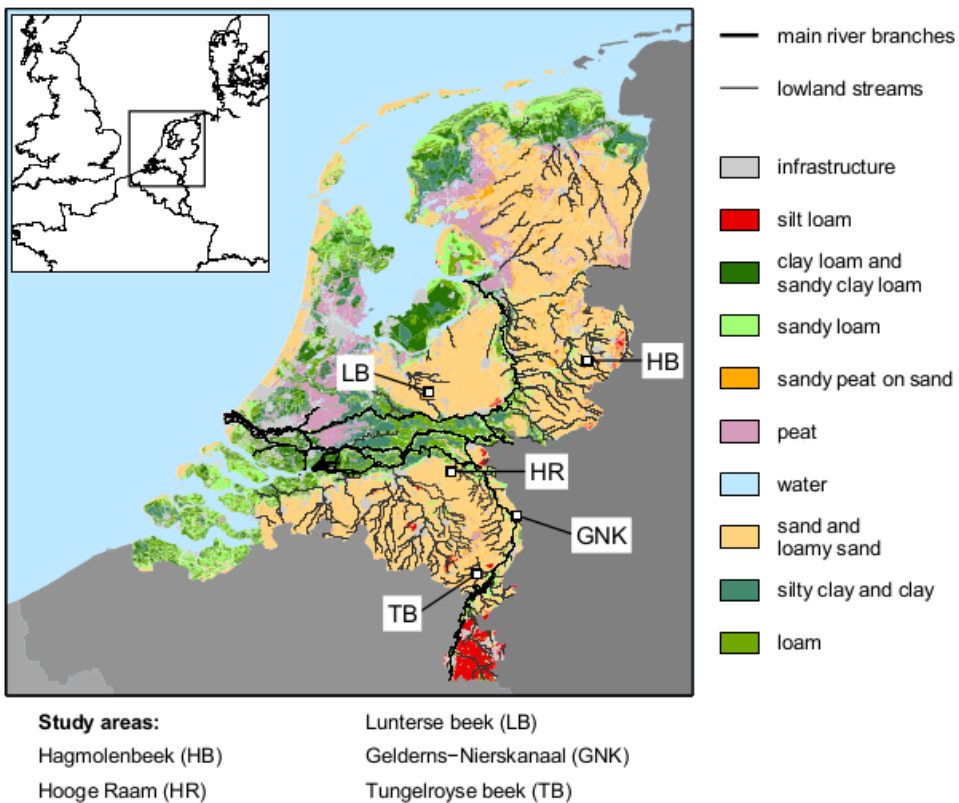


**Figure 1.3** Location of the five study areas in the Netherlands. The map of the Netherlands includes the main river branches, the location of all lowland streams (channel width > 3 m) and a simplified soil texture map (Alterra, 2006), interpreted to the USDA classification soil texture system.

The design principles are presented and evaluated based on morphological and hydrological surveys. An alternative approach has been implemented at an experimental study reach. Over a period of almost three years a field experiment has been performed, with a focus on the in-channel morphological processes. The design was based on general hydraulic geometry relations, established from a comprehensive data set described in Church & Road (1983). The aim of this project was to study the autogenous development of a straight channel.

In these four stream restoration projects, a monitoring scheme was implemented to study the morphological processes that evolved in the first 2-3 years after construction of the new channel. The length of the study reaches range between 300 and 600 m. This coincides with at least 2 meander loops in the re-meandered projects. The monitoring scheme included:

- Sequential morphological surveys along multiple cross-sections;
- Continuous discharge measurements;
- Continuous water level measurements;
- Sediment sampling from the channel bed.

The spatial and temporal resolution of the morphological surveys were chosen to be particularly high in two projects, i.e. the field experiment in the Hooge Raam and the re-meandered reach in the Lunterse beek. These projects aimed at gaining more insight into small-scale morphological processes (width/bend and event scale) and the interaction with the floodplain. Alternate bars formed eight months after construction of the straight experimental study reach in the Hooge Raam. Alternate bar dynamics was studied based on detailed morphological surveys. Similar morphological surveying methods have been applied in the Lunterse beek. Soon after construction works had ended, a chute cutoff event occurred. In the period following the chute cutoff in the Lunterse beek, riparian vegetation emerged. These processes have led to an increase in monitoring efforts at this study reach, focussing on riparian vegetation development, sedimentation sequencing, and discharge dynamics.

The field campaigns captured processes at the engineering time scale, which is most relevant for water authorities. The geological time scale gives more insight into stability of meander bends, and is more fundamental in nature. A historical reconstruction has been made for the re-meandering projects (i.e. Hagmolenbeek, Lunterse beek and Tungelroyse beek) and for the Gelderns-Nierskanaal. The historical analysis of the three re-meandering projects focusses on the dynamics of the channel planform before channelisation. Long-term morphological developments have been studied in the Gelderns-Nierskanaal, which has been constructed by the end of the 18th century as a straight channel. Within decades, the channel evolved into an active meandering channel. The processes that lead to this planform change have been studied using historical material and field surveys.



## 2 | Lowland Stream Restoration



---

Based on: EEKHOUT, J. P. C., HOITINK, A. J. F., DE BROUWER, J. H. F., & VERDONSCHOT, P. F. M. (*submitted*). Morphological assessment of reconstructed lowland streams in the Netherlands. Submitted to *Advances in Water Resources*.

## 2.1 Introduction

Halfway the 20th century, groundwater management in agricultural areas led to channelisation of the majority of lowland streams in the Netherlands. The design of the straightened streams aimed at reducing the flood risk and meeting the hydrological requirements for the adjacent agricultural fields. The small sinuous streams were redesigned to become straight, to obtain an increased cross-sectional area and to become controlled by weirs. The effects of these measures included degradation of the benthic ecology in the streams (Verdonschot & Nijboer, 2002).

The vast majority (96%) of lowland streams in the Netherlands are severely impacted by anthropogenic influences (Nienhuis *et al.*, 2002; Verdonschot & Nijboer, 2002), reflecting the need for stream restoration in the Netherlands. Over the past 25 years, many water authorities in the Netherlands have set goals to restore degraded streams. Stream restoration in the Netherlands has largely been triggered by the Water Framework Directive (WFD; Council of the European Communities, 2000), in which it is stated that all water bodies should achieve a good quality status by 2015, with extensions until 2027. The main objective of stream restoration in the Netherlands is to achieve a good ecological status. The second objective is to increase the retention of water within the catchment, which follows from a National Water Act (WB21; Ministerie van Verkeer en Waterstaat, 2000). Other objectives are related to hydrological conditions (to prevent groundwater damage to crops on agricultural fields and to assure wetland conditions of natural areas) and recreation (to combine measures with an increase of recreational facilities).

The most common practice for stream restoration in the Netherlands is so-called *re-meandering*. This mainly implies the construction of a sinuous channel planform. Stream restoration also includes the removal of weirs, to increase the longitudinal connectivity within the stream. Frequently, old historic maps are used as a source of inspiration for the planimetric design of the channel planform, e.g. to estimate the width of the meander belt and channel sinuosity. One-dimensional flow models (e.g. SOBEK Channel flow; Deltares, 2011) are used to find the most suitable cross-sectional dimensions, including channel width and channel depth. The aim of modelling exercises with such models is to find the dimensions that satisfy the following requirements: (1) flood risk reduction, (2) optimal groundwater conditions for adjacent agricultural fields and (3) improvement of the conditions beneficial for benthic ecology. The first requirement is related to the National Water Act (Ministerie van Verkeer en Waterstaat, 2000), and implies the construction of lowered floodplain areas surrounding the sinuous channel. The second requirement only applies to lowland streams within agricultural areas (the majority of the

**Table 2.1** Hydrological and ecological constraints for the design of the three stream restoration projects. Not all constraints were used in each stream restoration project. The constraints that were not used are denoted with n/a (not available).

	period	Hagmolen-beek	Lunterse beek	Tungelroyse beek
<b>Hydrological constraints:</b>				
Inundation frequency (days yr <sup>-1</sup> )		10-20	160-200	> 100
Groundwater level (m -surface elevation)	summer	n/a	1	n/a
	spring	n/a	n/a	0.50-0.80
	winter	n/a	n/a	0.30-0.50
<b>Ecological constraints:</b>				
Flow velocity (m s <sup>-1</sup> )	summer	> 0.10	> 0.10	> 0.20
	spring	0.20-0.40	n/a	0.10-0.50
	winter	n/a	0.60-0.80	< 1.00
Water depth (m)	summer	n/a	> 0.20	0.20-0.70

catchments in the Netherlands), and aims at maintaining the existing ground water levels in the adjacent agricultural fields. The third requirement follows from the Water Framework Directive, which aims at increasing the ecological status of the streams.

Table 2.1 shows details of the design principles, that served as a basis for the three stream restoration projects under study. The hydrological constraints are related to flooding frequency and groundwater needs. Flooding frequency differs between 10 to 200 days per year. The flooding occurrence is related to the bankfull discharge. The bankfull discharge is obtained from a flow duration curve, in which the expected frequency corresponds to the total inundation period. The groundwater constraints will determine the depth of the channel bed below the floodplain elevation. These values are commonly obtained from groundwater models. The ecological constraints are obtained from a 1D-flow model. The obtained channel dimensions are adjusted such that the highest discharges correspond to bankfull conditions.

In the design process, little attention has been paid to the morphological developments, that may occur after channel construction. Nevertheless, the Dutch water authorities are concerned with sediment transport and the associated morphological changes after the realization of a stream restoration project. These concerns include longitudinal and lateral channel adjustments. The objective of this study is to characterize and understand the channel bed adjustments in the three selected lowland streams subject to a stream restoration program. The selected streams all represent conditions typical for the Netherlands, but are different in bed slope, sediment grain size and channel width.

## 2. Lowland Stream Restoration

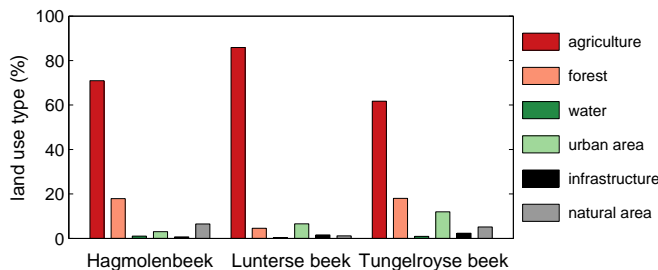


**Figure 2.1** Land use type (%) in each of the three catchments.

## 2.2 Study Areas

The streams under study are located in three different provinces of the Netherlands (Figure 2.2). The catchments are located in aeolian-sand deposits and land use is dominated by agriculture (Figure 2.1). Climatological conditions can be considered constant throughout the Netherlands, with the average yearly precipitation amounting to 793 mm (KNMI, 2014). Channel construction in the three stream restoration projects ended between June 2010 and October 2011. The overall stream restoration strategy included the construction of a sinuous channel planform, removal of weirs, and lowering of the floodplains. Table 2.2 shows characteristics of the three projects. Although the same restoration strategy was used in all three projects, the resulting channel characteristics differ. Constructed channel widths range from 2.0 m to 12.9 m, and constructed channel slopes from  $0.08 \text{ m km}^{-1}$  to  $0.96 \text{ m km}^{-1}$ .

Several site specific characteristics can be observed from the sketches of the study areas (Figure 2.2). In the Hagemolenbeek (panel b) the re-meandered channel partly follows the straightened channel, at the location where an existing bridge was maintained. Here, the channel dimensions increase, compared to the rest of the study reach. In the Lunterse beek (panel a), the re-meandered channel crosses the straightened channel at several locations. A weir is located upstream from the study reach. A peat deposit is located in the upstream part of the study reach. The Lunterse beek is also subject to extensive analyses in Chapters 5 and 6. The study reach of the Lunterse beek analysed in this chapter, includes the re-meandered channel reach upstream from the bend where a cutoff event occurred (Chapter 5). This choice was made to facilitate comparison with the morphological processes that occurred in the two other study reaches discussed in this chapter. The study reach of the Tungelroyse beek (panel c) is located upstream from an area where a straightened channel was maintained, causing an increase of the channel dimensions at the downstream end of this study reach.

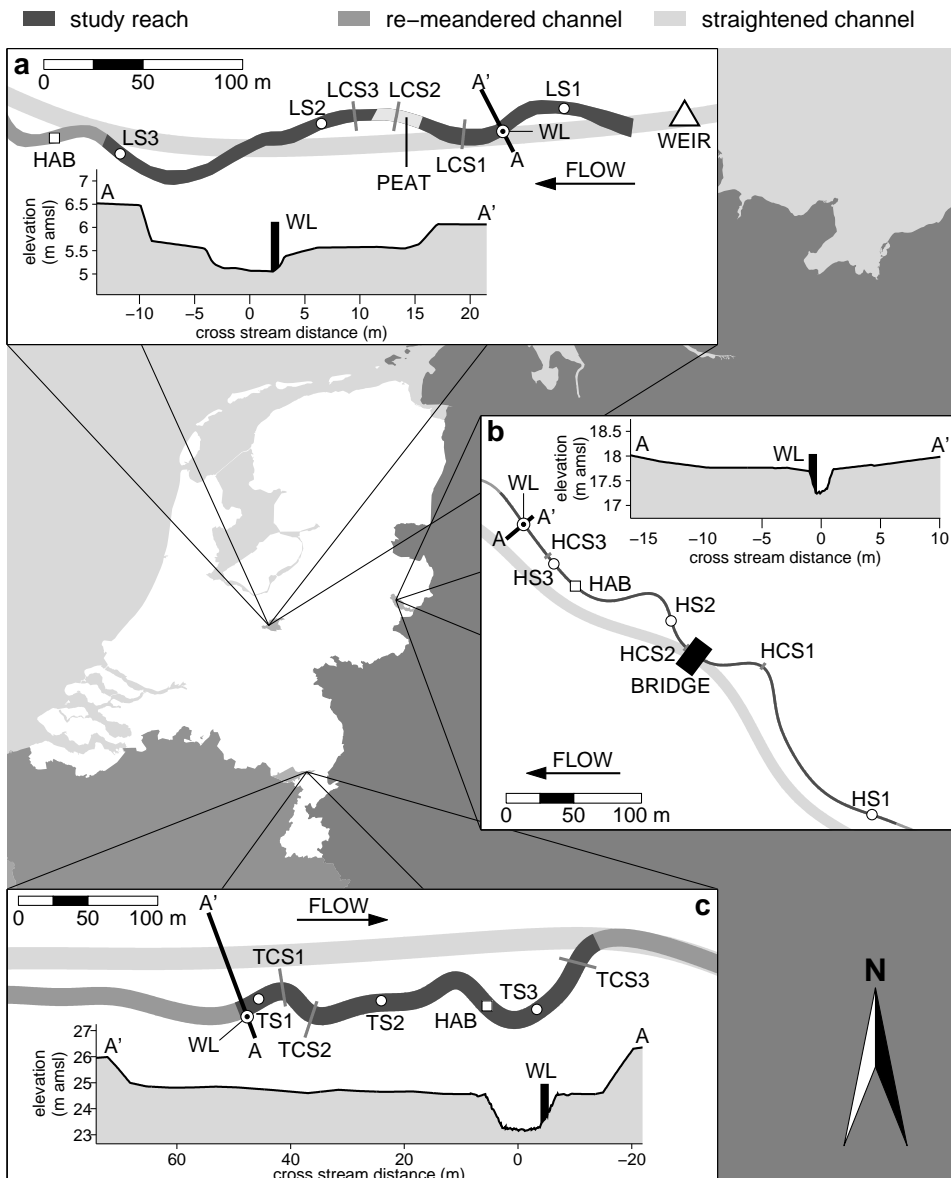


**Figure 2.2** Locations of the study areas in the Netherlands and sketches of the extent of the study areas Lunterse beek (a), Hagemolenbeek (b), and Tungelroyse beek (c). The sketches include the study reach (dark grey), re-meandered channel (grey) and straightened channel (light grey), the sediment sample locations (S1,S2,S3), the locations of the cross-sections CS1,CS2 and CS3, the location of the habitat survey (HAB), and the location of the water level gauge (WL), including the cross-section at that location (A-A'). The sketches also include the location of a weir and a peat deposit in the Lunterse beek (panel a) and the location of a bridge in the Hagemolenbeek (panel b).

**Table 2.2** Characteristics of the study areas.

	Hagmolen-beek	Lunterse beek	Tungelroyse beek
Longitude	52° 12' 59" N	52° 4' 46" N	51° 14' 42" N
Latitude	6° 43' 22" E	5° 32' 37" E	5° 53' 10" E
Altitude (m a.m.s.l.)	17.8	5.2	23.3
Catchment area (km <sup>2</sup> )	59.5	63.6	116.1
Mean daily discharge (m <sup>3</sup> s <sup>-1</sup> )	0.15	0.31	1.01
Yearly peak discharge (m <sup>3</sup> s <sup>-1</sup> )	1.00	3.55	4.77
Annual coeff. of flow variation <sup>a</sup> (-)	123.2 <sup>b</sup>	138.5 <sup>b</sup>	77.4 <sup>c</sup>
Sediment size (μm)	188	258	141
Restored channel length (km)	1.7	1.6	9
Width (m)	2.0	6.5	12.9
Depth (m)	0.4	0.4	1.4
Channel slope (m km <sup>-1</sup> )	0.50	0.96	0.08
Sinuosity (-)	1.20	1.24	1.32
Length of study reach (m)	385	250	380
Surveying period (from - to)	Sept. 2010 - July 2012	October 2011 - August 2013	June 2011 - August 2013

<sup>a</sup>standard deviation divided by average discharge (Poff & Ward, 1989)

<sup>b</sup>between harsh intermittent and intermittent flashy (Poff & Ward, 1989)

<sup>c</sup>between intermittent flashy and intermittent runoff (Poff & Ward, 1989)

## 2.3 Material & Methods

Historical maps were available for each of the three streams. The historical maps give a clear view of the channel evolution in time, possible anthropogenic modifications and allow to estimate the period when channelisation measures were implemented. Historical maps were available for the Hagmolenbeek from 1892-1995 (9 maps), for the Lunterse beek from 1872-1995 (8 maps) and for the Tungelroyse beek from 1896-1988 (9 maps). The channel centerline was extracted from the digitized historical maps. For each map a channel reach was selected that did not show any anthropogenic influence in the period before straightening. The length of these channel reaches ranged from 1.2 to 2.5 km. The sinuosity was determined for these channel reaches by dividing the channel length by the length of the channel reach after straightening.

A standardized monitoring scheme was implemented for all three projects. The monitoring focused on morphological and hydrological parameters. Monitoring activities were focused on study reaches with a length between 250 and 380 m. The lengths of the study reaches were chosen such that they captured at least

two complete meander wavelengths. Morphological data were collected using Real Time Kinematic (RTK) GPS-equipment (Leica GPS 1200+), with a one-year interval between the surveys. The RTK-GPS equipment allows to measure a point in space with an accuracy of 1 to 2 cm. Morphological data were collected along 30 to 69 cross-sections during each survey. The water level was recorded at each cross-section, from which the water level slope was determined.

The channel width and channel bed elevation were determined at each individual cross-section. The channel width is defined as the distance between the two channel bank tops. The location of the channel bank tops in each cross-section were marked during the field surveys. The channel bed elevation was obtained by subtracting the hydraulic radius from the average elevation of the two opposing crests of the channel banks. The hydraulic radius is defined as the cross-sectional area divided by the wetted perimeter. The average channel slope over the total length of the study reach was determined by fitting a straight line through the channel bed elevations.

The in-channel habitat patterns were obtained at 20-m subsections of the three study reaches (HAB; Figure 2.2). Each year, three pattern sketches were made of the channel bed, distinguishing substrate (sand, gravel and silt), macrophytes and algae.

Sediment samples were taken at three locations along the channel, i.e. upstream, half way, and downstream of the study reaches (S1,S2,S3; Figure 2.2). Samples were taken during the first and last morphological surveys. The sediment samples were dried for 24 hours in an oven at 105° Celsius. The dried samples were sieved using a stack of eight sieves, with mesh sizes ranging from 63-2000  $\mu\text{m}$ . The weight of each subsample was determined and the cumulative grain size distribution was established. The median grain size was derived from the cumulative grain size distributions.

Discharge was measured continuously at a measurement weir, located outside the study areas. Discharge was sampled at a one-hour frequency for the Hagmolenbeek and Lunterse beek and at a 15-minute frequency for the Tungelroyse beek. Water level was measured continuously using a water level gauge inside the study reach (WL; Figure 2.2). Water level was sampled at a one-hour frequency. Since short-term water level variation may relate to local effects at the water surface, further analysis focusses on the daily-averaged time-series for discharge and water level.

Discharge and water level time-series were combined to determine the cross-sectional average flow velocity  $\bar{u}$  and dimensionless bed shear stress (Shields stress)  $\theta$ . The cross-sectional flow area was determined based on the water level and cross-

## 2. Lowland Stream Restoration

**Table 2.3** Average water level slope and Shields parameter for each.

	Hagmolen-beek	Lunterse beek	Tungelroyse beek
Water level slope ( $\text{m km}^{-1}$ )	0.69	0.43	0.08
Shields parameter (-)	0.052	0.042	0.067

sectional shape at the water level gauge (Figure 2.2). Values of  $\bar{u}$  were obtained by dividing the discharge by the cross-sectional flow area.

Assuming near-uniform flow conditions, Shields stress was estimated according to:

$$\theta = \frac{R \frac{\Delta \zeta}{\Delta x}}{d_{50} s} \quad (2.1)$$

where  $R$  is the hydraulic radius (m),  $\frac{\Delta \zeta}{\Delta x}$  is the longitudinal water level slope (-),  $d_{50}$  is the median grain size (m), and  $s = (\rho_s - \rho)/\rho$  is the relative submerged specific gravity of the sediment (-), with  $\rho = 1000 \text{ kg m}^{-3}$  the density of water and  $\rho_s = 2650 \text{ kg m}^{-3}$  the density of sediment. The longitudinal water level slope  $\frac{\Delta \zeta}{\Delta x}$  was based on the average measured longitudinal water level (Table 2.3). The median grain size  $d_{50}$  was obtained from the average of the sediment samples from the first survey.

The cross-sectional average Shields stress time-series were used to determine the time windows when the Shields stress exceeds the critical Shields stress (Shields parameter), corresponding to the periods when sediment may have been actively transported. The Shields parameter depends on the grain size and is defined as (Van Rijn, 1993):

$$\theta_{cr} = 0.24 D_*^{-1} \quad \text{for } 1 < D_* \leq 4 \quad (2.2a)$$

$$\theta_{cr} = 0.14 D_*^{-0.64} \quad \text{for } 4 < D_* \leq 10 \quad (2.2b)$$

where  $D_*$  is the particle parameter:

$$D_* = \left[ \frac{(s - 1)g}{\nu^2} \right]^{1/3} d_{50} \quad (2.3)$$

where  $g = 9.81 \text{ m s}^{-2}$  is the gravitational acceleration and  $\nu = 10^{-6} \text{ m}^2 \text{ s}^{-1}$  is the kinematic viscosity of water.

## 2.4 Results

### 2.4.1 Historical Maps

Figure 2.3 shows the historical channel centerline evolution of the three streams, derived from the historical maps. The sinuosity was determined for each of the channel centerlines (Figure 2.3d). Both the Hagemolenbeek and Tungelroyse beek hardly show any variation of the sinuosity in the period before straightening, when the sinuosity was stable around a value of 1.26 and 1.20, respectively. The figures also show that both streams were first partly straightened, between 1925 and 1935, before the channels were completely straightened between 1935 and 1955. The Lunterse beek shows a stronger morphological activity in the period before straightening. In this period, the sinuosity varied between 1.14 and 1.25. The Lunterse beek was straightened between 1953 and 1962.

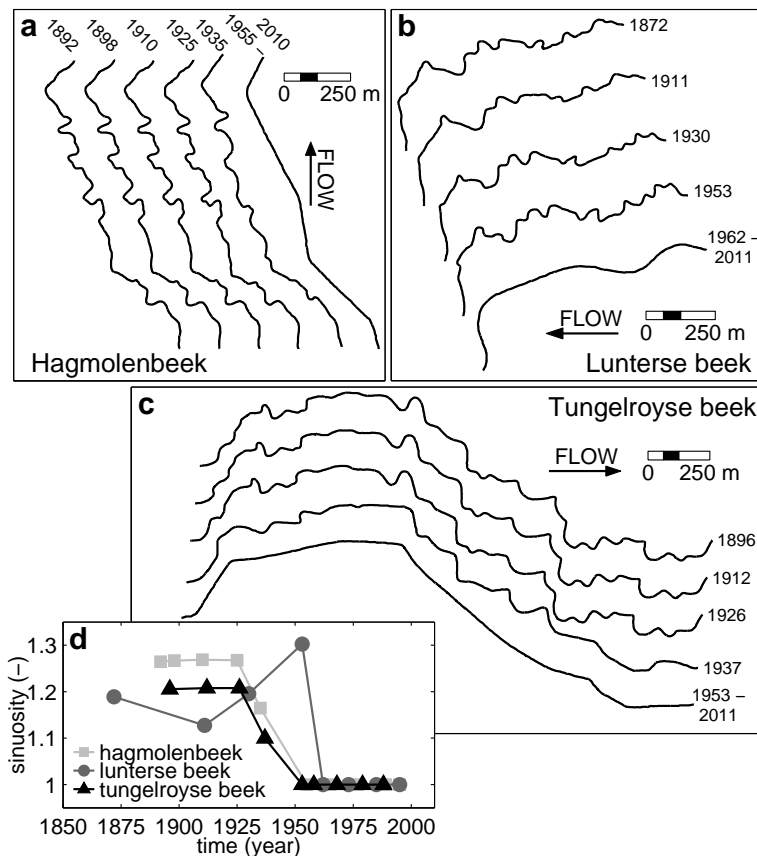
### 2.4.2 Morphological Surveys

Figure 2.4 shows the temporal changes of the channel width (upper panels) and channel bed elevation (lower panels) along the channel centerline. The figure indicates the location where the re-meandered channel crosses the formerly straightened channel (Hagemolenbeek and Lunterse beek) and the location of the peat deposit (Lunterse beek).

At two locations in the Hagemolenbeek, changes in channel width and channel bed elevation were observed. One location is situated where the re-meandered channel partly follows the old straightened channel, which coincides with the location of a bridge. The channel bed elevation before re-meandering was partly maintained. During the two-year monitoring period, this section of the channel was filled with sediment. The other location is located in the bend just upstream from the bridge. Here, a channel width increase and channel incision were observed from year 0 to year 2. A minor form of channel incision is observed in the downstream half of the study reach.

Most variation in channel width and bed elevation was observed in the Lunterse beek. The channel width increased by 1 to 3 meters at two sections of the channel. At these two sections, the re-meandered channel crossed the formerly straightened channel. Channel incision occurred at two locations along the channel centerline: upstream and downstream from the peat deposit. Sediment was deposited downstream of the streamwise coordinate 175 m. Most of the changes in channel width and bed elevation occurred during the first year after construction of the re-meandered channel. In the second year, only minor changes occurred.

## 2. Lowland Stream Restoration



**Figure 2.3** Temporal evolution of the channel planforms derived from the historical maps of the Hagmolenbeek (a), the Lunterse beek (b), the Tungelroyse beek (c). Panel (d) shows the temporal evolution of sinuosity.

During the two-year survey period, hardly any changes in channel width were observed in the Tungelroyse beek. Changes were more apparent in the temporal evolution of the bed elevation. Channel incision occurred between streamwise coordinates 125 and 150 m. Deposition of sediment occurred around streamwise coordinates 175 m and 250 m, and downstream from streamwise coordinate 350 m. The latter is most evident for cross-section TCS3 (Figure 2.5).

Figure 2.5 shows three examples of cross-sections for each study reach. HCS1 from the Hagmolenbeek shows the bend where both channel widening and channel bed incision occurred. Channel widening is mainly related to bank erosion. Here, bank erosion occurred gradually, from year 0 to year 2, and amounts up to 1.05 m (62% of the channel width). Channel bed incision also occurred gradually and amounted up to 0.25 m (44% of the channel depth). HCS2 shows the rate of sedi-

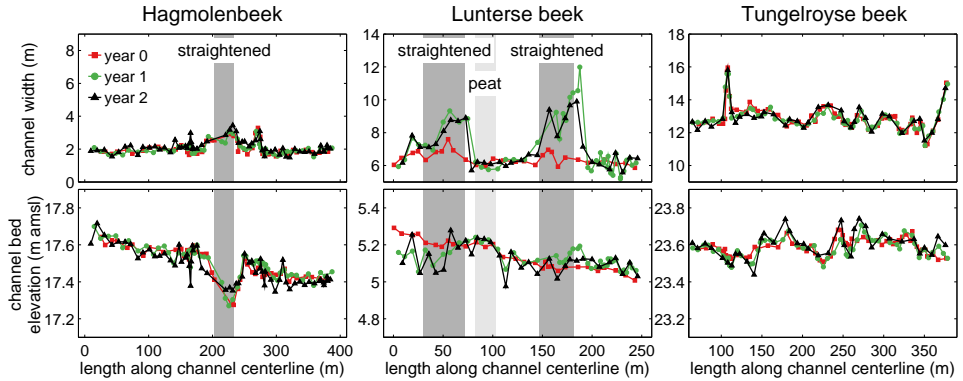


**Figure 2.4** Channel width and channel depth along the channel centerline at year 0 (red squares), year 1 (green circles) and year 2 (black triangles). The location where the re-meandered channels cross the straightened channels are indicated with dark grey (Hagemolenbeek and Lunterse beek). The location of the peat deposit in the Lunterse beek is indicated with light grey.

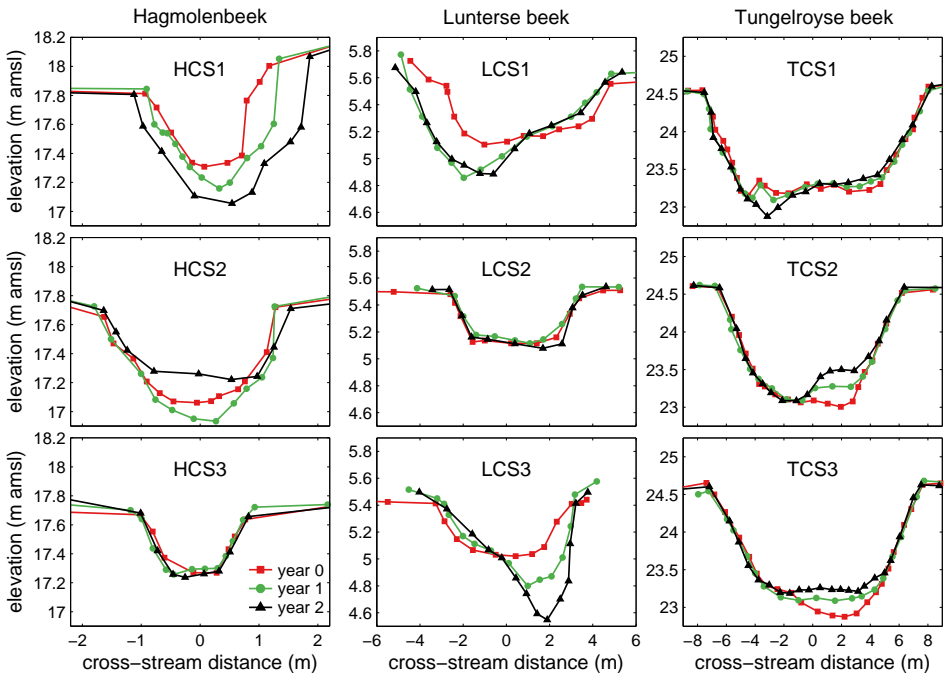


**Figure 2.5** Three examples of the temporal evolution of cross-sections in the three streams at year 0 (red squares), year 1 (green circles), and year 2 (black triangles). The location of the cross-sections correspond to the locations as shown in Figure 2.2.

## 2. Lowland Stream Restoration

mentation of the channel near the bridge. Here, the constructed channel width (3.0 m) exceeded the channel width of the rest of the channel. Deposition of sediment locally exceeded 0.29 m (37% of the channel depth). HCS3 shows an example of a cross-section from the downstream half of the study area. Only minor changes occurred here, even though Figure 2.4 suggests aggradation of sediment in this part of the study reach.

In the Lunterse beek, channel widening and incision occurred on a larger scale. LCS1 shows a location along the channel where the re-meandered channel crosses the formerly straightened channel. It shows a cross-section where bank erosion occurred next to incision of the channel bed near the eroding bank. This resulted in a typical asymmetric cross-sectional shape, as found in meandering rivers. The upstream cross-section also shows that morphological adjustments mainly occurred in the first year. At this location, bank erosion amounted to 1.4 m (19% of the channel width). Channel incision amounted to 0.22 m (55% of the channel depth). LCS2 shows a cross-section surrounded by peat deposits. Few morphological adjustments occurred in this section of the channel. LCS3 shows that just downstream of the peat deposits, channel incision occurred. As opposed to other locations along the channel, here the morphological development took place gradually. In the first year, incision amounted up to 0.22 m and in the second year up to 0.25 m, reaching 130% of the channel depth in total.

Figure 2.4 showed that few changes in channel width were observed in the Tungelroyse beek. TCS1 shows the cross-section where the channel was constructed, with a channel width exceeding the rest of the channel; 15.7 m against an average of 12.9 m. At this location, located in a bend, channel incision of the outer bank and aggradation of the inner bank occurred. TCS2 shows point bar development in the inner bend. Here, sediment was deposited in the inner bend, resulting in a gradual increase amounting to 0.27 m in the first year and 0.22 m in the second year. TCS3 is located at the downstream end of the study reach and shows the channel bed gradually aggregated over the two-year period, by 0.23 m in the first year and 0.13 m in the second year.

Figure 2.6 shows the channel slopes for each of the three surveys per stream. The channel slope in the Hagemolenbeek did not change over the two-year period. Both the Lunterse beek and the Tungelroyse beek show decreasing channel slopes over time. The decrease of channel slope in the Lunterse beek was most dramatic in the first year. This was mainly caused by channel incision at the upstream end of the study reach. In the second year, a slight increase of the channel slope was observed. The Tungelroyse beek featured negative channel slopes for the surveys after one and two years, which can be attributed to local channel bed adjustments.

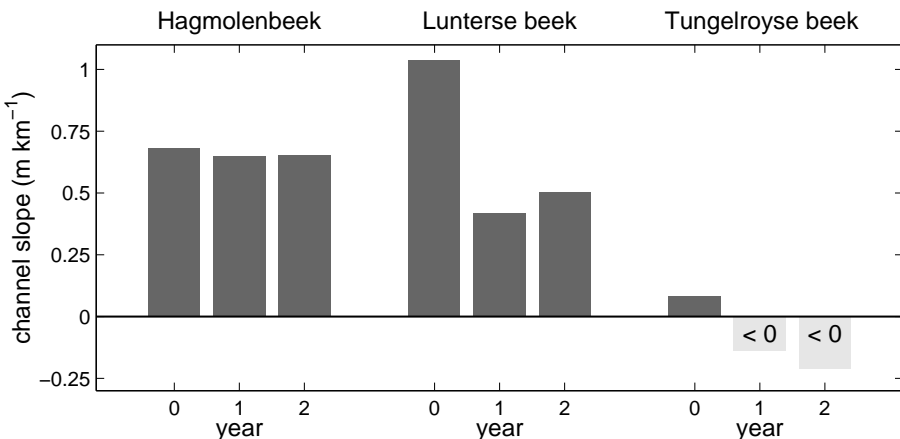


**Figure 2.6** Channel bed slope ( $\text{m km}^{-1}$ ) derived from the lower panels of Figure 2.4.

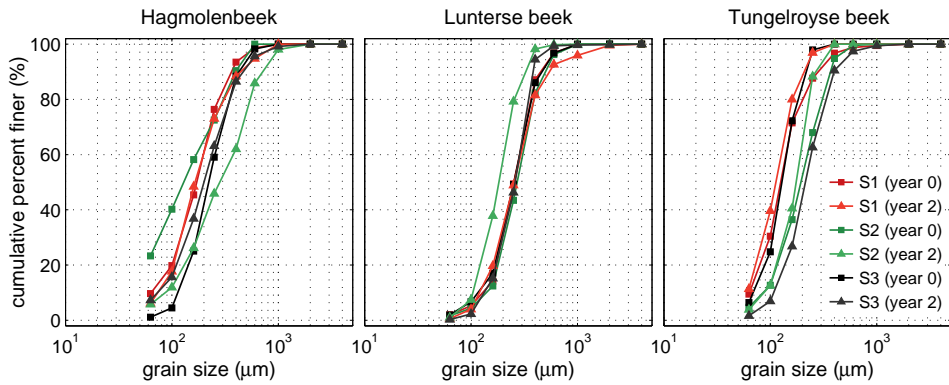
**Table 2.4** Median grain size ( $\mu\text{m}$ ) of each sediment sample, derived from the grain size distributions (Figure 2.7). The sample locations are shown in Figure 2.2.

	Hagmolenbeek		Lunterse beek		Tungelryse beek	
	Year 0	Year 2	Year 0	Year 2	Year 0	Year 2
S1	171	165	252	254	125	113
S2	129	282	271	182	194	175
S3	222	200	253	259	128	214
Average	188	203	258	227	141	179

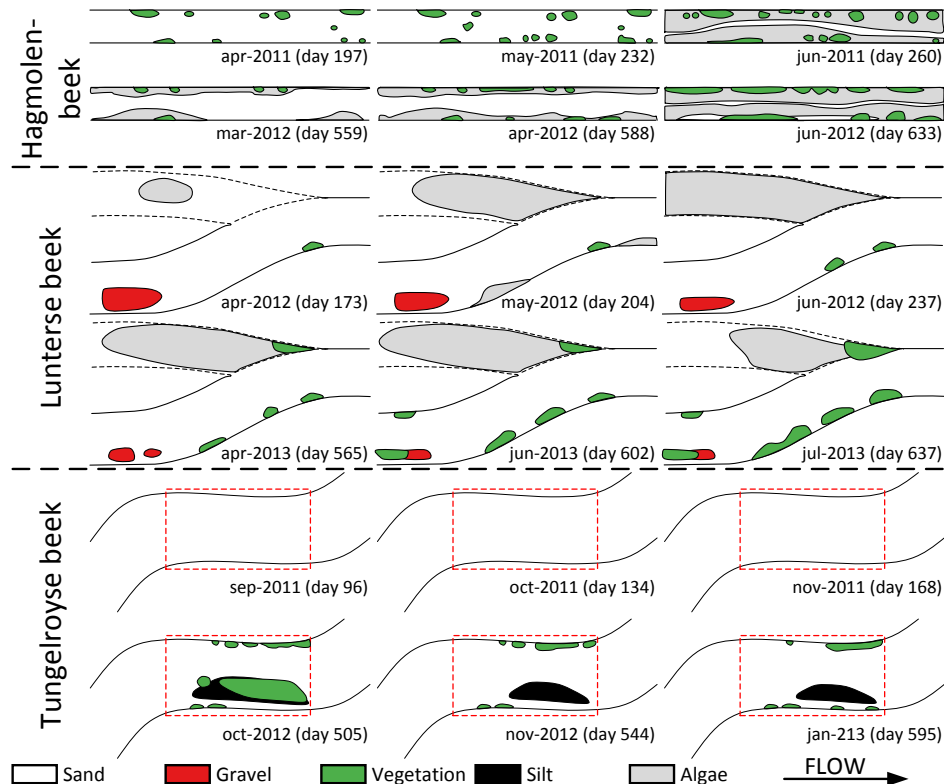
### 2.4.3 Grain Size Analysis

Figure 2.7 shows the grain size distributions for the three sample locations in each of the three streams, both at the start and at the end of the monitoring period. Table 2.4 lists the median grain sizes established from the sediment samples. Only small changes in bed material composition have occurred during the two-year study period. In each of the three streams, two out of three sample locations show negligible changes. Especially in the Lunterse beek, all except one of the grain size distributions remain nearly identical. In each stream, one sample location differs from this observation, i.e. location HS2 and LS2, and location TS3. Eventually, this caused a change in average median grain size, with an increase in the Hagmolenbeek and Tungelroyse beek and a decrease the Lunterse beek.

## 2. Lowland Stream Restoration



**Figure 2.7** Grain size distribution taken during year 0 (squares) and year 2 (triangles). Samples were taken at three locations along the channel centerline: S1 (red), S2 (green) and S3 (black). The sample locations are shown in Figure 2.2.



**Figure 2.8** Temporal evolution of the in-channel habitat pattern on a 20-m study reach. The sample locations are shown in Figure 2.2.

#### 2.4.4 Habitat Patterns

Figure 2.8 shows the evolution of the in-channel habitat patterns. All three study reaches were constructed in bare sandy soil. Within the first year several habitat types appeared in the Hagemolenbeek and in the Lunterse beek. In the Tungelroyse beek the channel bed still consisted of bare soil after the first year. In each study reach, macrophytes emerged, mainly near the channel banks. Also other habitat types were observed: algae in the Hagemolenbeek and Lunterse beek, gravel in the Lunterse beek and silt in the Tungelroyse beek. Since the habitat surveys were mainly concentrated in the summer period in the Hagemolenbeek, the amount of algae cover as observed from the figure may not represent the entire year.

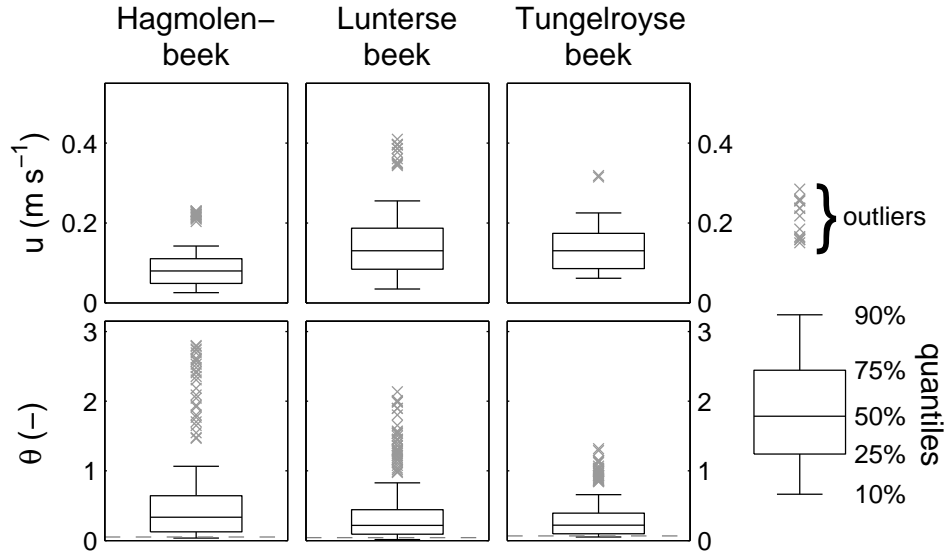
#### 2.4.5 Hydrological Results

Figure 2.9 shows Box-and-whiskers plots of the cross-sectional average flow velocity and Shields stress. The lowest cross-sectional average flow velocities occurred in the Hagemolenbeek, where the median value amounts to  $0.08 \text{ m s}^{-1}$ . The cross-sectional average flow velocities in the Lunterse beek and Tungelroyse beek were similar, with median values amounting to  $0.13 \text{ m s}^{-1}$ . Most variation in cross-sectional average flow velocity is observed in the Lunterse beek. Here, values reach up to  $0.41 \text{ m s}^{-1}$ . The least variation is observed in the Hagemolenbeek.

The highest Shields stresses are observed in the Hagemolenbeek, where the median Shields stress amounts to 0.34. The median Shields stresses in the Lunterse beek and Tungelroyse beek are slightly lower, both amounting to 0.22. The distribution of the Shields stress differs among the three streams. The broadest distribution is observed in the Hagemolenbeek and the narrowest in the Tungelroyse beek. Apart from these differences, the fraction of time for which the threshold for sediment motion is exceeded is similar for all three study reaches, amounting to 87%, 84%, and 81% of the time for the Hagemolenbeek, Lunterse beek and Tungelroyse beek, respectively.

## 2.5 Discussion

Longitudinal channel bed adjustments were observed in all three study areas. The longitudinal channel bed adjustments were observed at channel sections where the re-meandered channel either crosses the formerly straightened channel (Hagemolenbeek), downstream from a weir and a peat deposit (Lunterse beek) or upstream from a straightened channel section (Tungelroyse beek). In the Hagemolenbeek, longitudinal adjustments mainly occurred in the channel bend that was subject to



**Figure 2.9** Box-and-whiskers plots (median, 25th and 75th percentiles within the box and 10th and 90th percentiles as whiskers) of the cross-sectional averaged flow velocity  $\bar{u}$  ( $\text{m s}^{-1}$ ) and cross-sectional average Shields stress  $\theta$  (-). The dashed lines in the lower plots indicate the Shields parameter. A value  $X$  is considered to be an outlier when the value is outside the range between  $Q_{25} - w(Q_{75} - Q_{25})$  and  $Q_{75} + w(Q_{75} - Q_{25})$ , with  $w = 1.5$ . Outliers are plotted with grey crosses.

bank erosion and at a location where the re-meandered channel crosses the formerly straightened channel. At this location, where a bridge was located, the cross-section was initially both deeper (59%) and wider (34%) than the average values for the rest of the study reach. It is likely that the increase of channel dimensions caused flow velocities to decrease in this area, eventually leading to aggradation. Geometrical effects may have been responsible for the aggradation of the channel bed at the downstream end of the Tungelroyse beek. Here, the re-meandered channel eventually flows into the straightened channel, resulting in an increase of channel width.

In the Lunterse beek, a weir was maintained upstream from the study reach. At the upstream end of the study reach, channel incision was observed. It is likely that a lack of sediment transport past the weir resulted in an imbalance in sediment transport downstream of the weir. Consequently, more sediment may have been entrained because of the difference between the actual sediment transport and the transport capacity in this section, resulting in channel incision. A similar situation may have occurred downstream of the peat deposit. The peat area may trap sediment from upstream, interrupting the along channel sediment transport.

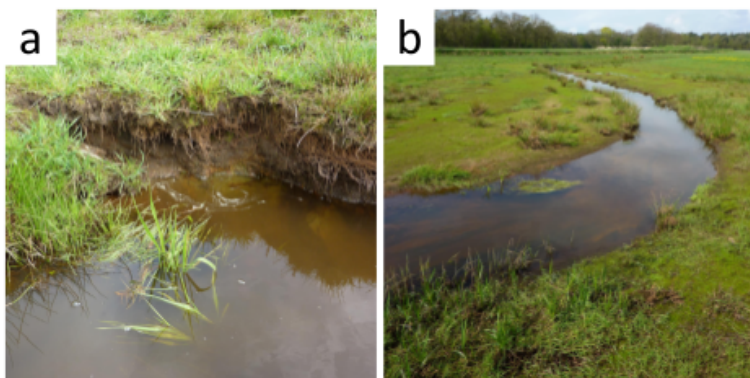


**Figure 2.10** Photos from (a) the channel bank where extensive bank erosion occurred, and (b) a channel bend with similar curvature where no morphological changes occurred.

Downstream of the peat deposit, sediment was available and must have been entrained to increase the sediment transport towards its transport capacity, causing channel bed incision.

These examples show that most of the longitudinal channel bed adjustments are related to exogenous influences, viz. width variation, a weir and a peat deposit, as opposed to autogenous processes related to instability in the coupled system of the water motion, sediment transport and bed morphology. These exogenous influences resulted in backwater effects and variation of sediment transport capacity.

Lateral channel adjustments occurred in all three study reaches. Bank erosion was observed in the Lunterse beek and the Hagemolenbeek, and was also related to exogenous influences. In the Lunterse beek, bank erosion was observed in areas where the re-meandered channel crosses the formerly straightened channel. At these locations, the former channel was filled with sediment prior to the construction of the new channel. It is very likely that this resulted in a less consolidated floodplain, which was prone to erosion. In the Hagemolenbeek, channel width adjustments were observed at a location where a non-cohesive sandy layer was overlain by a vegetated upper layer (Figure 2.10a). Erosion of the sandy layer undermined the upper cohesive layer, causing failure of the overhanging upper layer. A bend with similar curvature is located downstream of the bridge, where limited morphological adjustments were observed. The channel banks of this bend did not consist of this particular structure (Figure 2.10b).

Both in the Lunterse beek and in the Tungelroyse beek, asymmetrical cross-sections have been observed. The development of the asymmetrical cross-sections may be related to autogenous processes, featuring erosion in the outer bend and

## 2. Lowland Stream Restoration

deposition in the inner bend. In the Lunterse beek, both types of processes occurred, whereas in the Tungelroyse beek only deposition of sediment in the inner bend occurred.

Channel bed development also occurred at the habitat scale. Analysis of habitat patterns show that a gravel bar and a silt bar formed in the Lunterse beek and in the Tungelroyse beek, respectively. These habitat types may be related to the occurring flow regime. Figure 2.9 shows that the highest Shields stresses were observed in the Hagmolenbeek and the lowest Shields stresses in the Lunterse beek and Tungelroyse beek, although the Lunterse beek shows a broader distribution. The low Shields stresses in the Tungelroyse beek may explain the formation of a silt bar. Similar habitat dynamics have been observed in other lowland streams, but under similar flow conditions (Wolfert, 2001). In the Hagmolenbeek, almost the entire channel cross-section was covered with algae. In each stream, macrophytes appeared near the channel banks. Their presence may be related to the flow conditions, although it is likely that nutrient availability and other influences (e.g. temperature, shading) play a more important role in the distribution of these habitat types.

The rate at which the channel bed is adjusting to a new morphological equilibrium can be estimated by calculating the morphological time scale based on a parabolic approximation of the bed evolution equation (De Vries, 1975). The morphological time scale  $T$  characterises the time needed for the channel bed to develop towards uniform flow conditions, and is defined as:

$$T = \frac{(1 - e)3L^2Bi_b}{b\tilde{Q}_s} \quad (2.4)$$

where  $e = 0.4$  is the fraction of the sediment volume occupied by pores (-),  $L$  is a characteristic longitudinal length scale (m),  $B$  is the channel width (m),  $i_b$  is the channel slope,  $b$  is an exponent representing the degree of nonlinearity in the relation between sediment transport and depth-averaged flow velocity (-), and  $\tilde{Q}_s$  is the yearly averaged volumetric sediment transport ( $\text{m}^3 \text{ year}^{-1}$ ). The channel width  $B$  and the channel slope  $i_b$  follow from the constructed channel conditions. The value of  $b$  is equal to the exponent in case of a power law dependence  $q_s \propto u^b$ , attributed  $b = 4$  here. This corresponds to a value used for sand-bed rivers, following Crosato & Mosselman (2009) and Kleinhans & van den Berg (2011). The yearly volumetric sediment transport  $\tilde{Q}_s$  is estimated using the Engelund & Hansen (1967) sediment transport equation:

$$\tilde{Q}_s = \frac{0.05\bar{u}^2R^{1.5}\left(\frac{\Delta\zeta}{\Delta x}\right)^{1.5}B}{(s-1)^2\sqrt{gd_{50}}} \quad (2.5)$$

The median grain size  $d_{50}$  is obtained from Table 2.4.

**Table 2.5** Sediment transport rates and morphological time scales.

	Hagmolen-beek	Lunterse beek	Tungelroyse beek
Sediment transport $\tilde{Q}_s$ ( $\text{m}^3 \text{ year}^{-1}$ )	123	332	299
Morphological time scale $T$ (year)	20.3	36.9	6.5

The morphological time scale is estimated by adopting a characteristic length scale of 2 km, which is an estimate of the average length of stream restoration project in the Netherlands. For the Tungelroyse beek, this length is within the range where flow may be nonuniform ( $L < 3R/i_b$ ), limiting the applicability of the parabolic model in a strict sense. Despite this, the results offer an estimation of the characteristic response time for lowland streams, that can be used in a qualitative manner. Table 2.5 lists the yearly sediment transport and morphological time scale for the streams under study. Yearly sediment transport rates were similar for the three streams. The morphological time scales of the three streams are in the order of years to decades. These results suggest that longitudinal channel bed may adjust to a new equilibrium within years after implementation of stream restoration measures in lowland streams.

Table 2.1 lists the principles used in the design of the three studied streams. The ecological constraints include minimum and maximum flow velocity and water depth values, which reflect the abiotic conditions relevant for the typical benthic ecology. The ecological constraints differ per season. The time-averaged values for the cross-sectional average flow velocity and water depth were estimated based on the discharge and water level time-series. In nearly all cases, the flow velocity conditions in the spring and in the summer are lower than the design values, with cross-sectional average flow velocities around  $0.07 \text{ m s}^{-1}$  in the Hagmolenbeek and around  $0.10 \text{ m s}^{-1}$  in the Lunterse beek and Tungelroyse beek. For winter conditions, these values increase to around  $0.10 \text{ m s}^{-1}$  in the Hagmolenbeek,  $0.18 \text{ m s}^{-1}$  in the Lunterse beek, and  $0.15 \text{ m s}^{-1}$  in Tungelroyse beek. The Tungelroyse beek is the only case meeting the design criterion for flow velocity in winter conditions. The water depths are evaluated for summer conditions only, averaging  $0.34 \text{ m}$  in the Hagmolenbeek,  $0.25 \text{ m}$  in the Lunterse beek, and  $0.79 \text{ m}$  in the Tungelroyse beek. The Lunterse beek is the case to meet the design criterion for water depth in summer conditions. These figures show the current design procedure to be deficient for the flow velocity and water depth targets and justifies a reconsideration of the design procedure for lowland stream restoration in the Netherlands.

## 2.6 Conclusions

Three stream restoration projects have been evaluated focusing on morphological developments over a two-year period. During this period, longitudinal and lateral channel adjustments have been observed. Longitudinal channel bed adjustments were significant in each of the three streams, and were related to exogenous influences. Hydraulic structures (e.g. bridges and weirs), channel width variation and heterogeneity of the channel substrate caused channel bed incision and aggradation, and consequently, channel slope adjustments. Lateral channel adjustments were only observed in a limited number channel bends. Bank erosion was related to floodplain heterogeneity, which may be considered an exogenous influence. Other lateral channel adjustments were the result of autogenous morphological processes, including point bar formation due to secondary flow. In several bends, deposition of sediment in the inner bend was observed, which was associated with bank erosion in a limited number of cases, resulting in asymmetrical cross-sectional profiles.

The fine sediment characteristics (median grain size 125-250  $\mu\text{m}$ ) and relatively small flow depths cause Shields stresses to exceed the Shields parameter for over 81% of the time. Despite this, no significant changes in sediment composition were observed, most likely resulting from uniformity of the prevailing sediment. At the habitat scale, changes occurred that may be related to the flow conditions, leading to the formation of a gravel bar and a silt bar. These observations are particularly relevant for the abiotic conditions for benthic ecology, showing that within 2-years' time natural processes may develop a habitat pattern in a restored lowland stream.

# 3 | Alternate Bars



---

Based on: EEKHOUT, J. P. C., HOITINK, A. J. F., & MOSELMAN, E. 2013. Field experiment on alternate bar development in a straight sand-bed stream. *Water Resources Research*, **49**, 8357-8369.

## 3.1 Introduction

Alternate bars in rivers and streams are an instability phenomenon related to differences in the characteristic length scales for the adjustment of flow and sediment transport to irregularities at the channel bed. The vast majority of the experimental support for the existing theory relies on laboratory experiments assuming a constant discharge. Field studies are rare, which causes the practical applicability of existing theory to remain largely unclear. Aiming to verify the predictive capacity of existing bar theory, here a large-scale field experiment is presented in which alternate bars form under variable discharge conditions.

A key parameter for the development of alternate bars is the width-to-depth ratio of the channel. Alternate bars occur only within a limited range of this ratio. Wider and shallower channels give rise to multiple bars, rather than alternate bars (Parker, 1976; Colombini & Tubino, 1990). Narrower and deeper channels do not produce any bars at all (Struiksma *et al.*, 1985). The range for alternate bars can be expected to cover higher width-to-depth ratios in systems of overall erosion and lower ratios in systems of overall sedimentation, because bed degradation reduces the number of bars at a given width-to-depth ratio, whereas bed aggradation increases the number of bars (Germanoski & Schumm, 1993). A linear stability analysis of the mathematical equations provides values of the temporal growth rate, the migration speed, the wavelength and the spatial damping factor for alternate bars at specific conditions of flow and sediment (Hansen, 1967; Callander, 1969; Blondeaux & Seminara, 1985; Struiksma *et al.*, 1985). Linear stability analysis provides information on how bar amplitudes change in time and space, but not on the values of the amplitudes themselves. The latter can be obtained from weakly nonlinear stability analysis (Colombini *et al.*, 1987; Schielen *et al.*, 1993). Theoretically, linear and weakly nonlinear stability analyses apply to infinitesimally small amplitudes only, but experimental findings show they work well for larger amplitudes.

Two special cases arise from two different simplifications of the general linear analysis. Hansen (1967), Callander (1969) and Blondeaux & Seminara (1985) assume that the spatial damping factor is equal to zero, so that all bars have the same height. This implies they assume an infinitely long channel without any influence from upstream or downstream boundaries. The alternate bars are supposed to start growing spontaneously at the same time everywhere, without any gradients in bar amplitude. The resulting migration speed and wavelength correspond to the bars with the largest temporal growth rate. The alternate bars of this first special case are called ‘migrating bars’, ‘migrating free bars’ or, less precisely but widespread,

'free bars'. Struiksma *et al.* (1985) assumed that the temporal growth rate and the migration rate are equal to zero, which means that the bars neither migrate nor grow or decay in time. This is assumed to correspond to bars that are induced by some local, non-migrating geometrical forcing, such as a transverse dam in part of the cross-section or an abrupt change in channel curvature. The alternate bars of this second special case are called 'steady bars', 'nonmigrating bars', 'spatial bars' or, less precisely but widespread, 'forced bars'. They are significantly longer than the migrating bars (Olesen, 1984) and offer an explanation for overdeepening or additional scour along the outer bank of river bends (Struiksma *et al.*, 1985; Parker & Johannesson, 1989). Both special cases assume a constant discharge, but Tubino (1991) extended the analysis of migrating bars to varying discharges. Tubino (1991) showed that bar amplitude varies in response to the rising and falling stages of a flood event. The weakly nonlinear theory predicts the final bar amplitude, after applying the theory to a sequence of typical flood events.

Both migrating bars and nonmigrating bars have been reproduced under laboratory conditions (e.g. Tubino, 1991; Lanzoni, 2000; Crosato *et al.*, 2011; Venditti *et al.*, 2012). Migrating bars occurred in laboratory experiments, even though Blondeaux and Seminara's condition of absent boundaries, or boundaries without any influence, were not met. Nonmigrating bars forced by a local geometrical forcing have also been reproduced in laboratory flumes. These laboratory experiments demonstrate that the equilibrium bed topography that is eventually reached, when the condition of small amplitudes is no longer satisfied, has more or less the same wavelength and spatial damping as the nonmigrating bar pattern formed initially from a flat bed (Struiksma *et al.*, 1985). Long-duration laboratory experiments by Crosato *et al.* (2011) show migrating bars to be transient features that eventually develop into nonmigrating bars if the discharge remains constant. The presence of nonmigrating bars suppresses migrating bars (Seminara & Tubino, 1989; Lisle *et al.*, 1991), but Crosato *et al.* (2011) argue, nonetheless, that migrating bars could be re-generated episodically if the discharge varies. The slowly evolving nonmigrating bars result most probably from geometrical forcing at the boundaries, because their generation requires a permanent nonmigrating forcing. The convective nature of alternate bars implies that the pattern would disappear from an infinitely long channel after removal of all local geometrical forcing (Defina, 2003; Federici & Seminara, 2003). Once a pattern of nonmigrating bars persists, each bar can be seen as a new nonmigrating forcing for the next bar downstream (and upstream in case of a super-resonant width-to-depth ratio). As a result, the bar amplitude eventually becomes uniform along the channel, irrespective of initial spatial variations (Crosato *et al.*, 2011).

### 3. Alternate Bars

The vast majority of the experimental support for the existing theory relies on laboratory experiments. Field studies are rare and add complexity to the river system by large discharge variations, bank erosion, heterogeneous sediment, vegetation development and changes in the longitudinal stream profile due to reach-scale erosion and sedimentation. One of the first to report on a field study on alternate bar behaviour was Lewin (1976), who investigated the development of alternate bars in a straightened gravel-bed stream (River Ystwyth, Wales) over a period of one year. His results are mainly qualitative, however, they give a good overview of the initial stages of bar development in a straight river channel. Welford (1994) presented a field experiment on alternate bar behaviour in a straightened gravel-bed stream (Embarra River, USA). He tested the alternate bar theory for unsteady flows of Tubino (1991) against the results of his field experiment. Welford (1994) concluded that the process of bar formation in his field experiment occurred under different flow conditions, and in a different manner than predicted by the Tubino (1991) model. Tubino *et al.* (1999) refer to Welford (1994) as a properly designed field prototype, concluding that in spite of its approximate character, which mainly resides in the assumption of weak unsteadiness, the model was able to replicate observed trends in bar amplitude and to reproduce the distinct lag between flow variability and bed response exhibited by field observations. Recently, Rodrigues *et al.* (2012) studied two migrating bars in a side channel of the river Loire (France). The side channel was only inundated during flood events. Rodrigues *et al.* (2012) showed the resulting morphodynamics for a single discharge peak, where bar migration was observed during the falling limb of the discharge peak. A field scale experiment was performed by (Venditti *et al.*, 2012, St. Anthony Falls Laboratory, Minneapolis, USA), focusing on alternate bar dynamics under varying sediment supply conditions. They showed that their nonmigrating bars vanished when the sediment supply was terminated. Until now, Welford (1994) remains the only field study that actually tested the applicability of existing bar theory.

Here, the results from a field experiment are presented, over a period of almost three years. The straight channel was allowed to evolve autogenously from initially flat bed conditions, subject to discharge variation, where alternate bars formed over a period of eight months after the start of the experiment. In this experiment bar elongation, bar migration, bar amplitude growth and subsequent bar decay were observed. These processes can be related to both migrating and nonmigrating bars, therefore, these field observations were compared with two lines of research. The predictive capacity for the case of migrating bars was evaluated with the theory of Tubino (1991) and for the case of nonmigrating bars with a simple physics-based predictor for the number of river bars (Crosato & Mosselman, 2009), which is based

on the nonmigrating bar theory by Struiksma *et al.* (1985).

## 3.2 Study Area

The stream under study is the Hooge Raam ( $51^{\circ} 42' 56''$  N,  $5^{\circ} 42' 7''$  E), a tributary of the river Meuse (Figure 3.1a). The catchment (Figure 3.1b) covers an area of 42.8 km<sup>2</sup>. The elevation within the catchment varies between 9 and 22 m above mean sea level. The stream can be characterized as a lowland stream. The average yearly precipitation amounts to 793 mm (KNMI, 2014). The subsurface of the catchment mainly consists of aeolian-sand deposits. The mean daily discharge is 0.22 m<sup>3</sup>s<sup>-1</sup> and the peak discharge in the study period was 5.67 m<sup>3</sup>s<sup>-1</sup> (Figure 3.2a).

In the summer of 2009, a stream restoration project was completed over a length of about 1 km (Figure 3.1c). The downstream part of the project was restored by constructing a sinuous channel pattern, based on the historical planform observed on maps dating from the period before straightening. Figure 3.1e shows the initial channel cross-section of this part of the channel. In the upstream part, a straight channel was created, with the purpose to study autogenous meander initiation. The length of this experimental reach is 600 m, with an initial channel slope of 1.8 m km<sup>-1</sup>. The channel had a constructed width of 7.5 m and a constructed depth of 0.4 m (Figure 3.1d). The design was based on general hydraulic geometry relations, established from a comprehensive dataset described in Church & Road (1983). The initial channel was constructed 1.2-1.6 m below ground level, due to the upstream and downstream connection with the existing incised channel bed. The initial profile of the cross-section featured a small floodplain section, which was considered too narrow. For this reason, the floodplain was lowered 660 days after the start of the experiment (Figure 3.1d), creating a better connectivity between the channel bed and the surrounding area, both from a morphological and an ecological perspective. The bed sediment consists of cohesionless fine sands, with a median grain size of 218 µm (Figure 3.2b).

## 3.3 Materials & Methods

The experimental reach has a length of 600 m. Figure 3.3 shows three aerial photos taken 225, 352 and 862 days after the start of the experiment. Water is flowing from the bottom to the top. The middle photo shows a regular pattern of alternate bars in the downstream part of the experimental reach. In the upstream part, however, dense vegetation growth resulted in an irregular bed morphology, without a clear

### 3. Alternate Bars

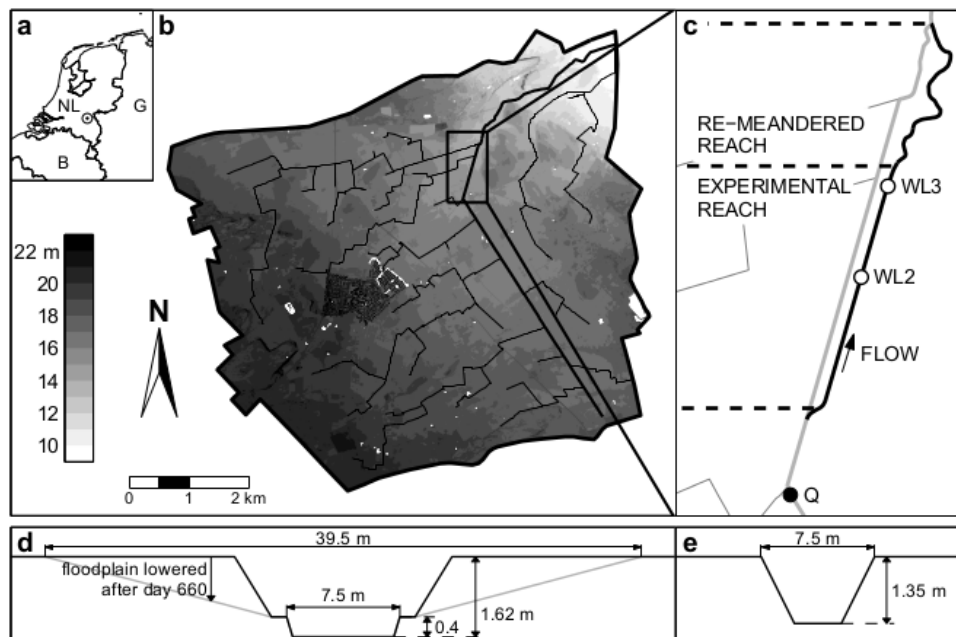


**Figure 3.1** Overview of the study area: (a) geographic location (b) digital elevation model of the catchment, (c) schematic diagram of the study area, where Q indicates the location of the discharge station and WL2 and WL3 the locations of the water level gauges, (d) design cross-section of the experimental reach, with in grey the floodplain after lowering, and (e) the design cross-section of the re-meandered reach.

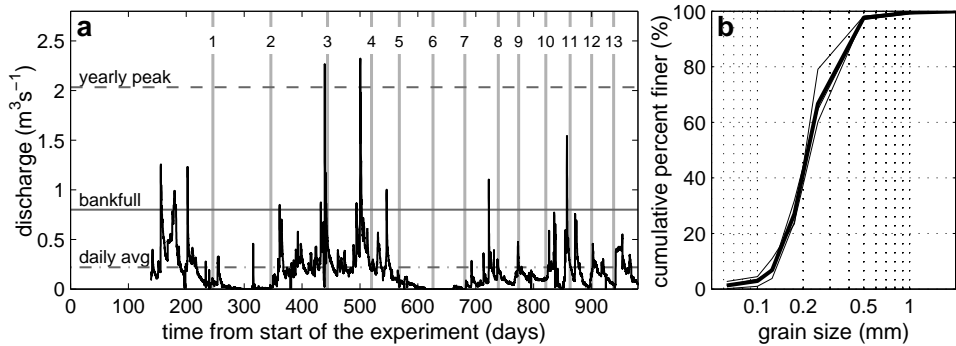


**Figure 3.2** (a) Discharge hydrograph of the channel under study. The grey horizontal lines denote the yearly peak discharge (dashed), bankfull discharge under initial constructed channel conditions (solid) and daily average discharge (dash-dotted). The 13 surveys are indicated with the grey vertical lines. (b) Grain size distributions from bed material samples, taken at 3 locations in the experimental reach. The bold line denotes the average from all three samples.



**Figure 3.3** Aerial photos of the experimental reach, taken at 225, 352 and 862 days after the start of the experiment. Water is flowing from the bottom to the top. The middle photo shows a clear difference between the vegetated area (upstream) and the regular pattern of alternate bars (downstream).

pattern of alternate bars. The dense vegetation in the upstream part emerged around 320-350 days after the start of the experiment (July 2010). The break in the development within the two parts of the experimental reach coincides with a border in land ownership. The sudden change in vegetation may relate to differential nutrient supply from the neighbouring agricultural lands. The analysis focusses on the morphodynamics of the downstream part, where alternate bars developed, initially unhindered by vegetation growth, over a length of 280 m. The entire 600 m of the experimental reach, including the upstream vegetated part, was surveyed twice, namely just after construction was completed and during the last survey.

Bed elevation data from 13 GPS-surveys were analysed. Bed elevation data were collected using Real Time Kinematic (RTK) GPS-equipment (Leica GPS 1200+). The RTK-GPS equipment measures a point in space with an accuracy of 1-2 cm. The number of points collected during each individual survey ranged from 600 to 2250, with an average of 1900 point measurements. Digital Elevation Models (DEMs) of each of the datasets were constructed. To do so, a Triangular Irregular Network (TIN) was made using Delaunay triangulation. Subsequently, the TIN was interpolated on a grid using nearest neighbour interpolation, with a grid spacing of 0.2 m. A grid was used to allow for a quantitative comparison among the serial DEMs. An anisotropy factor of 4 was used within the interpolation routine, to

### 3. Alternate Bars

account for the lower density of the collected data in the longitudinal direction. The anisotropy factor was derived by dividing the average distance between the cross-sections (2.8 m) by the average distance between the survey points in cross-sectional direction (0.7 m).

The temporal evolution of the alternate bars was studied by analysis of three geometrical variables, i.e. the bar wavelength, bar amplitude and longitudinal bar position. The latter was used to determine the bar migration speed. The bar wavelength and longitudinal bar position were evaluated based on longitudinal channel bed profiles. From these longitudinal channel bed profiles local extremes were derived, i.e. bar tops/troughs. This was done by first subtracting the average longitudinal channel bed slope from the bed topography data. Second, the data were filtered using a LOESS regression algorithm (Tate *et al.*, 2005).

The bar wavelength, bar position, bar top and bar trough are defined in Figure 3.4. Topographic data from the fifth field survey (day 520) are used in this example. The method was applied to the longitudinal profiles for both sides of the channel. In this example, the profile on the left side is shown. Figure 3.4a includes the measured longitudinal channel bed profile, the LOESS filtered longitudinal channel bed profile, and the channel gradient. Figure 3.4b shows the longitudinal channel bed profile after detrending the bed topography by removing the channel slope, in which zero-crossings can easily be detected. Figure 3.4b illustrates the adopted definitions of bar wavelength and longitudinal bar position. The bar wavelength is defined as the length between two successive bar troughs. The longitudinal bar position is defined by the center of gravity above the average channel slope, defined as:

$$pos_j = \frac{\sum_{\substack{s_{i,j}=Z_{2,j} \\ Z_{1,j}}}^{Z_{1,j}} (s_{i,j} - Z_{1,j}) \eta_{i,j} \Delta s}{\sum_{\substack{s_{i,j}=Z_{2,j} \\ Z_{1,j}}} \eta_{i,j} \Delta s} + Z_{1,j} \quad (3.1)$$

where  $pos_j$  is the location of bar  $j$ ,  $Z_{1,j}$  and  $Z_{2,j}$  are zero-crossings and  $s_{i,j}$  is the location of a certain cell  $i$  with elevation  $\eta_{i,j}$  and width  $\Delta s$ . The width  $\Delta s$  is equal to the grid spacing of 0.2 m.

The longitudinal bar position is used to determine the bar migration speed. The bar migration speed is determined by the bar migration distance divided by the time between two successive surveys ( $\Delta pos / \Delta t$ ). Bar elongation was observed during the experiment. Therefore, the resulting longitudinal bar growth was also determined, which is defined as the difference in bar wavelength between two successive surveys divided by the time between the two surveys ( $\Delta \lambda / \Delta t$ ).

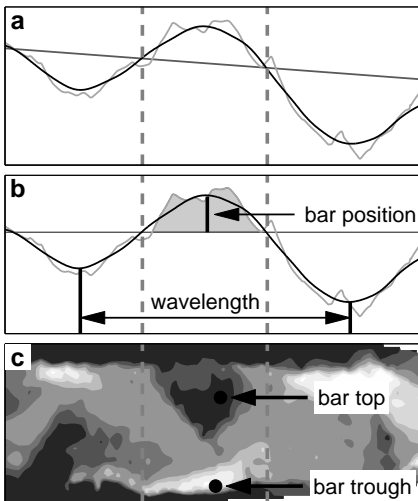


**Figure 3.4** Definition of bar characteristics, with an example of the fifth field survey (day 520): (a) the measured longitudinal channel bed profile on the left side of the channel (light grey), the longitudinal channel bed profile after applying the LOESS regression (black) and the channel gradient (dark grey), (b) detrended longitudinal channel bed profile and (c) bed topography data. Panel (b) gives definitions for bar wavelength and bar position. Panel (c) gives definitions for the locations of bar top and bar trough, their difference being the bar amplitude.

Figure 3.4c shows the bed topography from the fifth field survey. The bar amplitude is determined by the difference between the local maximum and local minimum, within the area between two zero crossings and the channel banks. The local maximum and local minimum represent the bar crest and bar trough of a particular bar, respectively.

Discharge data were collected upstream of the experimental reach at a discharge measurement weir, marked by Q in Figure 3.1c. The discharge measurement weir was operational from day 140 until the end of the experiment. Discharge data were collected with a one-hour frequency. Water level data were measured at two locations along the experimental channel, marked as WL2 and WL3 in Figure 3.1c, located at 325 and 547 m from the upstream end of the experimental reach, respectively. The water level gauges were operational from day 660 until the end of the experiment. Water level data were collected with a one-hour frequency. Longitudinal water level profiles were measured during 6 of the 13 surveys. During the eleventh field survey (day 863), a clear mark indicating the highest water level in the preceding period was observed. The date and time of this high-water event could be traced back from the measured water level time series at the two water level gauges.

### 3. Alternate Bars

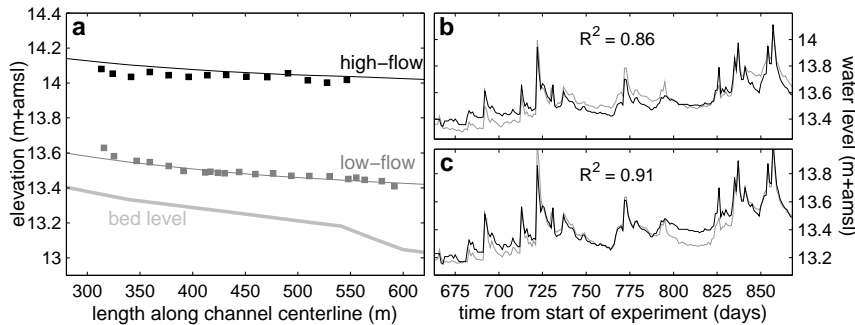


**Figure 3.5** Results from (a) model calibration and (b and c) model validation. The squares in panel (a) denote the measured water levels during the survey and the lines the modelled water levels. The thick light grey line denotes the bed level. Panels (b) and (c) show the validation results for the water level gauges WL2 and WL3, located at  $x = 325$  m and  $x = 547$  m, respectively. The grey lines represent the measured water levels and the black lines represent the modelled water levels.

The cross-sectional average flow velocity in the experimental reach was obtained from discharge and an estimation of hydraulic roughness, using a model implementation of the Saint Venant equations (SOBEK Channel flow, Deltares, 2011). Longitudinal water level measurements revealed an M1-backwater curve (see Figure 3.5a), caused by the narrower cross-sectional shape near the downstream end of the study reach (compare Figure 3.1d and 3.1e). The backwater curve causes the flow velocities to slightly decrease in the downstream direction.

In the hydrodynamic modelling exercise, the temporal changes of the channel dimensions were taken into account, i.e. variation of the channel slope and the floodplain lowering after day 660. Discharge was imposed at the upstream boundary and water level at the downstream boundary. The hydrodynamic model was calibrated using measured longitudinal water level profiles. A low-flow case (day 774,  $Q = 0.22 \text{ m}^3\text{s}^{-1}$ ) and a high-flow case (high-water mark at day 857,  $Q = 1.73 \text{ m}^3\text{s}^{-1}$ ) were selected from the available observed longitudinal water level profiles. The calibration was performed by adjusting the bed and floodplain roughness values, which yielded optimal Chézy values of 13 and  $10 \text{ m}^{1/2}\text{s}^{-1}$ , respectively. The Chézy value in the floodplain was attributed a lower value to represent the presence of vegetation. Figure 3.5a shows the results of the calibration procedure. The hydrodynamic model was validated using the measured water level time series (Figures 3.5b and 3.5c). The modelled water level time series at both locations compare well with the measurements ( $R^2 = 0.86$  for the upstream and  $R^2 = 0.91$  for the downstream location). Both panels show the highest degree of agreement during periods of high flow. Low flows are either under- or over-predicted.

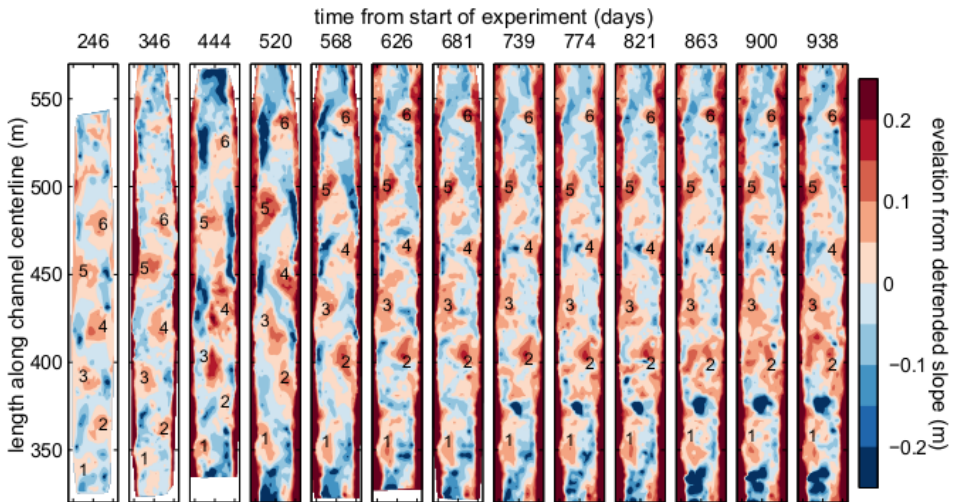


**Figure 3.6** Detrended bed topography data from the 13 GPS-surveys. The numbers indicate the location of the six individual bars. Water is flowing from bottom to top.

## 3.4 Experimental Results

First, the results from the 13 morphological surveys are presented. The first survey was performed 246 days after the start of the experiment. Figure 3.6 shows the bed topography data of the morphological surveys. For the first five surveys, the individual bars can be distinguished relatively easily. At the fifth survey, a more or less sinuous thalweg appears in the channel. The alternate bars grow both in length and in amplitude in the first five surveys. As time evolves, the morphology of the channel increases in complexity. The alternate bars become repeatedly connected and disconnected from each other, and from day 739 onwards several scour holes appear in the channel in the upstream part of the experimental reach, around 325 m and 380 m from the upstream end of the study reach.

In total, six bars were identified that appear in the data from the 13 surveys, i.e. three on the left side and three on the right side of the channel. The most downstream bar was excluded from the analysis, because it was possibly affected by the downstream boundary. Figure 3.7 shows the temporal evolution of the bar wavelength (a), bar amplitude (b), bar migration (c) and bar elongation (d). The bar wavelength initially increases in time up until the fifth survey, after which an equilibrium wavelength is reached, averaging 75.7 m. The evolution of the bar amplitude is more irregular. The bar amplitude decreases from the first to the second survey and increases from the second to the fourth survey. At the fourth

### 3. Alternate Bars

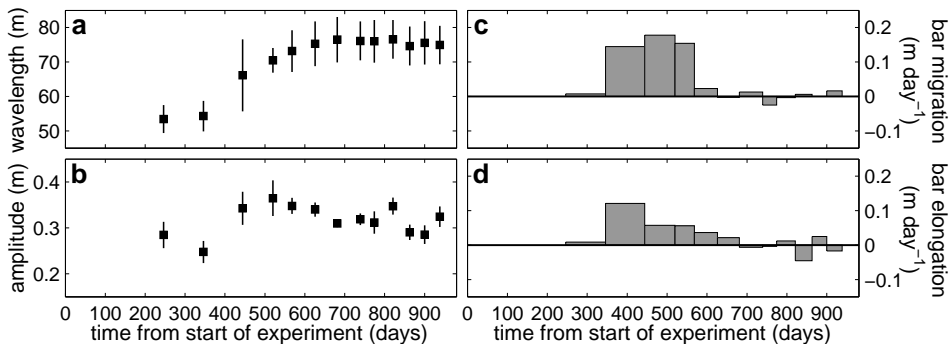


**Figure 3.7** Evolution of (a) the average bar wavelength, (b) the average bar amplitude, (c) bar migration, and (d) bar elongation. The length of the error bars in panels (a) and (b) are defined as the standard deviation divided by the square root of the number of bars ( $\sigma/\sqrt{n}$ ).

survey, the maximum average bar amplitude is reached, amounting to 38.3 cm. After the fourth survey, a downward sloping trend is visible, with slight increases of bar amplitude only around the 10th and 13th surveys. The latter is mainly caused by the irregular topography at the end of the experiment (Figure 3.6), which complicated the identification of local extremes, needed to describe the bar tops and bar troughs.

Figure 3.7c shows bar migration occurred especially between day 346 and day 568, with an average bar migration speed of  $0.17 \text{ m day}^{-1}$  in this period. Bar elongation (Figure 3.7d) was restricted to the period between day 346 and day 681. This period of bar elongation largely overlaps the period of bar migration. In addition, bar migration rates are of the same order of magnitude as the bar elongation rates. The observed bar migration are arguably interpreted as a side effect of bar elongation, rather than actual bar migration.

Figure 3.8a shows the average cross-sectional bed level for the experimental reach, just after construction was realized (day 0) and at the end of the experiment (day 938). The figure shows an overall decline of the bed slope. Where the longitudinal profile initially had an average slope of  $1.8 \text{ m km}^{-1}$ , it decreased to  $0.9 \text{ m km}^{-1}$  after 938 days. Figure 3.8b shows the development of the channel slope in the downstream part of the experimental reach. The channel slope decline occurred gradually from the start of the experiment until day 520, after which it stabilized. The channel slope decline is most probably caused by a backwater effect, which were observed during several morphological surveys. The right most aerial photo of Figure 3.3 shows that at the downstream end of the experimental reach (upper part of the photo) water inundates the floodplain, as a result of the backwater effects.

Figure 3.9 shows cross-sections at successive bar tops, for surveys carried out

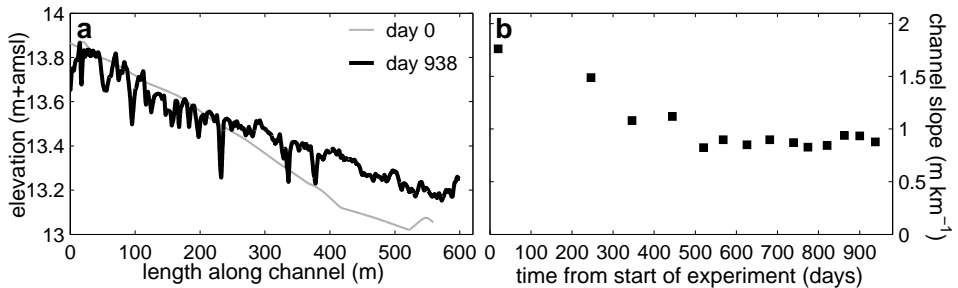


**Figure 3.8** (a) The longitudinal channel bed profile just after construction (gray) and after 938 days from the start of the experiment (black). The black line shows increased bed levels in the downstream part of the channel, causing a reduction of the longitudinal channel bed slope. (b) The temporal evolution of the channel slope in the downstream part of the experimental reach.

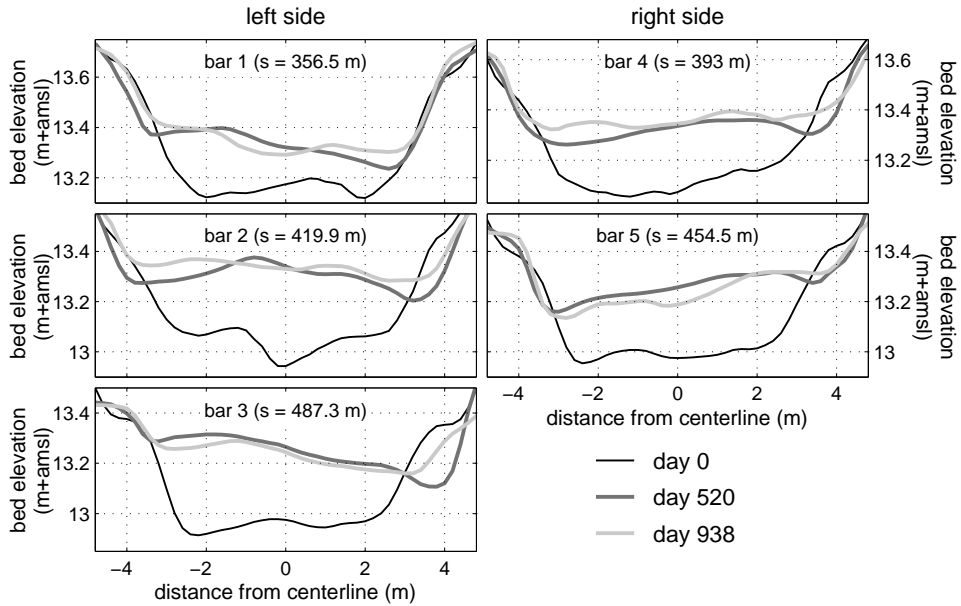
immediately after construction of the stream, at day 520 and at day 938. All panels show both aggradation of the channel bed and erosion of the channel banks from the start of the experiment until day 520. Aggradation of the bed is most apparent for the bars located in the downstream section of the experimental reach, summing up to 0.30 m for both bars 2 and 3. Erosion of the channel banks is apparent at all individual bar locations. Channel bank erosion shows the highest rates for bar 3, which amounts to more than 1 m over 520 days. Morphological changes between days 520 and 938 are mainly restricted to sedimentation of the bar troughs, up to 0.10 m for bar 3. This holds for all bars except for bar 5, which hardly shows any morphological change between days 520 and 938. Sedimentation of the bar troughs explains the decrease of bar amplitude, as shown in Figure 3.7b.

Table 3.1 summarizes some of the results obtained from the field experiment. Both the average discharge and the average water depth reflect the seasonal variation, as shown in Figure 3.2a. The response of the flow to the declining channel slope is mainly reflected in the average flow velocity and average Shields parameter. Each of these three flow characteristics show decreasing values in response to the declining channel slope.

## 3.5 Predictive Capacity of Bar Theory

Theoretical models by Tubino (1991) and Struiksma *et al.* (1985) have the potential to predict the occurrence of migrating bars and nonmigrating bars, respectively. The input for both models is basically restricted to flow velocity, grain size, channel width, channel depth, and channel slope. The bar models were applied by adopting

### 3. Alternate Bars



**Figure 3.9** Channel cross-sections at each of the five bars from three surveys: just after construction (black), at day 520 (dark grey) and at day 938 (light grey). The figure shows sedimentation over the full width of the channel from the start of the experiment. Additionally, sediment is deposited in the bar troughs in the period between day 520 and day 938.

**Table 3.1** Characteristics from the periods between the 13 successive surveys.

from - to (days)	discharge <sup>a</sup> ( $\text{m}^3\text{s}^{-1}$ )	water depth <sup>a</sup> (m)	flow velocity <sup>a,b</sup> ( $\text{m s}^{-1}$ )	channel slope ( $\text{m km}^{-1}$ )	Shields stress <sup>a,c</sup> (-)	wd-ratio <sup>d</sup> (-)
0 - 246	0.29	0.27	0.17	1.80	1.36	18.6
246 - 346	0.02	0.04	0.14	1.49	0.17	19.7
346 - 444	0.26	0.26	0.14	1.08	0.78	16.8
444 - 520	0.34	0.31	0.15	1.12	0.97	17.0
520 - 568	0.23	0.28	0.11	0.82	0.64	14.8
568 - 626	0.04	0.07	0.09	0.90	0.18	15.1
626 - 681	0.00	0.01	0.02	0.85	0.03	15.5
681 - 739	0.11	0.16	0.10	0.90	0.39	15.6
739 - 774	0.11	0.17	0.11	0.87	0.41	15.8
774 - 821	0.13	0.23	0.12	0.83	0.52	15.5
821 - 863	0.21	0.36	0.13	0.84	0.85	15.6
863 - 900	0.16	0.21	0.11	0.94	0.54	15.2
900 - 938	0.16	0.21	0.12	0.94	0.56	15.5

<sup>a</sup> time-averaged

<sup>b</sup> from 1D-flow model

<sup>c</sup>  $\theta = \tau/C^2 d_{50} s$ , with  $\tau = u^2 \rho g / C^2$ ,  $C = 13 \text{ m}^{1/2} \text{s}^{-1}$ ,  $d_{50} = 218 \mu\text{m}$  and  $s = 1.65$

<sup>d</sup> width-to-depth ratio, determined at bankfull discharge (constr. channel),  $Q = 0.8 \text{ m}^3 \text{s}^{-1}$

the reach-average flow velocities obtained from the 1D-flow model. Since both theoretical models assume uniform flow conditions, the application to the gradually varied flow of this case may seem inconsistent, but the observed rhythmic pattern of the five retained alternate bars does not show any systematic trends that can be interpreted as signs of a backwater effect.

### 3.5.1 Theory by Tubino (1991)

The model of Tubino (1991) simulates migrating bar development in response to a varying discharge. The model predicts bar dynamics under unsteady flow conditions. Here, the analysis is limited to the temporal dynamics of the unsteadiness parameter  $\tilde{U}$ , which is directly linked to the occurrence of migrating bars. This results in a quasi-steady analysis, in which a reference state was defined for each of the 13 surveys separately. The reference state is defined by three dimensionless parameters, i.e. the mean width-to-depth ratio  $\tilde{\beta}$ , the mean roughness parameter  $\tilde{d}_{50}$ , and the mean Shields parameter  $\tilde{\theta}$  (dimensionless variables are denoted with a tilde):

$$\tilde{\beta} = \frac{0.5B}{\bar{h}_0} \quad (3.2)$$

$$\tilde{d}_{50} = \frac{d_{50}}{\bar{h}_0} \quad (3.3)$$

$$\tilde{\theta} = \frac{S}{s\tilde{d}_{50}} \quad (3.4)$$

where  $B$  is the width of the channel,  $\bar{h}_0$  is the reach-averaged flow depth (in the reference state),  $d_{50}$  is the median grain size,  $S$  is the bed slope, and  $s = (\rho_s - \rho)/\rho$  is the relative submerged specific gravity of the sediment. For the case study presented here,  $B = 7.5$  m and  $d_{50} = 218 \mu\text{m}$  are assumed.

The reference state is selected by choosing a set of parameters satisfying the following two conditions:

$$\tilde{\varepsilon}(\tilde{\theta}, \tilde{d}_{50}) = \frac{\tilde{\beta} - \tilde{\beta}_c(\tilde{\theta}, \tilde{d}_{50})}{\tilde{\beta}_c(\tilde{\theta}, \tilde{d}_{50})} = \tilde{\delta} \quad (3.5)$$

$$\tilde{q}_{th}(\tilde{\theta}, \tilde{d}_{50}) = \frac{q_{th}}{\bar{q}_0(\tilde{\theta}, \tilde{d}_{50})} = 1 - \tilde{\delta} \quad (3.6)$$

where  $\tilde{\varepsilon}$  and  $\tilde{\delta}$  are perturbation parameters,  $\tilde{\beta}_c(\tilde{\theta}, \tilde{d}_{50})$  is the critical value of the width-to-depth ratio for the formation of migrating alternate bars,  $\bar{q}_0(\tilde{\theta}, \tilde{d}_{50})$  is the average flow discharge per unit width,  $q_{th}$  is the minimum value of  $\bar{q}_0(\tilde{\theta}, \tilde{d}_{50})$ , and  $\tilde{q}_{th}(\tilde{\theta}, \tilde{d}_{50})$  is the dimensionless value of  $q_{th}$ .

### 3. Alternate Bars

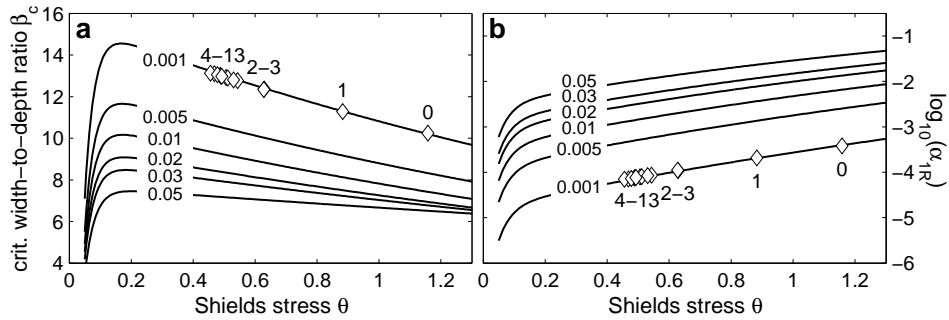


**Figure 3.10** (a) The critical value of the width-to-depth ratio  $\tilde{\beta}_c$  above which migrating bars can develop. (b) The linear growth rate of bar amplitude on the slow time scale associated with bar development  $\tilde{\alpha}_{1R}$ . Both  $\tilde{\beta}_c$  and  $\tilde{\alpha}_{1R}$  are plotted against the Shields stress  $\tilde{\theta}$  for six values of the roughness parameter  $\tilde{d}_{50}$ . The markers  $\diamond$  show the values for  $\tilde{\beta}_c$  and  $\tilde{\alpha}_{1R}$ , which were obtained for the constructed conditions (0) and conditions for each survey (1-13). Solid lines are adopted from Tubino (1991);  $\tilde{\beta}_c$  and  $\tilde{\alpha}_{1R}$  are extrapolated for the Shields stress  $\tilde{\theta} > 0.5$ .

Values of  $\tilde{\beta}_c$  are obtained from Figure 3.10a, which shows  $\tilde{\beta}_c$  as a function of  $\tilde{\theta}$  and  $\tilde{d}_{50}$  based on the idealized model. The minimum value of the discharge was used, because the flow conditions nearly permanently exceed the threshold for sediment motion. From the discharge time series, 13 flood waves were identified, with peak values exceeding  $0.8 \text{ m}^3\text{s}^{-1}$ , i.e. the bankfull discharge under constructed channel conditions (at day 0). Accordingly,  $q_{th}$  was set to the minimum discharge recorded during these flood waves, which amounted to  $Q_{\min} = 0.064 \text{ m}^3\text{s}^{-1}$ , and hence,  $q_{th} = Q_{\min}/0.5B = 0.017 \text{ m}^2\text{s}^{-1}$ .

The unsteadiness of the flow and morphology can be quantified based on the unsteadiness parameter  $\tilde{U}$ , which is defined as:

$$\tilde{U} = \frac{\tilde{\sigma}}{\tilde{\varepsilon}\tilde{\alpha}_{1R}} \quad (3.7)$$

where  $\tilde{\sigma}$  is the dimensionless angular frequency of the flood wave and  $\tilde{\alpha}_{1R}$  the linear growth rate of bar amplitude on the slow time scale associated with bar development. The dimensionless angular frequency of the flood wave  $\tilde{\sigma}$  is expressed as a ratio between the average travel time along the channel reach and the characteristic period of the flood, defined as:

$$\tilde{\sigma} = \frac{\sigma 0.5B}{\bar{u}_0} \quad (3.8)$$

where  $\sigma = 2\pi/\tau$  is the angular frequency of the flood wave, with  $\tau$  the characteristic rise time of the flood wave, and  $\bar{u}$  is the reach-averaged flow velocity, derived from the 1D-flow model results. The characteristic rise time of the flood wave was derived from the discharge time series. From the 13 selected flood waves, the average rise

time amounted to 22 h. The linear growth rate of the bar amplitude  $\tilde{\alpha}_{1R}$  is obtained from Figure 3.10b, which shows  $\tilde{\alpha}_{1R}$  for different values of both  $\tilde{\theta}$  and  $\tilde{d}_{50}$ .

Figure 3.11a shows the unsteadiness parameter  $\tilde{U}$  for all surveys. For each survey the bed slope  $S$  was obtained and the 1D-flow model results and reference conditions, defined by equations 3.5 and 3.6, were used to obtain  $\bar{u}_0$  and  $\bar{h}_0$ . Positive/negative values of  $\tilde{U}$  are controlled by the perturbation parameter  $\tilde{\varepsilon}$ , since  $\tilde{\sigma}$  and  $\tilde{\alpha}_{1R}$  are always positive. The perturbation parameter  $\tilde{\varepsilon}$  becomes positive/negative when  $\tilde{\beta}$  is larger/smaller than  $\tilde{\beta}_c(\tilde{\theta}, \tilde{d}_{50})$ , which corresponds to the unstable/stable regime, respectively. The unstable regime corresponds to conditions where migrating bars develop. The stable regime corresponds to conditions where migrating bars do not develop or vanish. In the unstable regime, three subregimes can be identified based on  $\tilde{U}$ , controlled by the dimensionless angular frequency of the flood wave  $\tilde{\sigma}$ : (1)  $\tilde{U} \sim \mathcal{O}(1)$ , bar development is affected by flow unsteadiness; (2)  $\tilde{U} \gg 1$ , bars develop on a much longer time scale than that associated with the flow unsteadiness; (3)  $\tilde{U} \ll 1$ , bars develop on a much shorter time scale than that associated with the flow unsteadiness.

Figure 3.11a shows that the unsteadiness parameter was positive during all surveys, corresponding to the migrating bar regime. Immediately after construction of the channel, conditions corresponded to the first subregime, i.e.  $\tilde{U} \sim \mathcal{O}(1)$ . This implies that at the start of the experiment, the time scale of migrating bar development was expected to be similar to the time scale of flow variation. Soon after construction, conditions gradually developed towards the second regime, i.e.  $\tilde{U} \gg 1$ , in which the time scale of migrating bar development is larger than the characteristic time scale of flow variation.

Here, the analysis is restricted to the unsteadiness parameter, whereas the theory by Tubino also presents expressions for bar amplitude and bar wavelength. Efforts to quantify bar amplitude and bar wavelength were hampered by: (1) the apparent focus on gravel-bed rivers, which explains the limited Shields domain for which results are presented ( $\tilde{\theta} < 0.5$ ), and (2) the lack of information on the imaginary parts of the model parameters.

### 3.5.2 Theory by Struiksma *et al.* (1985) and Crosato & Mosselman (2009)

The physics-based second-order linear model by Struiksma *et al.* (1985) predicts wavelength and spatial damping of bar formation. Struiksma *et al.* (1985) assumed that the temporal growth rate and the migration rate are equal to zero. The theory was applied using the same parameter values as in the Tubino model, except for the discharge, by adopting bankfull discharge conditions, following Crosato & Mos-

### 3. Alternate Bars

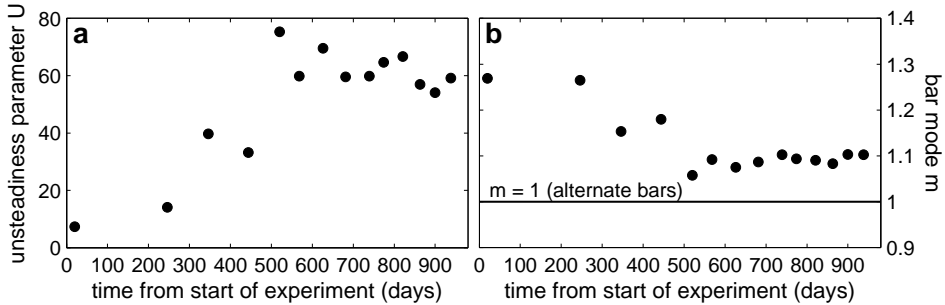


**Figure 3.11** Temporal evolution of: (a) the unsteadiness parameter  $\tilde{U}$  and (b) the bar mode  $m$ .

selman (2009), and except for the bed slope effect on sediment transport direction, by employing formulations by Talmon *et al.* (1995).

The bar regime can be computed adopting the longitudinal damping coefficient of nonmigrating bars  $L_D$ . The system complies with Blondeaux and Seminara's resonant conditions when this coefficient equals zero. When the coefficient is positive/negative, the system is sub-resonant/super-resonant, respectively. The longitudinal damping coefficient reads:

$$\frac{\lambda_w}{L_D} = \frac{1}{2} \left( \frac{\lambda_w}{\lambda_s} - \frac{b-3}{2} \right) \quad (3.9)$$

where  $\lambda_w$  is the adaptation length of the flow,  $\lambda_s$  is the adaptation length of a bed disturbance and  $b$  is the degree of nonlinearity in the relation between sediment transport and depth-averaged flow velocity, which is equal to the exponent in case of a power law dependence  $q_s \propto u^b$ . A value  $b = 4$  was attributed, corresponding to a value used for sand-bed rivers, following Crosato & Mosselman (2009) and Kleinhans & van den Berg (2011).

The adaptation length of the flow  $\lambda_w$  characterizes the longitudinal distance needed for the decay of perturbations in the transverse distribution of flow velocity, generated by an upstream disturbance. The adaptation length for the flow is formulated as:

$$\lambda_w = \frac{\bar{h}_0}{2C_f} \quad (3.10)$$

where  $C_f$  is the friction factor defined by  $C_f = g/C^2$ , in which  $g = 9.81 \text{ m s}^{-2}$  is the gravitational acceleration in the Netherlands and  $C$  the Chézy coefficient set to  $13 \text{ m}^{1/2}\text{s}^{-1}$ , which is adopted from the 1D-flow model.

The adaptation length of a bed perturbation  $\lambda_s$  characterizes the longitudinal distance needed for the decay of perturbations in the lateral water depth profile

created by an upstream disturbance, which is defined as:

$$\lambda_s = \frac{1}{\pi^2} h_0 \left( \frac{B}{\bar{h}_0} \right)^2 f(\theta_0) \quad (3.11)$$

where  $f(\theta_0)$  accounts for the effect of gravity on the direction of sediment transport over transverse bed slopes, which is formulated as (Talmon *et al.*, 1995):

$$f(\theta_0) = 9 \left( \frac{d_{50}}{\bar{h}_0} \right)^{0.3} \sqrt{\theta_0} \quad (3.12)$$

where  $\theta_0$  is the reach-averaged value of the Shields stress, defined by:

$$\theta_0 = \frac{\bar{u}^2}{C^2 s d_{50}} \quad (3.13)$$

The wavelength of nonmigrating bars  $L_P$  is formulated as follows:

$$\frac{2\pi}{L_P} = \frac{1}{\lambda_w} \left( \frac{\lambda_w}{\lambda_s} - \left( \frac{\lambda_w}{L_D} \right)^2 \right)^{1/2} \quad (3.14)$$

Crosato & Mosselman (2009) derived a predictor for the number of bars per cross-section from the theory by Struiksma *et al.* (1985). For a river with a width-to-depth ratio  $\beta$ , the bar mode  $m$  of the incipient bars can be determined by:

$$m = \frac{\beta}{\pi} \sqrt{(b-3)f(\theta_0)C_f} \quad (3.15)$$

where the nearest integer of bar mode  $m$  relates to the most probable number of bars per cross-section. A bar mode  $0.5 < m \leq 1.5$  suggests a series of alternate bars.

Figure 3.11b shows the results for the bar mode  $m$ , which describes the bar regime. Equation 3.15 predicts values around 1, which corresponds to a bar mode with alternate bars. The temporal evolution of  $m$  shows a decreasing likelihood of the development of nonmigrating bars, which is shown in Figure 3.11b by a decrease of  $m$ . Similar to the results from the Tubino model, this is mainly caused by the decreasing channel slope.

## 3.6 Discussion

The first stages of bar development in the experiment show strong similarities with the field description by Lewin (1976) and the numerical model results of Defina (2003). Lewin (1976) offers a clear view on the first stages of bar growth in a coarse grained channel bed. He showed that initially, alternate bars developed with bar wavelengths corresponding to 3 times the channel width. In a subsequent stage,

### 3. Alternate Bars

these bars developed into alternate bars with a wavelength of 7.5 times the channel width. The alternate bars migrated in downstream direction during exceptionally high flows. The evolution of the bar amplitude was not reported. Defina (2003) developed a numerical model to study alternate bar dynamics and applied the model to the steady flow experiments described by Lanzoni (2000), showing initial bar elongation and an increase of bar amplitude. The results show that especially bar amplitude developed towards an equilibrium value. Figure 3.12 presents a cartoon summarizing the wavelength, amplitude and migration development of the bars in the present experiment. Combining results from Lewin (1976), Defina (2003) and this study, which feature contrasting conditions of bar material, elongation of alternate bars may be a general feature occurring in the initial stages of bar development.

The bar development summarized in Figure 3.12 is markedly different from the results presented by Welford (1994). Welford (1994) showed migrating bars formed during the falling limb of a single discharge peak, which vanished during the subsequent periods of low flow. Alternate bars developed sequentially, rather than uniformly, as in this experiment. Welford (1994) classified the discharge regime in the straightened section of the Emberras River based on an annual coefficient of flow variation (Poff & Ward, 1989). The latter coefficient amounted to 52.6, which classified the discharge regime in the transition between intermittent runoff and perennial runoff. In the case of the Hooge Raam, the annual coefficient of flow variation amounts to 119.5, corresponding to an intermittent flashy to harsh intermittent discharge regime. While Welford (1994) classified the flow variability in the system as fairly high, in this case the flow variability was even higher. In the Tubino model, this flow variability is captured in the characteristic rise time of the flood wave. A flashy discharge regime with high flow variability results in short rise times. This causes an increase of the unsteadiness parameter  $\tilde{U}$ , which reduces the likelihood of the occurrence of migrating bars. In this field case, this corollary may explain the absence of migrating bars. Flashy discharge hydrographs are typical for highly modified lowland catchments, like in The Netherlands. Migrating bars are not likely to appear under these conditions.

Despite several differences in the underlying assumptions, the theoretical models by Tubino (1991) and Struiksma *et al.* (1985) both contain a capacity to predict the main bar developments as observed. Both models predict the occurrence of alternate bars immediately after construction of the channel, and both models predict that the conditions for the bars to prevail become increasingly unfavourable in time. Migrating bars are characterized by a smaller wavelength compared to nonmigrating bars and are typically migrating in the downstream direction. The

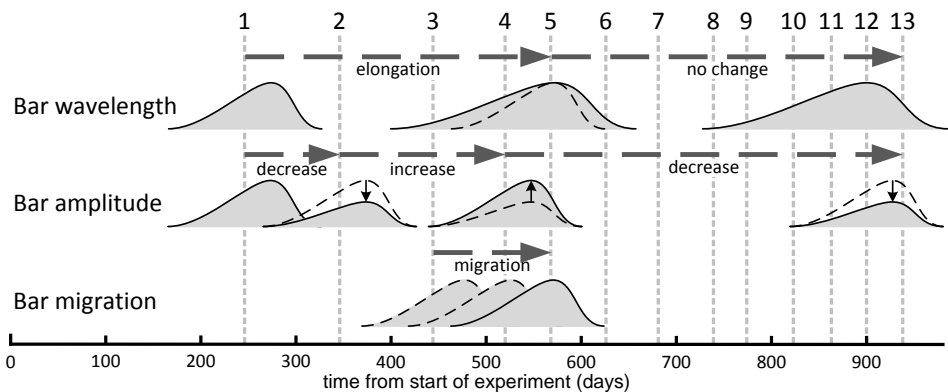


**Figure 3.12** Schematic diagram of the temporal evolution of bar wavelength, bar amplitude and bar migration.

laboratory experiments described in Tubino (1991), used to validate the model, show migration speeds of about 10 bar wavelengths per day. Migration speeds of 0.17 meter per day were observed, which is equal to  $3 \cdot 10^{-3}$  bar wavelengths per day. These small migration rates and the coincidence between bar migration and bar elongation suggest that the alternate bars can be classified as nonmigrating. It is plausible that migrating bars have triggered the start of bar development in the initial stage of the experiment. From the second survey onwards, the Tubino model predicts the time-scale of migrating bar development to become much larger than the time scale of the flow variation ( $\tilde{U} \gg 1$ ). The model may be correct in reproducing the observation, but the information available is insufficient to establish the model performance rigorously.

The results from this field experiment show an initially regular alternate bar pattern until halfway the experiment. In the second half of the experiment, the regular bar pattern evolved to become irregular. To quantify the increased irregularity of the bed topography, the raw bed elevation data was subtracted from the filtered elevation data. Figure 3.13 shows an increase of the standard deviation of these residuals from around 0.020 m to 0.035 m. Arguably, the bed forms in the final stages of the experiment are merely relics from initially regular bar pattern. Figure 3.14 shows how vegetation cover increases towards the end of the experiment. The vegetation cover on the bars may be responsible for stabilizing the initial bar pattern.

The Crosato and Mosselman model predicts the development of nonmigrating alternate bars throughout the experiment, with values for bar mode  $m$  around 1, suggesting bars to prevail during the entire experiment. The bar mode  $m$  shows a tendency to decrease towards  $m = 1$ , caused by the declining channel slope. This

### 3. Alternate Bars

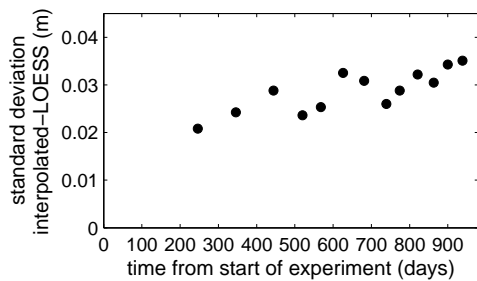


**Figure 3.13** Standard deviation of the difference between the raw bed elevation data and corresponding LOESS filtered data.

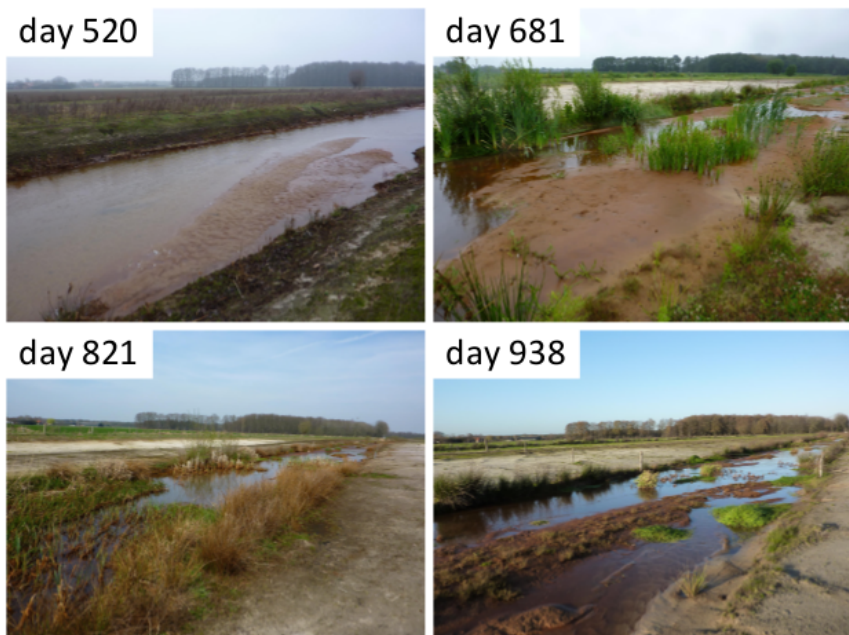


**Figure 3.14** Photos of alternate bar 2, taken at 520, 681, 821 and 938 days after the start of the experiment.

could be interpreted as a decreasing likelihood of alternate bar development. In a recent study, Venditti *et al.* (2012) showed that termination of upstream sediment supply caused alternate bars to disappear, both under laboratory and field conditions. In their field experiment, the channel slope reduced to half the initial value, with the main longitudinal adjustment being upstream erosion. In this experiment, channel slope decline was mainly caused by downstream deposition of sediment. The end result is similar for both cases: a decreased regularity of the initial alternate bar pattern.

The theoretical bar models applied in this case study assume uniform flow and channel bed conditions. The field results show that these conditions were not met during the entire study period. A backwater effect is held responsible for the declining bed slope, hence, flow was not uniform over the whole length of the experimental reach. Besides, the experimental reach was subject to a flashy discharge hydrograph. Most of the time, the flow conditions did not correspond to the average flow conditions, as used in the two bar theories. Furthermore, the vegetated upstream part of the experimental reach may have had an influence on the sediment supply to the downstream part. These constraints may have influenced bar dynamics and may also explain the deviation between field observations and model results, near the end of the experiment. A logical next step would be to apply a numerical model to this case study, to study these constraints in more detail.

## 3.7 Conclusions

This chapter presents the results from a field experiment where alternate bars developed within eight months after the start of the experiment. From the obtained field data a sharp view on the initial increase of bar wavelength and bar amplitude was obtained. These findings are consistent with existing field studies on alternate bars, suggesting that the growth and elongation of alternate bars may be a general feature occurring in the initial stages of bar development. A period of bar migration was recorded, which coincided with the period of bar elongation. The migration rates were several orders of magnitude smaller than those presented previously in laboratory experiments. This suggests the observed alternate bars can be classified as nonmigrating bars, rather than migrating bars.

Using the obtained dataset, the predictive capacity of two bar theories was established: (1) the theory by Tubino (1991) for migrating bars and (2) the theory by Struiksma *et al.* (1985) and Crosato & Mosselman (2009) for nonmigrating bars. Both theories predicted the occurrence of alternate bars under the constructed channel conditions. Halfway the experiment, the regular pattern of alternate bars

### 3. Alternate Bars

evolved into an irregular bed topography, and bar amplitudes were subject to decline. The two bar theories correctly predicted a decreasing likelihood of alternate bars throughout the experiment, mainly caused by the decline in channel slope that occurred in the first half of the experiment.

The common practice in lowland stream restoration is the construction of a sinuous planform, with the aim of increasing the spatial flow variability, which is considered crucial for the abiotic conditions for benthic ecology. Alternate bars potentially have the same effect on the flow and are therefore sometimes considered to be an alternative, for the common practice within lowland stream restoration. This study shows that the initial conditions, controlled by the channel slope, were favourable for the formation of alternate bars. A backwater curve, due to a narrow cross-sectional shape near the downstream end of the study reach, caused the channel slope to decline. After the channel slope declined, the conditions promoting bar development vanished. As a consequence, the regular pattern of alternate bars disappeared. The final channel slope of the presented case study is at the upper end of the range of slopes occurring in lowland streams. Therefore, stream restoration practitioners in lowland areas should not aim at autogenous development of alternate bars, but use other means for increasing the spatial flow variability. In other geographic regions, with steeper slopes and continuous sediment supply, alternate bars could be an alternative for the common practice of stream restoration.

## 4 | Initiation of Meandering



---

Based on: EEKHOUT, J. P. C., HOITINK, A. J. F., & MAKASKE, B. 2013. Historical analysis indicates seepage control on initiation of meandering. *Earth Surface Processes and Landforms*, **38**, 888-897.

## 4.1 Introduction

River meander dynamics has intrigued many scientists throughout history. Recently, the interest in meander behaviour has intensified in the context of stream restoration projects aiming at restoring sinuous/meandering planforms and subsequent free morphological behaviour. Meander dynamics have been studied by applying analytical and numerical models. Ikeda *et al.* (1981) was among the first to develop a meander model that includes a description of the river flow and bed topography, simulating lateral channel shift. Their modelling approach was the basis of a number of subsequent meander models (e.g., Richardson, 2002; Abad & García, 2006; Coulthard & Van de Wiel, 2006). Blondeaux & Seminara (1985) and Struiksma *et al.* (1985) showed the importance of coupling the hydrodynamic equations with the conservation equation of sediment. This has led to meander migration models based on the full Saint Venant equations (e.g., Crosato, 1987; Johannesson & Parker, 1989; Howard, 1996; Stolum, 1996; Sun *et al.*, 1996, 2001; Zolezzi & Seminara, 2001). In many of these models, which capture much of our current understanding about river morphology, meandering initiates uniformly along the streamwise coordinate. Based on a historical analysis, this contribution shows how meandering initiates in isolated sections along a channel, which can be related to floodplain heterogeneity.

Initiation of meandering has been attributed to two types of instability responses, unified by Blondeaux & Seminara (1985). The first to emerge was the so-called *bar theory*, which considers the stability of the alluvial bed and shows that small perturbations in the channel bed may develop into an alternate bar pattern (Hansen, 1967; Callander, 1969; Engelund, 1970). At the pools between the bars, near-bank flow velocities and water depths are higher, resulting in localized bank erosion, and hence, a sinuous channel planform. *Bend theory* (Ikeda *et al.*, 1981) considers the planform instability of a straight channel and shows that a small perturbation of the channel centerline may lead to the development of meanders.

In most meander models developed so far, the migration rate is obtained by multiplying the near-bank excess flow velocity by a dimensionless erosion coefficient, which depends on the physical properties of the banks and their vegetation cover. The value of the erosion coefficient also depends on the numerical solution of the model (Crosato, 2007). For cases where field data is available, the coefficient is obtained empirically based on calibration, using observed erosion rates. These erosion rates are either measured in the field or obtained by remote sensing data (aerial/satellite imagery) or historical maps. Calibration of the erosion coefficient is a challenge, considering the heterogeneity of floodplain soils, the presence of

vegetation, and other causes of spatial variation. Often, observed erosion rates from field studies are lacking.

Recently, several studies have focused on the relation between floodplain characteristics and meander dynamics. Van Balen *et al.* (2008) addressed the spatial heterogeneity of bank erosion in a meander migration model, through the dependence of erosion rates on seepage flow in the banks. They showed a positive feedback may exist between seepage rates and bank migration: bank migration focuses groundwater flow, causing more seepage at the bank, which in turn enhances migration rates. Güneralp & Rhoads (2011) showed that heterogeneity in erosional resistance of the floodplain has a major influence on meander evolution. Motta *et al.* (2012a) presented an analytical meander model based on the work by Ikeda *et al.* (1981), coupled to a physics-based bank erosion module (Langendoen & Alonso, 2008; Langendoen & Simon, 2008). They simulated features of planform behaviour that are commonly observed in nature, but previously could not be simulated using the constant erosion coefficient approach. Following Güneralp & Rhoads (2011), Motta *et al.* (2012b) extended their model for the case of heterogeneous floodplain sediments. They concluded that complexity of the floodplain sediments contributes to the complexity of the channel planform.

Laboratory experiments have shown that it is possible to create a physical scale model of a meandering planform. Federici & Paola (2003) presented an experiment in which a meandering planform formed after some time. However, the meandering planform eventually evolved into a braided river pattern due to the lack of cohesion of the bank material. Therefore, the type of sediment plays a major role in the creation of meanders under laboratory conditions. Several sediment mixtures have been used, which all have a different way of adding cohesion to the material. In the past, solely cohesive material was used to create meanders in the lab (Friedkin, 1945; Schumm & Khan, 1971; Smith, 1998). More recently, mixtures of cohesive and noncohesive sediment were explored to achieve realistic river meandering in laboratory flumes, using for example silica flour (Peakall *et al.*, 2007; Van Dijk *et al.*, 2012). Braudrick *et al.* (2009) used alfalfa sprouts to obtain a stable meandering planform. Both Peakall *et al.* (2007) and Braudrick *et al.* (2009) also introduced an initial perturbation in the channel planform.

Considering the calibration requirements of bank erosion parameters in mechanistic models, and scaling issues in laboratory experiments, field studies and historical reconstructions are crucial in studying the timescales and spatial development characterizing channel development. Long-term field-scale reconstructions of meandering channels are limited by the availability of historical sources to reconstruct the meandering planform, especially before 1900. Planform reconstructions are mainly

#### 4. Initiation of Meandering

based on historical topographic maps (Pišút, 2002; Uribelarrea *et al.*, 2003; Timár *et al.*, 2008; Church & Rice, 2009; Hooke & Yorke, 2010) and aerial photographs (Warburton *et al.*, 2002; Uribelarrea *et al.*, 2003; Bartley *et al.*, 2008; Church & Rice, 2009; Hooke & Yorke, 2010), of which the latter are often available from the 1940s onwards. Recently, airborne LiDAR and satellite imagery have become customary tools for geomorphological studies (Charlton *et al.*, 2003; Timár *et al.*, 2008), offering a means of recognizing historical channel patterns (Seker *et al.*, 2005; Notebaert *et al.*, 2009).

The objective of this study is to contribute to the knowledge about the role of floodplain heterogeneity on the spatio-temporal developments of meander formation, by making a historical reconstruction of the meander behaviour and incision development of an initially straight channel.

## 4.2 Study Area

### 4.2.1 Engineering Works

The artificial channel under study, named Gelderns-Nierskanaal and centred at 51° 30' 54" N, 6° 11' 14" E, was constructed by the Prussians by the end of the 18th century, probably around 1770. The channel is located on the Dutch-German border in the south-eastern part of the Netherlands and runs from the river Niers in Germany to the river Meuse in the Netherlands (Figure 4.1). The purpose of the channel was to lower peak discharges in the downstream reaches of the river Niers, which is a tributary of the river Meuse. At the inlet of the channel, a weir controls the inflow of water. Inflow of water is regulated by an agreement between the Dutch and German water authorities, settled in 1952. Discharge is measured close to the inlet. Discharge data from 1971-2008 were used to calculate a mean daily discharge of 0.71 m<sup>3</sup>s<sup>-1</sup> and an average yearly peak discharge of 4.07 m<sup>3</sup>s<sup>-1</sup>.

The total length of the channel is 13.3 km. The banks of the German part of the channel were protected, to prevent lateral developments, whereas the Dutch part developed into a morphodynamically active meandering channel. The Dutch part, in turn, can be subdivided into two parts. Between the early 1900s and 1940s, the banks of the upstream part became protected with bank revetments. At present, those bank revetments are still visible at some locations, see Figure 4.3e. Two bridges are present in the upstream section, one at the Dutch-German border and one approximately 0.5 km downstream from the border. The downstream part of the study reach can be considered undisturbed regarding its geomorphology, with no erosion or flood controls, and the presence of only one bridge near the mouth

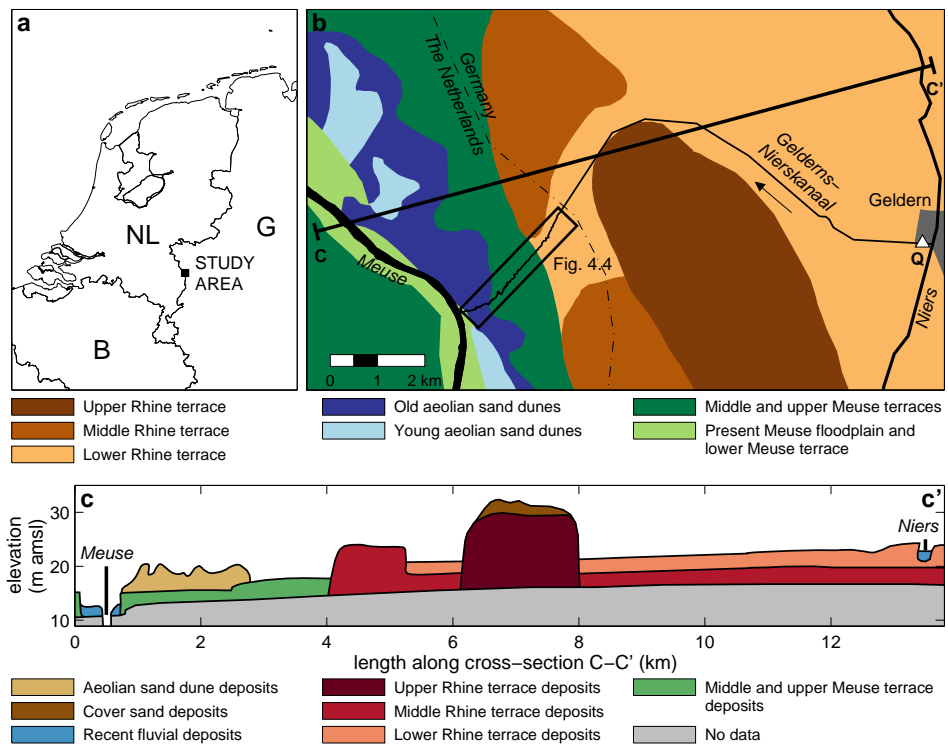


**Figure 4.1** Overview of the study area with (a) the location of the study area on the German-Dutch border, (b) a geomorphological map of the study area, where Q indicates the location of the discharge station and the rectangle indicates the location of Figure 4.4, and (c) a schematic cross-section showing sedimentary units across transect C-C' in panel (b). The terrace denominations ‘upper’, ‘middle’, and “lower” in panels (b) and (c) are used as relative indications of terrace levels in this figure and do not represent formal units in regional terrace classifications. Both (b) and (c) are adapted after Stiboka (1975), using data from Wolfert & De Lange (1990) and Van den Berg (1996).

of the channel where it debouches into the river Meuse. The study area is located in a deciduous forest, surrounded by several agricultural fields.

## 4.2.2 Geology

Figure 4.1 shows the main geomorphological units of the study area, in a plan view (panel b), and the related sedimentary units, in a cross-section (panel c). The sedimentary units are divided into aeolian, Rhine, and Meuse deposits. The Pleistocene Rhine and Meuse terrace deposits mainly consist of coarse sand and gravel. The recent river deposits in the floodplains along the rivers Meuse and Niers predominantly consist of clay. The aeolian deposits consist of fine to coarse sand. Figure 4.1 shows that the German part of the study area is mainly influenced by the

#### 4. Initiation of Meandering

river Rhine. Here, the channel follows a valley occupied by an abandoned (lower) Rhine terrace, between middle and upper Rhine terrace remnants. The upper Rhine terrace remnant explains why the channel was not constructed in a straight line from the city Geldern in Germany to the river Meuse in the Netherlands. The channel follows the northern edge of the upper Rhine terrace. On Dutch territory, the channel predominantly has scoured into Meuse terrace deposits. The channel flows across a middle/upper terrace, and crosses an area of aeolian sand dune deposits, before debouching into the river Meuse.

The study reach is located in the Dutch part of the channel with a length of 3.8 km, extending from the German-Dutch border to the outflow in the river Meuse. Here, the channel gradient varies between  $0.48 \text{ m km}^{-1}$  in the upstream section and  $3.8 \text{ m km}^{-1}$  near the mouth. The channel gradients in the upstream section are comparable to those in the Niers (Kasse *et al.*, 2005), to the lowland streams analysed by Wolfert (2001) and the lowland streams presented in Chapters 2, 5 and 6. The channel gradients in the downstream section correspond to the small streams found in the hilly landscape in the province of Limburg in the southern part of the Netherlands (e.g. De Moor & Verstraeten, 2008; De Moor *et al.*, 2008). The average bankfull width and depth are 8.8 m and 1.2 m, respectively.

The bed material varies along the channel. In the upper section the bed material mainly consists of (coarse) sand, with a median grain size of 0.80 mm (see Figure 4.2 for the grain size distributions). There are several weakly developed point bars located in the inner bends. The bed material in this section is typical for Dutch lowland streams, which mainly consists of sand (Wolfert, 2001). In the downstream section, the bed material gradually becomes coarser and is dominated by gravel, with a median grain size of 18.1 mm (Figure 4.2). The in-channel morphology changes in the downstream direction along the channel. A total of 67 gravel bars have been identified in the downstream section of the channel, which are only exposed during periods of low-flow. Figure 4.3a and 4.3b show examples of the point bars and mid-channel bars.

At several locations along the valley edge, a clear view of the Pleistocene terrace deposits was obtained (see Figure 4.3d and 4.3g). At those locations, sediment textures and layer thicknesses were determined *in situ*. The USDA soil texture classification was used to differentiate between the different grain sizes, using a sand ruler. Figure 4.4 shows the sample locations in the study area. Figure 4.5 shows the sedimentary succession at 10 locations along the valley edge. The exposed deposits mainly consist of median to coarse sand. At eight locations, a thick (0.3–1.2 m) gravel layer and/or gravelly sand layer was visible. This is most likely the source of the current bed sediment, which consists of gravel in the downstream

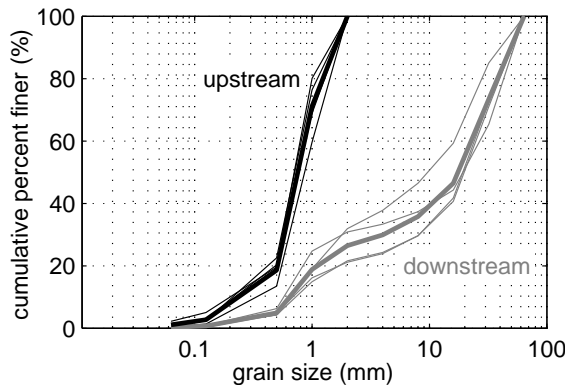


**Figure 4.2** Grain size distributions from bed material samples from 4 locations in the upstream part (black lines) and 4 locations in the downstream part (grey lines). The thick lines denote the average for upstream and downstream samples, respectively.

section of the channel. In a preliminary survey, red-brown coloured layers of sand were found at five locations along the valley edge, in which iron-rich groundwater oxidises and turns red when it comes in contact with air. The groundwater comes in contact with air in the upper part of the groundwater column, and therefore, the depth of the iron oxide gives an indication the upper extent of the historical groundwater table.

### 4.2.3 Hydrology

The purpose of the channel was to reduce flood risk in the downstream reaches of the river Niers. This suggests that no water was led into the channel during low flow periods, resulting in a non-natural discharge distribution. The Dutch and German water authorities, however, made an agreement in 1952 which defined a minimum discharge of  $0.5 \text{ m}^3\text{s}^{-1}$  and a maximum of  $7 \text{ m}^3\text{s}^{-1}$ . It is unknown how water discharge was distributed before that time.

Discharge time series of the Gelderns-Nierskanaal and Niers were compared to investigate the discharge distribution over the inlet of the channel and the downstream branch of the river Niers. Two discharge time series were used, both consisting of daily averaged discharge data. The discharge in the Gelderns-Nierskanaal was measured near the inlet (Figure 4.1). This discharge time series contains data covering the period between 1970 and 2008. The discharge in the river Niers was measured at the city of Goch between 1970 and 2006. For both data series, the monthly averaged discharge is shown in Figure 4.6. The figure also shows the 10%, 25%, 75% and 90% quantiles for every month.

#### 4. Initiation of Meandering

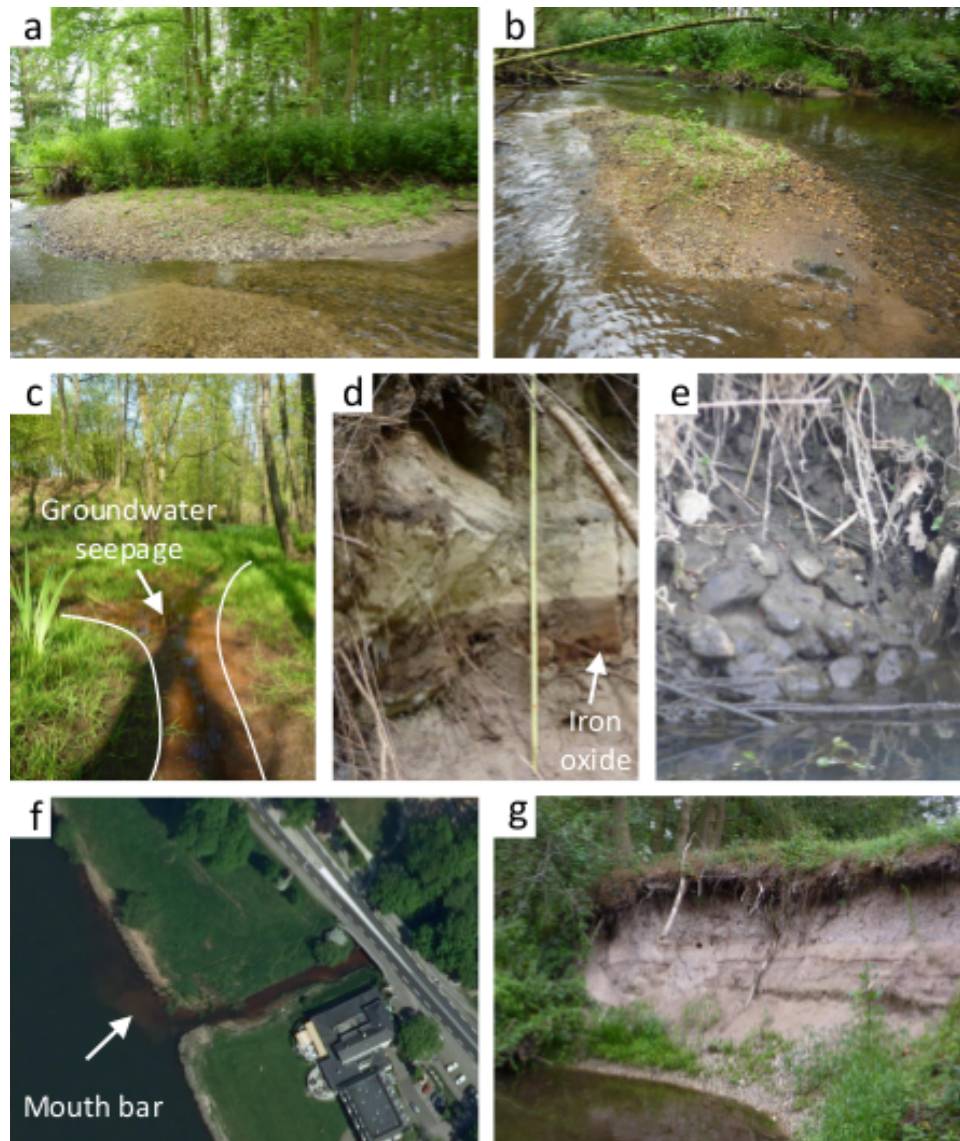


**Figure 4.3** Photos of the study area, illustrating (a) a point bar, (b) a mid-channel bar, (c) the valley floor showing groundwater seepage, (d) a sedimentary succession showing a thick iron oxide layer (thickness: 0.20 m), (e) the remnants of the bank protection, (f) an aerial photo (2008) of the area surrounding the confluence of the Gelderns-Nierskanaal and the river Meuse showing a mouth bar at the downstream side of the channel outlet (Copyright Eurosense B.V. 2008) and (g) valley edge erosion (height of exposed sediments: 2.5 m). See Figure 4.4 for photo locations.

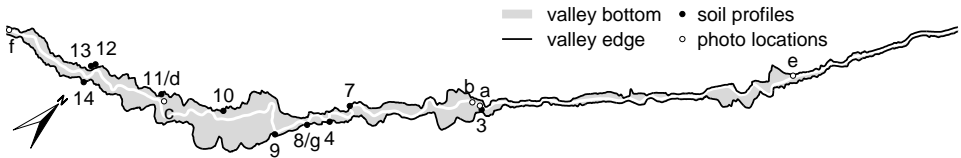


**Figure 4.4** Locations of the exposed valley edges and photo locations corresponding to Figure 4.3. The extent of this figure corresponds to the rectangle in Figure 4.1. Flow is from right to left.

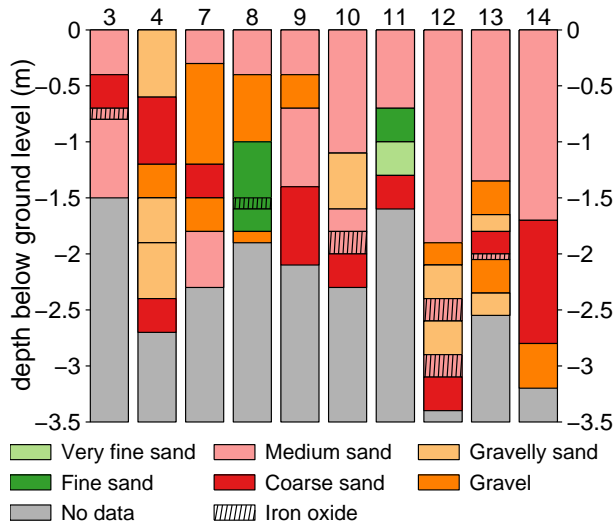


**Figure 4.5** Sedimentary successions at 10 locations, see Figure 4.4 for the locations in the study area. Ground level corresponds to the level of the valley edge into which the channel has incised.

As to the monthly average discharge (solid black line), both discharge time series show the same yearly pattern with high flows in January and February and low flows in August and September. The 25% and 75% quantiles also feature similar patterns for both data series. The 10% and 90% quantiles, however, show that the extremes in the river Niers are less pronounced than the extremes in the Gelderns-Nierskanaal. In other words, the peak discharges in January–February are relatively high in the Gelderns-Nierskanaal, compared to the river Niers. The same holds for low flows in the summer period. Thus, the discharge in the Gelderns-Nierskanaal is relatively flashy.

The study area is located in the river Meuse catchment ( $36,000 \text{ km}^2$ ). The river Meuse has a length of 900 km and is a rain-fed river. It is an important waterway in western Europe, navigable from the North Sea up to France (Nienhuis, 2008). In the

#### 4. Initiation of Meandering

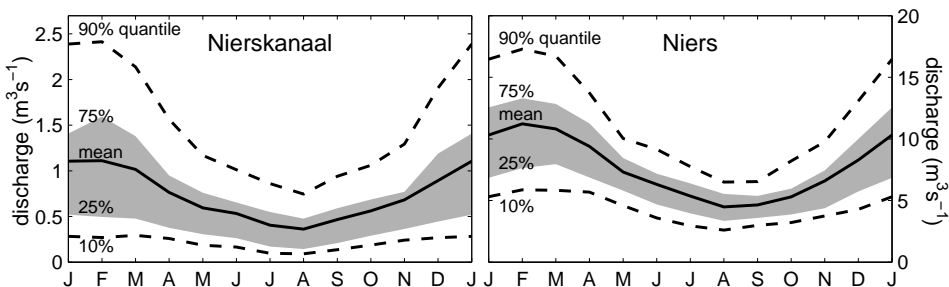


**Figure 4.6** Monthly averaged discharge for the Gelderns-Nierskanaal (upper panel) and river Niers (lower panel). Indicated in gray are the 25% and 75% quantiles and with a dashed line the 10% and 90% quantiles.

19th century, navigation was impeded by sedimentation. Since the 19th century the river Meuse has been subject to measures aiming to improve navigation. This started with dredging activities in the 19th century. In the 20th century, the measures became more rigorous. Several meanders were cutoff, hundreds of groynes were build, lateral canals were constructed, and, most importantly, from 1930 onwards the water level was fully controlled by six weirs in the Dutch part of the river Meuse (Nienhuis, 2008). All of this may have had an impact on the bed morphology of the Gelderns-Nierskanaal near the confluence with the river Meuse.

Water level data from the river Meuse were analysed to evaluate the dynamics of the downstream boundary (i.e. the downstream water surface level) of the Gelderns-Nierskanaal. At 14 locations water levels were measured daily. From these locations, two are in the vicinity of the confluence with the Gelderns-Nierskanaal, 4 km upstream and 6 km downstream from the mouth of the Gelderns-Nierskanaal, respectively. Both water level time series span a period from 1850 until the end of the 20th century. Figure 4.7a shows yearly averaged water levels in the period 1850-1984/1995 for these two locations. The figure clearly shows that the weirs were operational in the river Meuse from 1930 onwards, causing a water level increase of about 2 m from 1929 to 1930. Regression analysis shows there is a water level increase before the weirs were operational, for both locations. The cumulative water surface rise is equal to 0.31 m and 0.46 m for the upstream and downstream location, respectively. After the weirs became operational, the increasing trend is still visible, although less pronounced.

Bed level measurements have been performed from 1916 onwards, with irregular intervals between the surveys. These bathymetry data were collected along cross-river transects with a 100 m spacing, and width-averaged within the navigable section of the channel. Subsequently, bed levels were averaged per river kilometre

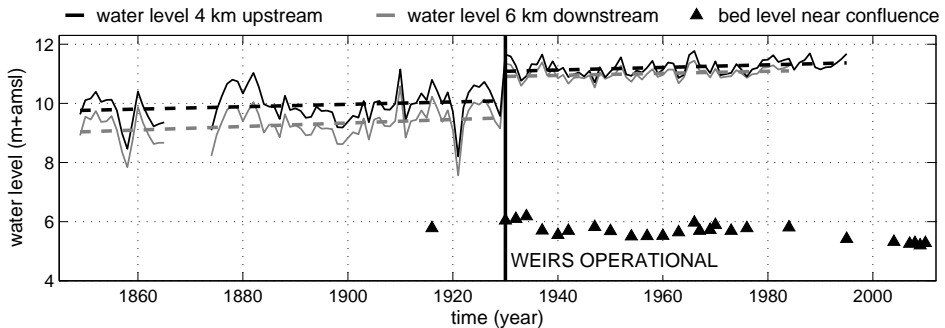


**Figure 4.7** Historical yearly averaged water levels and bed levels from the river Meuse. The water level time series correspond to two locations near the confluence of the Gelderns-Nierskanaal, as indicated.

(Van Dongen & Meijer, 2008). Figure 4.7 shows the change in bed level of the river Meuse at the confluence with the Gelderns-Nierskanaal. Between 1930 and 1940, dredging operations were performed in this section of the river Meuse (Van Dongen & Meijer, 2008), causing a decrease of the bed level. Overall the bed level shows only minor changes between 1940 and 2010. Therefore, it is concluded that the installation of the weirs in 1930 is the only substantial change at the downstream boundary of the Gelderns-Nierskanaal that has occurred since the construction of the channel. The installation of the weirs is the main cause of the rise in water surface level at the confluence with the Gelderns-Nierskanaal.

## 4.3 Materials & Methods

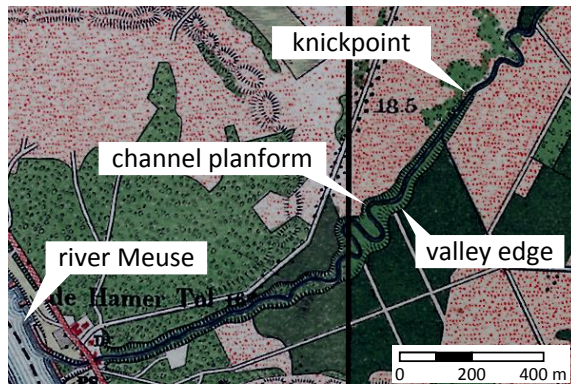
Planform characteristics were derived from 12 historical maps, covering the period between 1806 and 2006. The oldest historical document available was the Tranchot map, based on data from a survey carried out around 1806. Four topographic military maps were used, dating from 1840 to 1936, and seven general topographic maps, dating from 1941 to 2006. Figure 4.8 shows an example of the topographic map of 1895. The features that were derived from all maps are indicated in the figure, including the channel centerline, the incised valley boundaries and the knickpoint of the bed level indicating the upstream end of valley incision. Table 4.1 lists the details of all historical maps. Each map was scanned at a resolution of 600 dpi and georeferenced using ESRI ArcGIS™. Centerlines were manually digitized, with an average node-spacing of 10 m.

Figure 4.9 shows the channel centerlines derived from all 12 historical maps.

#### 4. Initiation of Meandering

**Table 4.1** Characteristics of historical topographic maps.

year	map type	scale
1806	Tranchot	1:25000
1840	topographic military map	1:50000
1895	topographic military map	1:50000
1926	topographic military map	1:50000
1936	topographic military map	1:50000
1941	topographic map	1:50000
1955	topographic map	1:25000
1965	topographic map	1:25000
1975	topographic map	1:25000
1982	topographic map	1:25000
1988	topographic map	1:25000
2006	topographic map	1:25000



**Figure 4.8** Topographic military map of 1895, showing features that were derived from the historical maps, viz. the channel centerline, the valley edges and a bed level knickpoint marking the upstream end of the valley incision.

Planform changes were evaluated based on total sinuosity  $S_{\text{total}}$ , computed by dividing the channel length  $L_{ch}$  by the valley axis length  $L_v$ . The valley axis is defined as the midline of the valley. An increase of  $S_{\text{total}}$  indicates an increase of channel length, which is the result of lateral migration of the channel. A decrease of total sinuosity in a meandering channel is mainly caused by meander cutoffs or by channel straightening through bank erosion. On the right-hand side of Figure 4.9 the total sinuosity is reported for the 12 channel centerlines. In the period between the construction of the channel until the mid 1930s,  $S_{\text{total}}$  increased. Between 1936 and 1955, a number of meander cutoffs occurred, which resulted in a decrease of  $S_{\text{total}}$ .

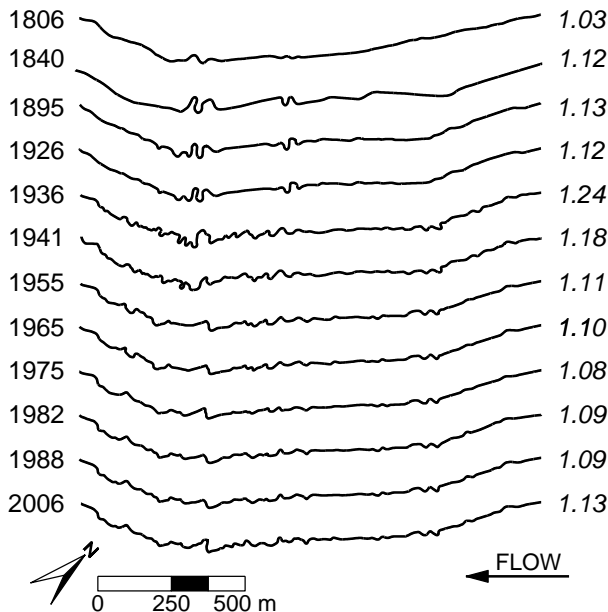


**Figure 4.9** Channel centerlines derived from the 12 topographic historical maps. Values on the right-hand side quantify the sinuosity of the Dutch part of the channel.

A Digital Elevation Model (DEM) was obtained from LiDAR surveys carried out between 1997 and 1998, which covered the entire Dutch part of the study area (Actueel Hoogtebestand Nederland, AHN, Van Heerd *et al.*, 2000). The LiDAR data resolution amounted to 1 point per  $4 \text{ m}^2$ , with a vertical accuracy of 0.20 m and a horizontal accuracy of 0.30 m. Outliers, vegetation and buildings were removed from the dataset to ensure the data represent the actual earth surface. The data were interpolated on a grid with a 1-m resolution, using linear interpolation. The DEM was used to identify the valley edges as shown in Figure 4.4, and to make an estimate of the valley incision since the construction of the channel.

In addition to the historical and remotely sensed data described above, field data were collected. In a first reconnaissance survey, traces of iron oxide and gravel layers in the sedimentary succession were found at several locations along the valley edge (Figure 4.5). Sedimentary successions were described at 10 locations along the valley edge where the sediment was exposed. Figures 4.3d and 4.3g show examples of these exposed terrace deposits. These 10 exposed locations were not evenly distributed over the valley length. Therefore, 49 cores were subsequently collected along the entire length of the valley to establish the spatial distribution of sediment properties. A hand auger was used for drilling down to 2.2 m below ground level. The depth of iron oxide layers in the profile was recorded at each

#### 4. Initiation of Meandering

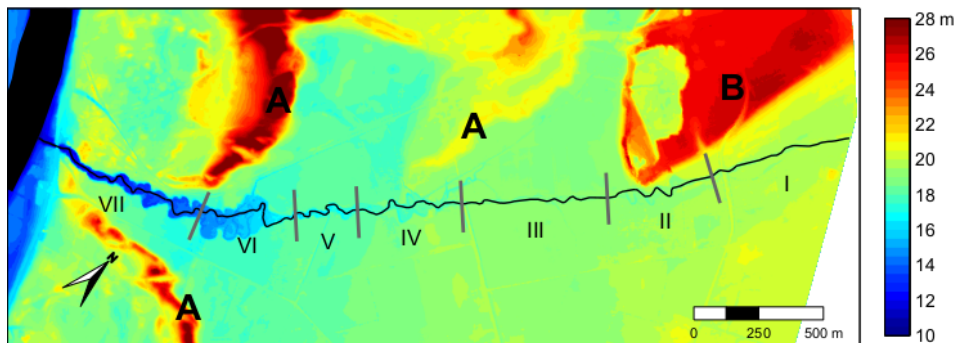


**Figure 4.10** Digital Elevation Model of the study area, including the centerline of the channel in 2006. Elevation is shown in meters above mean sea level. Several geomorphological units are indicated, i.e. the parabolic sand dunes near the confluence with the river Meuse (A) and a Rhine terrace near the German border (B). The Roman numbers label the sections indicated in Figures 4.11 and 4.12.

location. A distinction was made between profiles consisting solely of sand and profiles where gravel layers were present in the profile, in which the gravel layer depth was recorded as well. This resulted in a along valley view on traces of groundwater seepage and gravel.

## 4.4 Results

### 4.4.1 Valley Incision

Figure 4.10 shows the DEM of the study area including the 2006 channel centerline. Several geomorphological units discussed earlier can be recognized in this figure. Near the German border, a Rhine terrace remnant (B) borders the channel at its northern side. Moving in the downstream direction, a gentle westward slope of the land surface surrounding the channel is part of the Meuse terrace, also shown in Figure 4.1 (c). The most distinctive features are the parabolic sand dunes near the confluence with the river Meuse (A). These aeolian sand dunes date from the Younger Dryas period, approximately 12,000 years ago (Van den Berg, 1996). The dunes consist of coarse grained sand and show local elevation differences up to 20 m. The LiDAR data show the aeolian dunes have a larger extent than indicated in Figure 4.1, which was based on Stiboka (1975), indicating the accuracy limitations of the latter report.

When focussing on the area near the channel, the most notable feature in Figure 4.10 is the incised valley near the confluence with the river Meuse. The DEM shows

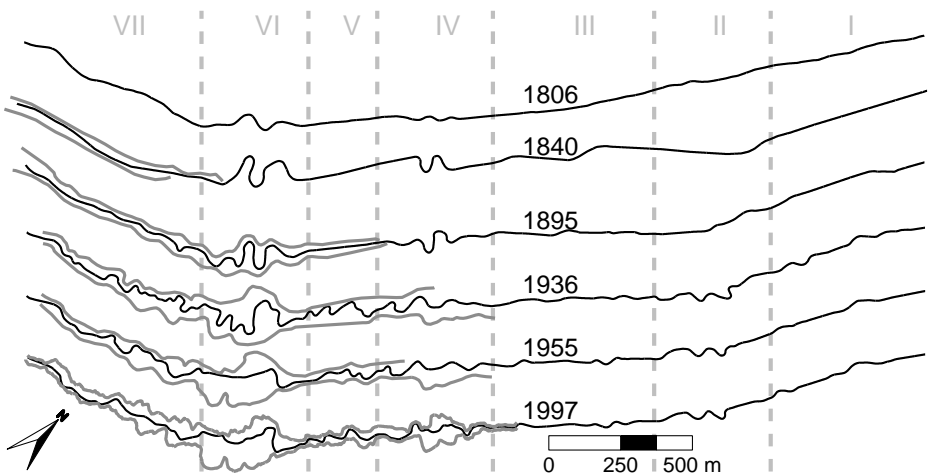


**Figure 4.11** Evolution of the channel centerline (black) and valley edge (grey). The valley edges from 1840, 1895, 1936 and 1955 are derived from topographic maps. The valley edge of 1997 is derived from the LiDAR data set. The Roman numbers label the sections in Figure 4.12.

the channel has incised over several meters (see also the upper part of Figure 4.12).

From historical maps it was possible to extract the valley edge, as shown for example in Figure 4.8. The first topographic map, dating from 1806, did not show any feature that would suggest the presence of a valley edge. From 1840 onwards, all maps depict valley edges, as illustrated in Figure 4.11. The map of 1926 did not show any change in the location of the valley edge compared to 1895. No changes are observed in the period from 1955 to 2006 either. Note that the valley edge of 1997 is derived from the LiDAR dataset, which includes much more detail than the valley edges derived from the historical maps.

Figure 4.11 shows that until 1840, the valley incision was concentrated in the reach downstream of the first meander (section VI). Upstream of that location no valley edges were drawn. The map of 1895 shows that the extent of the valley incision reached up to section IV. From 1936 onwards, the knickpoint location and valley width in the downstream reach of the Gelderns-Nierskanaal were constant, suggesting the valley incision to be stable in that period.

The top panel in Figure 4.12 shows the present longitudinal valley bottom profile. The valley bottom profile in the upstream part runs largely parallel to the valley edge, whereas the valley bottom in the downstream part becomes progressively deeper downstream. This pattern cannot be readily explained as a response to a draw-down curve of the channel bed level, creating erosion that progressively retreats in the upstream direction. The valley bottom profile has a bilinear shape

#### 4. Initiation of Meandering

with a knickpoint around 1.5 km from the Dutch-German border. Figure 4.11 shows that the present extent of the valley incision has been stable since the mid 1930s. Because the knickpoint coincides with the most upstream extent of the valley incision, it can be assumed that the knickpoint has also been stable ever since the 1930s.

Several processes played a role during the process of valley incision. Figure 4.3c shows the presence of overland flow within the incised valley during one of the field surveys, caused by water that was seeping out of the valley wall. The upper part of Figure 4.12 shows where an iron oxide layer was recorded, and at which depth. Iron oxide was found in almost all cores in the deeply incised part of the valley. The shape of the incision in this section shows similarities with so-called amphitheatre shaped canyons (Kochel & Piper, 1986; Howard & McLane, 1988; Schumm *et al.*, 1995), which are typically attributed to erosion by local seepage flow. The average depth where the iron oxide was found was 1.4 m below the level of the valley edge. Considering the current channel depth (1.2 m), this could have been below the constructed channel bed before incision. Arguably, seepage may have been triggered by valley incision, which in turn may have accelerated valley incision. Both seepage and meander dynamics may have contributed to the width of the incised valley. Seepage increases the moisture content of the valley wall, which enhances bank erosion at locations where the meander banks encounter the valley wall. This has resulted in a present day valley depth up to 9 m and a valley width up to 170 m, or 19 times the current channel width.

The knickpoint in the bed level profile coincides with the transition from coarse-grained bed sediment in the upstream part of the channel, and gravel in the downstream part (Figure 4.3a and 4.3b). Results from the 49 cores (Figure 4.12) reveal that in the valley wall two gravel layers are present, located upstream and downstream of the knickpoint in the valley bottom. The progressive retreat of the valley edge, illustrated in Figure 4.11, shows that it is likely that valley incision has initiated in the downstream reach and progressively proceeded in the upstream direction. This process will have continued until the gravel layer was reached, which consists of particles too coarse to be readily transported. From then onward, the valley incision will have been retarded, which may have been amplified by spreading of the gravel over the channel bed by the flow. The deposited gravel can act as an armouring layer, increasing the erosion resistance of the channel bed. The established changes in water levels in the river Meuse may also have had an effect on the incision rate of the valley. Both the presence of gravel on the channel bed and raised water levels in the river Meuse will have counteracted valley incision.

#### 4.4.2 Meander Dynamics

Spatial series of the local sinuosity are determined to discuss the meander dynamics of the channel over the past 240 years. Local sinuosity, denoted by  $S_{\text{local}}$ , was obtained by dividing the channel length within a moving window by a predefined length along the valley centerline. The moving window is 250 m long, which is roughly equal to three meander wavelengths.

Figure 4.12a shows spatial series of the local sinuosity for all 12 historical channel centerlines. The results from the 49 cores along the valley are included in the figure, and the elevation of the valley edge and valley bottom are indicated. The valley edge runs nearly horizontally in downstream direction until 1.5 km from the German-Dutch border. The increase in slope marks the transition between two Meuse terraces. Downstream of the transition, the valley edge again runs nearly horizontally. Near the outlet to the river Meuse, the peak in the surface level reflects the aeolian sand dunes in the area.

Figure 4.12b shows the temporal variability of the local sinuosity in each of the seven sections defined in Figure 4.12a. The 1806 channel centerline shows meandering has initiated in section VI, where sinuosity increased rapidly in time up to a maximum of around 2. Figure 4.11 shows that, in this section, meandering had initiated before valley incision had started. Meandering also initiated in section IV, in the period between 1806 and 1840. Both in section IV and in section VI, meandering developed independently, at least until 1926. From 1936 onwards, sections IV and VI had merged, which is reflected in an increase in sinuosity in section V.

Several meander cutoff events have occurred between 1926 and 1955. The remainders of those are shown in Figure 4.10, e.g. in section VI. Meander cutoffs result in a decrease in sinuosity. In section IV, cutoff events have occurred between 1926 and 1936. Most evident are the cutoff events in section VI. Figure 4.12b clearly shows a decrease of local sinuosity between 1936 and 1955. For both sections IV and VI, it can be concluded that the cutoff events are clustered within a 10 to 20 year time span. Using the meander model of Howard & Knutson (1984), Stølum (1996) showed from numerical simulations that cutoff events tend to cluster. This was subsequently confirmed by field research by Stølum (1996), who concluded that each cutoff has a tendency to trigger other cutoffs in its vicinity by causing accelerated local change. This explains the cutoff clustering in space and time as observed.

The upstream sections of the channel show little activity over the past 240 years. In section II, meandering has initiated between 1926 and 1936. The sinuosity in section II does not show any significant changes after 1936 (Figure 4.12b), which

#### 4. Initiation of Meandering

can be attributed to the construction of bank revetments between 1900 and 1940. Bank protection, albeit left unmaintained (see Figure 4.3e), may have prevented the channel from active meandering in the upper sections.

The valley bottom profile confirms the existence of a difference in morphodynamic behaviour between sections III and IV. Figure 4.12 shows a knickpoint at the boundary between the inactive upstream sections I through III, and the active downstream sections IV through VII. Both the upstream part and the downstream part show a nearly constant slope. The two parts may have developed to reach two alternative states of a morphological equilibrium, pertaining to laterally confined conditions and a more natural state with erodible banks, respectively.

#### 4.4.3 Initiation of Meandering

Figure 4.10 shows the current meandering planform including the DEM of the surrounding earth surface. Sections II, IV and VI, where meandering has initiated, are located in the direct vicinity of elevated sedimentary units, i.e. aeolian sand dunes and a Rhine terrace remnant. Each of the three hotspots for meander initiation coincides with the toe of a topographic high. Figure 4.12 shows that iron oxide was found in the Pleistocene terrace deposits at those spots, which is related to lateral groundwater seepage flows (Anderson, 1988). While it remains unknown whether seepage was present before the channel was constructed, it is likely that groundwater levels in the study area were affected by the construction of the channel.

In flat terrains, precipitation usually infiltrates the soil vertically. The vicinity of a terrace remnant or an aeolian dune, however, changes the groundwater flow in the surroundings of the channel. A topographic high causes the groundwater to flow in lateral direction away from the elevated terrain, causing groundwater seepage in lower parts of the landscape, e.g. valleys. Seepage through the valley walls increases the moisture content of the bank. Field research (Wilson *et al.*, 2007; Fox *et al.*, 2007; Van Balen *et al.*, 2008) and laboratory studies (Fox *et al.*, 2006; Lindow *et al.*, 2009; Fox & Wilson, 2010) have shown a positive correlation between seepage flow and bank instability and erodibility.

Results from the cores confirmed that iron oxide is present in the banks at each of the three spots of meander initiation, but occurred also in section (VII). In the latter section, the seepage has been related with the relatively deep valley incision, which was described earlier. In sections II, IV and VI iron oxide was found close to the level of the valley edge (< 1 m). This provides a clue that seepage has triggered meander initiation. The upper part of Figure 4.12 also shows that, especially in sections II and IV, and to some extent also in section VI, the subsurface mainly consists of sand. The subsurface of both sections III and V mainly consist of gravel.

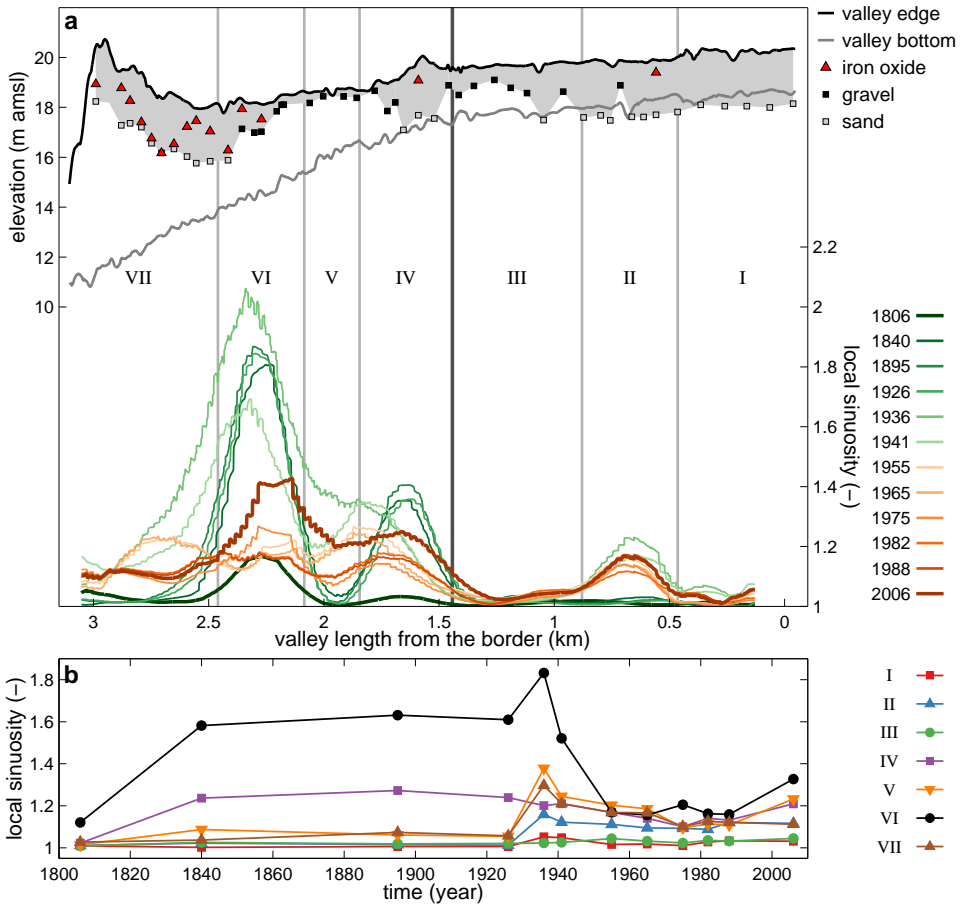


**Figure 4.12** Longitudinal (a) and temporal (b) variability of local sinuosity. Right vertical axis in panel (a): spatio-temporal variation of local sinuosity along the valley axis for all 12 historical channel centerlines. Local sinuosity is determined with a window-size of 250 m. Left vertical axis in panel (a): elevation of the valley edge and valley bottom in meters above mean sea level. The upper part of the figure shows the locations of cores, with a maximum depth of 2.2 m below the level of the valley edge. Red squared markers indicate locations where traces of iron oxide were found, solid black squares correspond to locations where the hand auger reached a gravel layer, and delineated squares indicate the deepest point to which the hand auger reached in a sand layer. The gray zone marks the coring depth and the extent of the sand deposits.

#### 4. Initiation of Meandering

A conclusion is made that meandering in the channel under study has initiated in channel reaches with a floodplain consisting of sand, at spots in the vicinity of topographic highs, where local seepage flow causes seepage erosion and enhances the erodibility of the banks, promoting fluvial erosion.

## 4.5 Conclusions

The objective of this study was to contribute to the knowledge about the role of floodplain heterogeneity on meander formation, by making a historical reconstruction of the development of an initially straight channel. A historical reconstruction was made of a channel constructed in the 18th century between the rivers Niers and Meuse, on the Dutch-German border. Within the Dutch part of the channel, meandering has initiated at three locations. The upstream part of the channel did not show any meander dynamics after the first meander had initiated, because of bank protection. Downstream of the protected bank area, the channel evolved into an actively meandering channel, featuring meander cutoffs.

From field evidence it appears that the sections of the channel where meandering has initiated correspond to sections of the channel where iron oxide was found within 1 m from the surface level, indicating groundwater seepage. The groundwater seepage originates from the banks and valley sides adjacent to higher elevated terrains, composed of terrace remnants and aeolian dunes. Since the subsurface of these sections mainly consists of sand, local seepage flow causes seepage erosion and enhances the erodibility of the banks, promoting fluvial erosion. The resulting bank erosion may have resulted in small perturbations in the channel planform. These perturbations in the initial planform, in turn, are the most plausible trigger for the initiation of meandering in this case study.

Meandering has initiated in three separate sections of the channel. The spatial variation in meander initiation was attributed to local differences in hydrology (seepage) and geology (presence of gravel). Recently, meander research focuses on the role of floodplain heterogeneity on meander dynamics, e.g. local differences in hydrology and geology. Commonly, a constant erosion coefficient is used for the whole river reach to parametrise bank erosion. The present study shows that spatial heterogeneities may assert a strong control over sinuosity developments over two centuries of planform change. These observations justify efforts to implement the influence of floodplain heterogeneity and the effect of seepage on bank erosion in meander models.

## 5 | Chute Cutoff



---

Based on: EEKHOUT, J. P. C., & HOITINK, A. J. F. (*under review*). Importance of backwater effects to the occurrence of a chute cutoff. Submitted to *Journal of Geophysical Research - Earth Surface*.

## 5.1 Introduction

In the Netherlands, stream restoration generally refers to the construction of low-sinuosity channels. After construction, these channels typically show limited morphological change in time, mainly due to oversized cross-sections. Occasionally, pronounced morphological changes occur, including bank erosion and meander cutoffs. This chapter reports on a recent chute cutoff event that occurred right after the realization of a stream restoration project, showing that backwater effects can play a crucial role in the occurrence of a chute cutoff.

Two main types of meander cutoffs have been identified. Neck cutoffs can develop by the progressive migration of an elongated bend into itself (Erskine *et al.*, 1992; Hooke, 1995). Chute cutoffs are shortcuts developing over a point bar or, over-bank, across a meander bend (Lewis & Lewin, 1983; Erskine *et al.*, 1992). Neck cutoffs are likely to occur in high-sinuosity meander bends and under low channel gradients (Lewis & Lewin, 1983). Chute cutoffs are more likely to occur in moderate to low sinuosity meander bends, and under high channel gradients (Lewis & Lewin, 1983). Few studies have focused on cutoffs in small streams, which occur at temporal and spatial scales small enough to investigate the phenomenon in detail.

Three mechanisms have been proposed in the literature to explain chute cutoff occurrence: (1) swale enlargement, (2) headcut propagation, and (3) embayment formation and extension (Constantine *et al.*, 2010). According to the first mechanism, a swale may channelise the flow during a flood, governing the predominant flow route on the floodplain. The second mechanism refers to a headcut at the downstream boundary of a meander bend propagating in the upstream direction. This chute mechanism mainly occurs in rivers with floodplains consisting of cohesive sediment, which acts to maintain the form of the headcut (Brush & Wolman, 1960; Gay *et al.*, 1998). The third mechanism considers the formation of an embayment as a result of localized bank erosion along the outer bank, upstream of the meander that undergoes cutoff. Subsequent floods extend the embayment, shifting it downstream until it intersects the riverbank downstream, forming a chute (Constantine *et al.*, 2010). Chute cutoff by embayment formation and extension is most likely to occur along large meandering rivers having steeply sloping floodplains. The headcut propagation and embayment formation are incisional processes that may act on well-established inner-bank floodplains, and are affected by reductions in floodplain surface roughness and floodplain heterogeneity (e.g. root depth and stratification). Both mechanisms are strongly related to flood events (Constantine *et al.*, 2010; Micheli & Larsen, 2011).

Lewis & Lewin (1983) were among the first to present a study on the occurrence of neck and chute cutoffs. They used historical sources to show the correlation between floodplain gradient and cutoff frequency, although this correlation was not so pronounced for chute cutoffs. More recently, historical sources have been used to find correlations between the occurrence of chute cutoffs and planform characteristics (Constantine *et al.*, 2010; Micheli & Larsen, 2011; Grenfell *et al.*, 2012). Micheli & Larsen (2011) found that meander bends that have been subject to a chute cutoff had higher values of sinuosity and entrance angle, and lower values of curvature, compared to other meander bends. Constantine *et al.* (2010) showed that chute cutoffs tend to form at the spot along the channel centerline where the curvature has its local maximum. Based on regression models, Grenfell *et al.* (2012) showed, with a statistical analysis, that the probability of chute initiation at a meander bend is a function of the bend extension rate, i.e. the rate at which a bend elongates in a direction perpendicular to the valley axis trend. Other planform characteristics such as sinuosity, curvature and entrance angle were shown not to be significantly different for bends with and without chute cutoff. Although historical sources of the river planform are very useful to study chute cutoff occurrence at large temporal and spatial scales, they may not provide sufficient information needed to predict the occurrence of chute cutoffs.

There are only a few case studies available that describe the occurrence of chute cutoffs in the field. Most of these offer qualitative rather than quantitative information, giving insight in the causal relationships involved in processes during chute cutoff events. The majority of these studies claim that the chute cutoffs under study occurred during periods of overbank flow (Johnson & Paynter, 1967; Hooke, 1995; Gay *et al.*, 1998; Zinger *et al.*, 2011). This was also observed under laboratory conditions (Jin & Schumm, 1987; Peakall *et al.*, 2007; Braudrick *et al.*, 2009; Van Dijk *et al.*, 2012). Even though these experiments were performed imposing constant bankfull conditions, overbank flow did occur, caused by changes in channel slope (Jin & Schumm, 1987) and in-channel sedimentation (Van Dijk *et al.*, 2012). Both field and lab studies show overbank flow is an inherent feature of the occurrence of chute cutoffs, although the magnitude and related frequency of the floods needed for chutes to develop is still unknown.

Existing quantitative field studies have focused on processes of sedimentation in cutoff channels and on post-cutoff morphodynamics in chute channels. Sedimentation processes in cutoff channels were investigated shortly after the cutoff occurred (Johnson & Paynter, 1967; Thompson, 1984; Hooke, 1995; Dieras *et al.*, 2013) and at sites where historical evidence was present (McGowen & Garner, 1970; Erskine *et al.*, 1992; Ghinassi, 2011; Toonen *et al.*, 2012). Sedimentation of the cutoff chan-

## 5. Chute Cutoff

nel exhibits a fining-upward sequence, from coarse sand or gravel/cobbles at the base to clay loam or sand at the surface (e.g. Erskine *et al.*, 1992; Hooke, 1995). Differences in grain size characteristics of the deposited material are related to the flow regime after the channel underwent cutoff. In a laboratory experiment, Peakall *et al.* (2007) showed that deposition of fine to medium sands (corresponding to the courser material in the experiment) coincides with continued flow through the cutoff, whereas deposition of fine-grained fills of clays and loams coincides with slow-moving or stagnant water in the cutoff channel.

Only recently, case studies describing post-cutoff morphodynamics were presented in the literature, where the collection of the morphological data mainly focused on the chute channel. Fuller *et al.* (2003) quantified in detail the magnitudes of sediment transfers associated with channel adjustments following cutoff, in a laterally active gravel-bed river. Their analysis shows that the initial morphological development was dominated by bed scour, followed by a period of extensive bank erosion and lateral channel migration. Zinger *et al.* (2011) estimated the amount of sediment produced by two chute cutoff events. They found that each event triggered the rapid delivery of sediment into the river, at rates one to five orders of magnitude larger than those produced by lateral migration of individual bends. They also found that much of this material was deposited immediately downstream, which led to significant changes in channel morphology.

The lack of process-based field studies is the main reason why the physical controls on processes of chute cutoff formation remain poorly understood (Grenfell *et al.*, 2012). Despite this, there have been several attempts to model the process of chute cutoff. Chute cutoff initiation has been incorporated into a one-dimensional meander migration model by Howard (1996). The model does not capture the flood flow across the point bar creating the chute, but predicts the influence of planform and topographic characteristics determining where and when chute cutoffs are expected to occur. Constantine *et al.* (2010) applied a two-dimensional depth-averaged hydrodynamic model to determine the influence of the channel curvature on the location where overbank flow incises the floodplain, causing the initial chute cutoff formation. Constantine *et al.* (2010) suggests that chute cutoff initiation is due to overbank flow escaping from the main channel, where the riverbank most strongly turns away from the downstream flow path.

Unlike other morphological processes that occur in meandering channels (e.g. bank erosion, neck cutoffs, meander migration), detailed analysis of field observations of chute cutoffs are still lacking (Micheli & Larsen, 2011). These observations are needed to better understand the mechanisms that cause chute cutoffs. Field evidence is presented of a chute cutoff event, which occurred within three months

after the realization of a stream restoration project. As part of a research project to establish post-project morphological changes in this stream restoration project, a detailed monitoring plan was implemented. The objective of this study is to reveal details of the hydrodynamic and morphological conditions before, during and after the chute cutoff event, to eventually increase understanding of the processes governing chute cutoffs.

## 5.2 Study Area

In October 2011 a stream restoration project was realized in a small lowland stream, entitled Lunterse Beek, located in the central part of the Netherlands ( $52^{\circ} 4' 46''$  N,  $5^{\circ} 32' 30''$  E), see Figure 5.1. A sinuous planform (with a sinuosity of 1.24) replaced a former straightened channel, where the course of the new channel crossed the former channel at several locations (Figure 5.1c). The channel was constructed with a channel width of 6.5 m, a channel depth of 0.4 m and a channel slope of  $0.96 \text{ m km}^{-1}$ . A lowered floodplain surrounded the channel, with an average width of 20 m (Figure 5.1d). At the downstream end of the study area, a bridge reduces the floodplain width to less than 10 m. The bed material mainly consists of fine sand, with a median grain size of  $258 \mu\text{m}$ . A 20 m channel reach, located upstream from the main study area, consists of peat (Figure 5.1d).

Figure 5.1b shows the location of the study area in the catchment. The catchment has an area of  $63.6 \text{ km}^2$ . The elevation within the catchment varies between 3 to 25 m above mean sea level. The study area is located in a mildly sloping area. The subsurface of the catchment mainly consists of aeolian-sand deposits. Agriculture is the main land-use in the catchment. The average yearly precipitation amounts to 793 mm (KNMI, 2014). The average daily discharge is measured at  $0.33 \text{ m}^3 \text{ s}^{-1}$  and the peak discharge during the study period was  $5.67 \text{ m}^3 \text{ s}^{-1}$ .

## 5.3 Material & Methods

### 5.3.1 Morphological Monitoring

The temporal evolution of the bathymetry has been monitored over a period of eight months. Morphological data were collected in the area covering the lowered floodplain, over a length of 180 m, indicated by light grey in Figure 5.1d. Morphological data were collected using Real Time Kinematic (RTK) GPS-equipment and an Acoustic Doppler Current Profiler (ADCP), see Figure 5.3 for the dates of the

## 5. Chute Cutoff

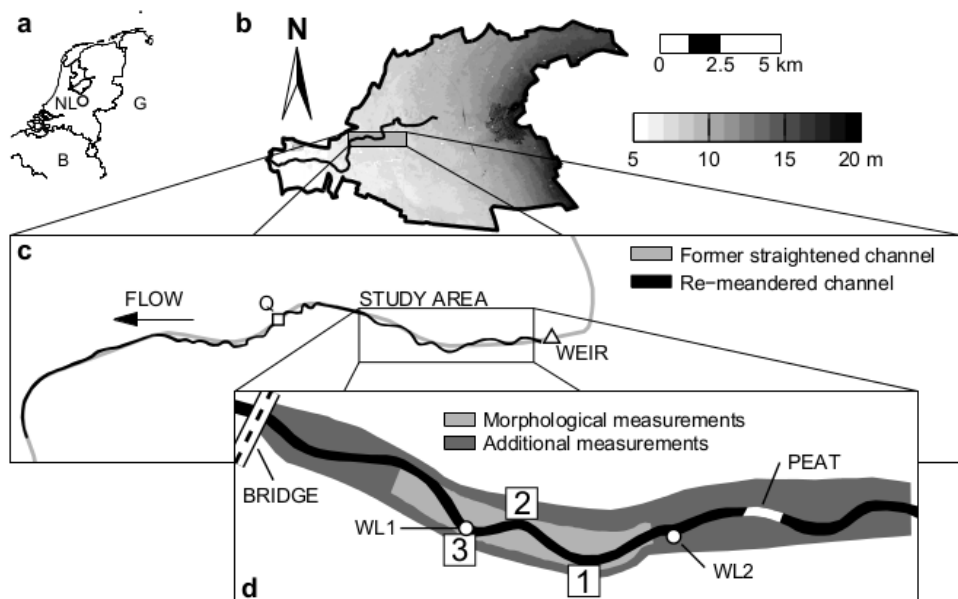


**Figure 5.1** Overview of the study area: (a) location of the study area in the Netherlands, (b) elevation model of the catchment, (c) planform of the restored reach, with the squared marker indicating the location of the discharge station (Q) and the triangular marker the location of a weir (WEIR), and (d) sketch of the study area, indicating the location of peat in white, the location of a bridge at the downstream end of the study area, the location of the water level gauges with circled markers and the three main bends with labels 1-3.

morphological surveys. RTK-GPS equipment (Leica GPS 1200+) was employed to measure surface elevation, with an accuracy of 1-2 cm. The surface elevation data were collected along cross-sections between the two floodplain edges. The number of points collected during each GPS-survey ranged between 379 and 1158, with an average of 831 point-measurements, see Table 5.1 which also provides point densities for each survey. The survey strategy proposed by Milan *et al.* (2011) is followed, focusing on breaks of slope. The point-density was increased in the vicinity of steep slopes (e.g. channel banks), and decreased the point-density on flat surfaces (e.g. floodplains).

An ADCP-survey was not included in the original monitoring plan, being part of a separate study commissioned by the water authority. Despite accuracy limitations, the bed level data from the ADCP-survey appeared valuable to the present study, as the survey took place just before the cutoff event. The ADCP-survey was undertaken with a Teledyne RDI StreamPro ADCP. The StreamPro ADCP is mounted on a float, with a length of 0.70 m and a width of 0.43 m. The ADCP uses four acoustic beams to measure the depth of the channel relative to the ADCP transducer, with

a sampling frequency of 0.5 Hz. Bed level data were recorded for water depths exceeding 0.10 m. The track of the float is measured using bottom tracking. An RTK-GPS antenna (Septentrio Altus APS-3) was mounted on the ADCP to be able to transform the local coordinates and measured channel depths to the Dutch coordinate system (RD-coordinates) and to elevation above mean sea level.

From four morphological surveys (three GPS-surveys and the ADCP-survey), bed elevation data were also obtained in the channel upstream from the study area. These measurements were focused on the channel bed rather than on the floodplain. Both datasets were combined to derive the evolution of the channel bed over a length of approximately 300 m, in the main study area and upstream. The bed elevation was obtained at each channel cross-section by averaging the measured cross-sectional data over the width of the channel bed, between the channel banks.

### 5.3.2 DEM Construction and Processing

Digital Elevation Models (DEMs) of each of the fourteen datasets were constructed. The data were transformed to  $s, n$ -coordinates using the method described by Legleiter & Kyriakidis (2007). Since the data were collected in cross-sections, an anisotropy factor was used within the interpolation routine, accounting for dispersion of the collected data in the longitudinal direction. The anisotropy factor was determined by dividing the average streamwise distance between the subsequent cross-sections by the average cross-stream distance between the individual point measurements. The data were split into a channel section and a floodplain section, to account for a higher density of point measurements in the channel than in the floodplain. A separate anisotropy factor was applied for the channel and the floodplain data. Table 5.1 lists the point density and anisotropy factors for all individual surveys, specified for the channel and floodplain sections.

The data were projected onto a curvilinear grid, following the channel centerline for the channel data and the valley centerline for the floodplain data. A Triangular Irregular Network (TIN) was constructed using a Delaunay triangulation routine in Matlab, following Heritage *et al.* (2009). Subsequently, the TIN was interpolated onto a grid using nearest neighbour interpolation, with a grid spacing of 0.25 m. After interpolation, the data were transformed back to  $x, y$ -coordinates. The interpolated channel and floodplain were then merged to facilitate the comparison between all six surveys.

Deposition and erosion patterns were obtained by subtracting two subsequent morphological surveys, yielding a DEM of Difference. Real morphological change can be different from apparent morphological change, which may arise from uncertainties in the individual DEMs, e.g. from instrumental errors or errors that arise

## 5. Chute Cutoff

**Table 5.1** Overview of the six morphological measurements, showing the survey date, the surveying equipment, the number of data points, the point density (PD) in points  $\text{m}^{-2}$  and the anisotropy factor (AF) as used in the interpolation routine, specified for the channel and floodplain data.

Measurement no.	1	2	3	4	5	6
Survey date (day)	0	64	93	133	191	231
Equipment	RTK-GPS	ADCP	RTK-GPS	RTK-GPS	RTK-GPS	RTK-GPS
No. data points	379	8394	956	918	742	1158
PD (all)	0.16	2.46	0.32	0.27	0.20	0.30
PD (channel)	0.25	4.09	0.44	0.34	0.31	0.45
AF (channel)	10.51	11.70	5.30	3.74	4.42	4.19
PD (floodplain)	0.12	2.21	0.24	0.24	0.15	0.24
AF (floodplain)	4.95	12.15	2.47	2.25	2.13	2.09

from the interpolation routine. The uncertainty can be established by determining the threshold level of detection (LoD). The method by Milan *et al.* (2011) was adopted to construct the spatially distributed LoD. Milan *et al.* (2011) account for the increase of spatially distributed error in a DEM near steep surfaces (e.g. channel bank edges), by inferring the relationship between the standard deviation of elevation errors and local topographic roughness. The method by Milan *et al.* (2011) was adjusted, by adopting a single linear regression model to obtain the spatial standard deviation of elevation error grids. The regression model was obtained after combining elevation errors and local topographic roughness values (Figure 5.2a), for all six surveys.

In each grid cell the LoD was obtained according to:

$$U_{crit} = t \sqrt{(\sigma_{e,1})^2 + (\sigma_{e,2})^2} \quad (5.1)$$

where  $U_{crit}$  is the critical threshold error,  $t$  is the critical Student's value and  $\sigma_{e1}$  and  $\sigma_{e2}$  are the standard deviation of elevation error, for the first and second survey, respectively. The threshold value is based on a critical a Student's  $t$ -value, at a chosen confidence level. Following Milan *et al.* (2011), a confidence limit equal to 95% was applied, which results in  $t \geq 1.96$  ( $2\sigma$ ). The elevation difference between two subsequent surveys at a particular grid cell is insignificant when  $z_{i,j}(new) - z_{i,j}(old) < U_{crit}$ , where  $z_{i,j}(new)$  and  $z_{i,j}(old)$  are the elevations of the two subsequent morphological surveys at grid cell  $i, j$ . A lower bound for the critical threshold error was adopted, to account for the accuracy of the RTK-GPS equipment. This lower bound was set to  $U_{crit} = 0.04$  m, which is 2 times the maximum error of the RTK-GPS equipment.

The channel centerlines were used to determine the temporal evolution of the planform characteristics. During each of the six surveys, the position of both channel

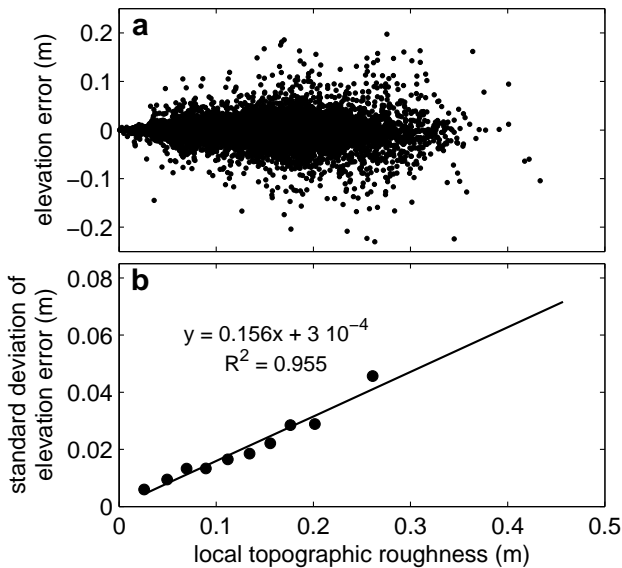


**Figure 5.2** Variation in elevation errors with local topographic roughness, (a) elevation errors for each measured x,y-coordinate for all six surveys, where elevation error increases with increasing local topographic roughness, (b) standard deviation of the elevation error for 10 classes of the local roughness. Panel (b) also includes the linear regression model and coefficient of determination.

banks were well-defined. The position of the channel centerline was subsequently derived from the average position of either bank. The curvature series were derived from the channel centerline. Zero-crossings of the curvature series coincide with the inflection points between the bends. The inflection points were used as a boundary between the bends. For each bend, the sinuosity and dimensionless wavelength were determined. The sinuosity was calculated by dividing the length of the channel between the inflection points by the wavelength of the bend, which is the straight-line distance between the inflection points. The wavelength was subsequently divided by the constructed channel width to obtain the dimensionless wavelength.

### 5.3.3 Hydrological Monitoring

Discharge data were collected downstream of the study reach at a discharge station, indicated with  $Q$  in Figure 5.1c. The discharge estimates were acquired with a one hour frequency. Figure 5.3 shows the discharge hydrograph over a period of 250 days. Water level data were measured at two locations along the study reach,

## 5. Chute Cutoff

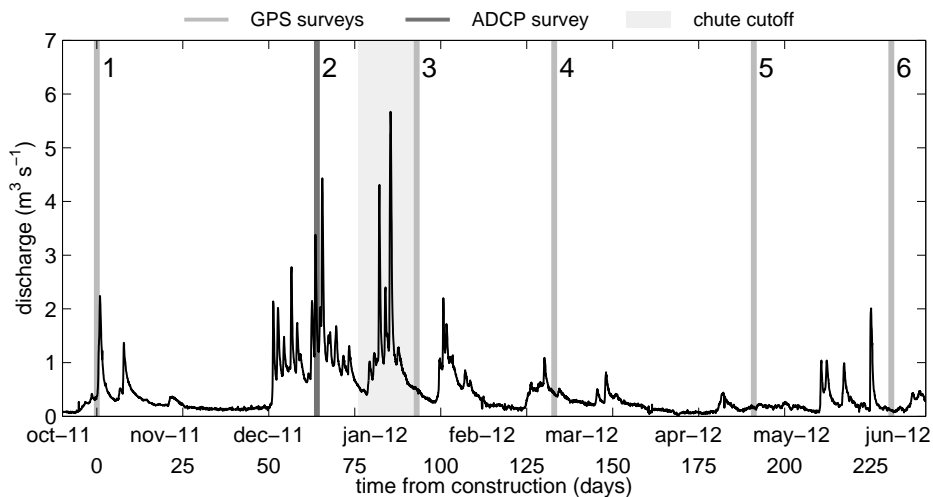


**Figure 5.3** Discharge hydrograph for the channel under study. The morphological surveys are indicated with the grey and dark grey vertical lines for the GPS- and ADCP-surveys, respectively. The chute cutoff took place in the period indicated in light grey.

indicated with WL1 and WL2 in Figure 5.1d. The water level gauges WL1 and WL2 started monitoring 54 and 103 days after construction of the channel had finished, respectively. Water level data were acquired with a one-hour frequency. Longitudinal water level profiles were measured using the RTK-GPS equipment during four of the five GPS-surveys.

### 5.3.4 Sediment Sampling

Grain size distributions were derived from two sets of sediment samples, taken with a sediment core sampler (KC Denmark Kajak Model A). First, sediment samples were taken from the channel bed and banks just after construction had finished. Sediment samples were taken at two cross-sections along the channel in the study area. Second, sediment samples were taken in the cutoff channel approximately one year after the construction had finished. A total of 10 cores were taken in the cutoff bend at the centerline of the constructed channel. At each location, the difference between the constructed channel and deposited sediment was determined, which ranged between 0.24 and 0.47 m below the surface. The samples were taken at two depths between the current surface level and the constructed channel bed, approximately at one quarter and three quarters of the depth of the deposited sediment. Sediment samples were dried in an oven for 24 hours at a temperature of 105° Celsius. Subsequently, the organic material was removed. The grain size distribution was obtained using a laser particle sizer (Sympatec Helos KR) and

subdivided into 57 classes, ranging from 0.12  $\mu\text{m}$  to 2000  $\mu\text{m}$ . The median grain size was derived from the cumulative grain size distributions.

### 5.3.5 Hydrodynamic Model

A Reynolds Averaged Navier Stokes model (Delft3D), using  $k-\epsilon$  turbulence closure, was employed to study the flow characteristics causing deposition of the sediment in bend 2, prior to the chute cutoff. To minimize boundary effects in the model results in the region of interest, the model domain was extended both in lateral and longitudinal direction. For this purpose, an additional morphological survey was performed at day 133. The model domain covered an area with a length of 425 m and an average width of 39 m, indicated by the dark grey colour in Figure 5.1d. The bathymetrical data were interpolated onto a curvilinear grid, with an average grid spacing of 2.35 m in stream-wise direction and 1.25 m in cross-stream direction. A finer cross-stream grid spacing of 0.8 m in the channel section was used to account for details of the bathymetry within the channel. Ten logarithmically distributed sigma-layers were defined in the vertical direction. The horizontal eddy viscosity was set to  $2.5 \text{ m}^2\text{s}^{-1}$ .

Discharge and water levels were imposed as upstream and downstream boundary condition, respectively. To find the discharge conditions that could explain the deposition of sediment in bend 2, a series of steady-state simulations was carried out imposing discharges ranging between 0.1 and  $5.7 \text{ m}^3 \text{ s}^{-1}$ , which corresponds to the range of observed discharges in the period under study (Figure 5.3). In these simulations, the water level boundary condition was derived from a discharge-water level relation ( $Q$ - $H$  relation), based on measured water level time series at water level gauge WL2. The measured water level data from WL2 were extrapolated to the downstream boundary of the model domain, based on measured water level slopes. Figure 5.4a shows the  $Q$ - $H$  relation and Figure 5.4b the longitudinal water level profile.

The model calibration was performed using the measured longitudinal water level profile from the first GPS-survey. In the calibration procedure, values of the Manning bed roughness coefficient were varied. The 20-m long channel section consisting of peat caused an increase in water level (Figure 5.4b), between 80 m and 100 m along the centerline coordinate. This was represented in the model by increasing the roughness in this area. Calibrated values of the Manning coefficient amounted to  $0.017 \text{ s m}^{-1/3}$  for sand and  $0.14 \text{ s m}^{-1/3}$  for peat. This resulted in a coefficient of determination of  $R^2 = 0.97$ . A validation simulation was performed using the measured longitudinal water level profile from the second GPS-survey. This resulted in a coefficient of determination of  $R^2 = 0.87$  (Figure 5.4b).

## 5. Chute Cutoff

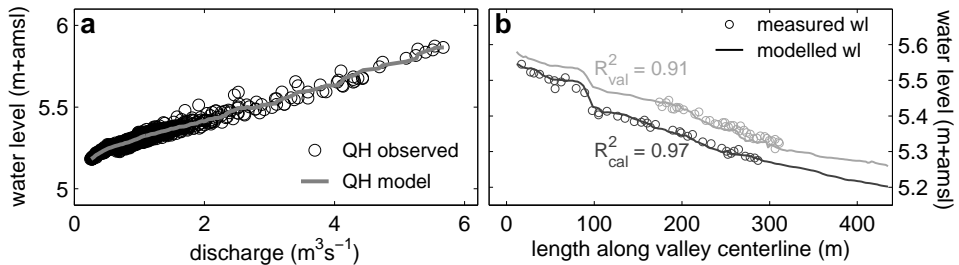


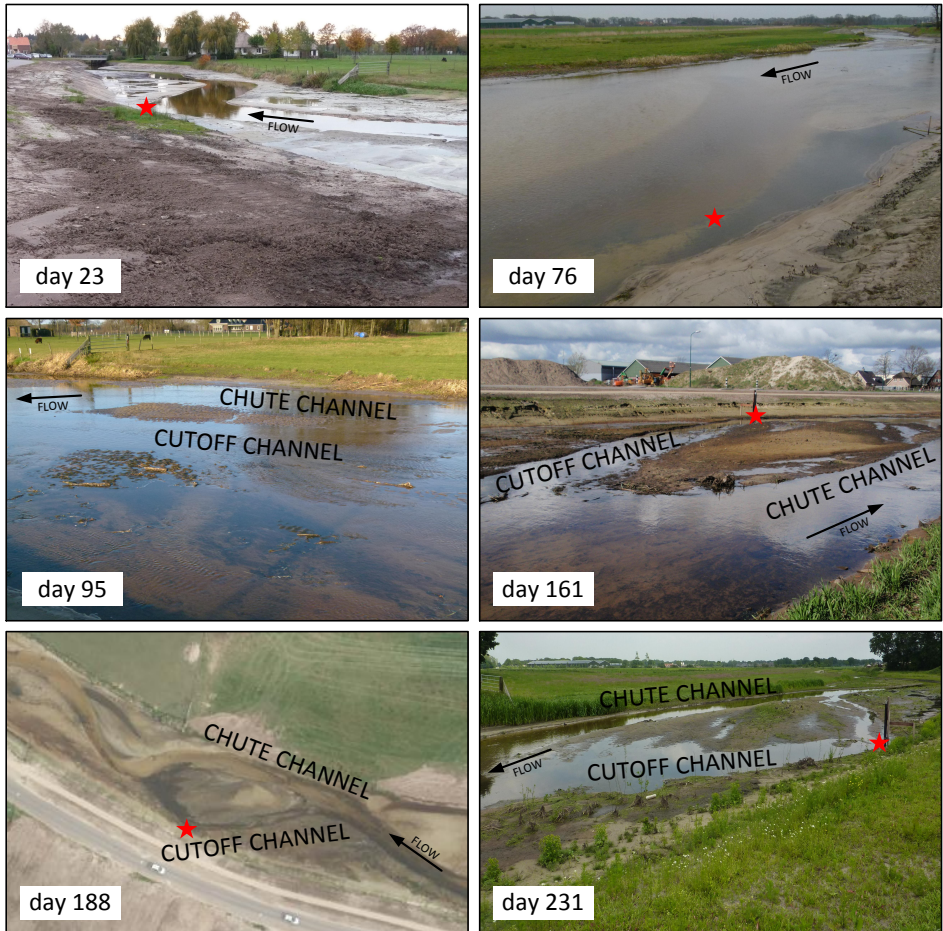
**Figure 5.4** Input for the hydrodynamic model, with (a) discharge-water level relation ( $Q$ - $H$  relation) and (b) the results of the calibration (dark grey) and validation (light grey) simulations. Panel (b) shows the measured and modelled longitudinal water level profile, including the coefficient of determination  $R^2$  as a measure of model performance.

## 5.4 Results

### 5.4.1 Field Results

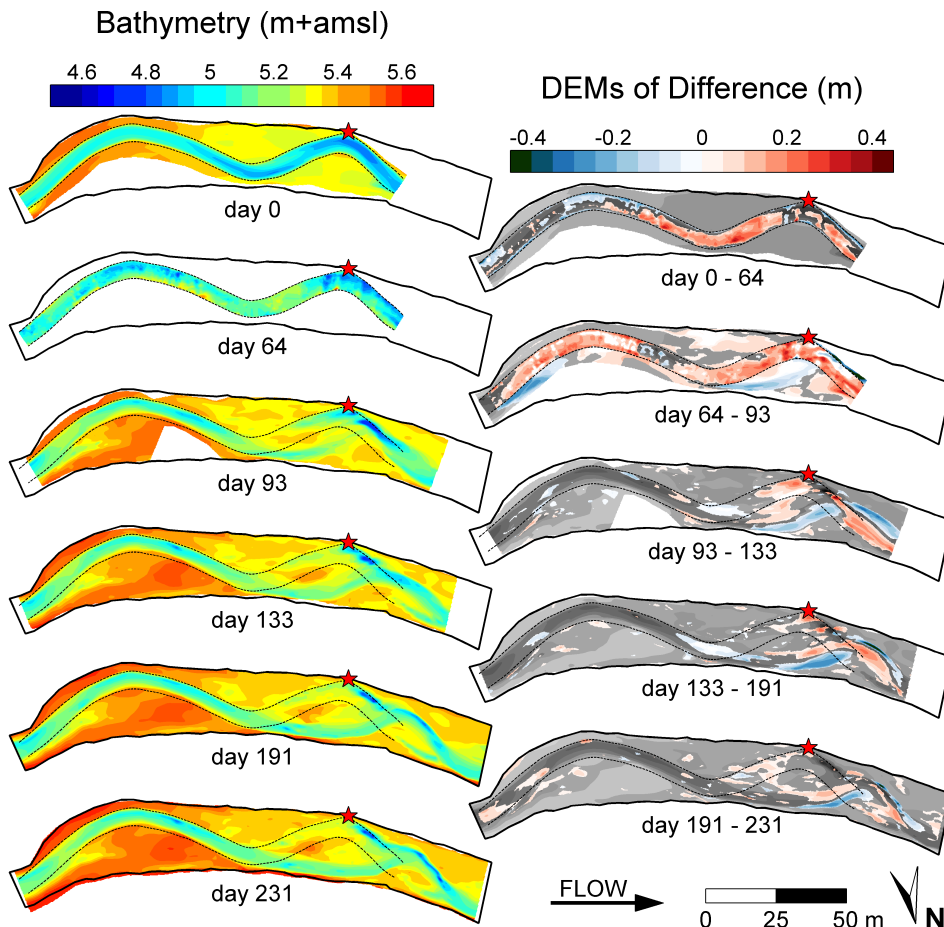
Figure 5.5 shows a sequence of 6 photos taken between 23 and 231 days after construction of the channel. The top-left figure shows the constructed sinuous channel planform. The photo clearly shows the channel was constructed in a lowered floodplain. Initially, the floodplain consisted of bare soil. After 95 days, the first distinction between the constructed (cutoff) channel and chute channel became visible. In the photo taken 161 days after construction and in subsequent photos, this distinction becomes more pronounced. The aerial photo (day 188) gives a good overview of the study area after the chute cutoff occurred. Vegetation started to appear after 231 days.

Figure 5.6 shows on the left side the bathymetry from the six morphological surveys, and on the right side the resulting erosion and deposition in the five subsequent periods. The first survey (day 0) shows the channel was constructed according to a regular sinuous pattern, with a sinuosity  $P = 1.24$ . Between the first two surveys, sediment was deposited in bend 2, with sedimentation locally exceeding 0.30 m. The third survey (day 93) shows more sediment was deposited in bend 2, which was at that moment cutoff from the main channel. The process of sedimentation of the cutoff channel continued in the subsequent period, albeit only in the downstream limb of the cutoff channel. The third survey shows an embayment had formed downstream of the apex of bend 2. This embayment continued to show incision into the floodplain at the fourth survey, resulting in a clear distinction between the constructed channel (indicated with the dashed lines) and the new channel.



**Figure 5.5** Sequence of photos from the study area. Photos are taken at 23, 76, 95, 161, 188 and 231 days after construction of the channel had finished. Flow is indicated with an arrow. The red stars indicate the apex of bend 3.

## 5. Chute Cutoff



**Figure 5.6** Digital Elevation Models and DEMs of Differences of all six morphological surveys. The number of days indicates the time since construction of the channel had finished. The dashed black lines indicate the location of the channel banks of the constructed channel. The red stars indicate the apex of bend 3, as indicated in Figure 5.5. On the left side of the figure, elevation is indicated in meters above mean sea level. On the right side of the figure, erosion is indicated in blue and deposition in red.

The newly formed channel bend migrated in downstream direction between the fourth and sixth survey, showing both erosion at the outer bank and accretion at the inner bank. Focusing on the upstream part of the study area, morphodynamic developments occurred between the second and third surveys in bend 1. In the upstream limb of bend 1, a topographic low had formed and sediment was also deposited around the apex of bend 1. In the subsequent surveys, only minor changes occurred in the upstream part of the study area.

Figure 5.7 shows the temporal evolution of both the channel centerline and the

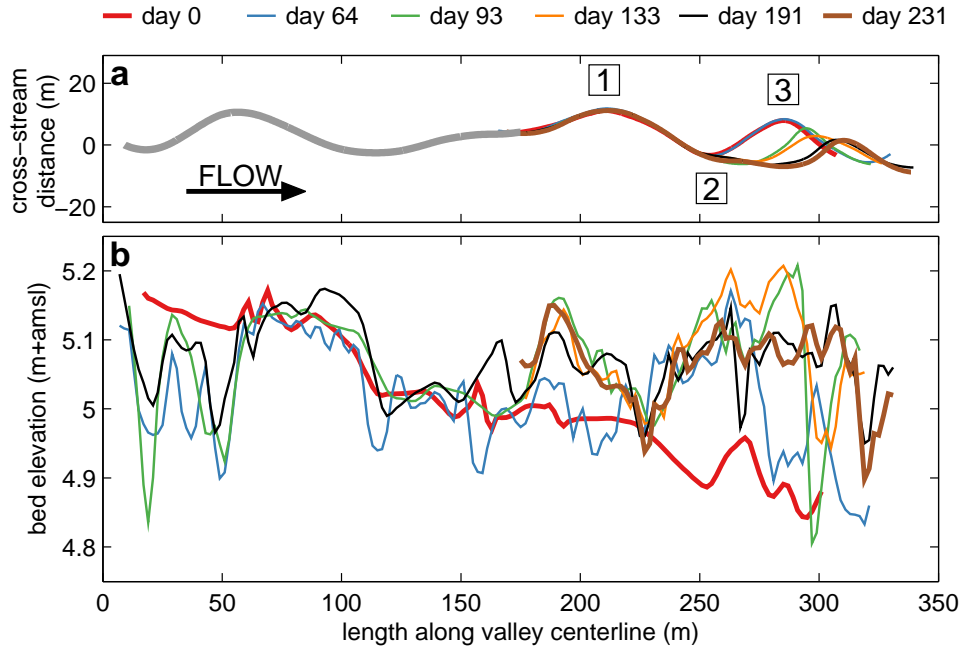


**Figure 5.7** (a) Temporal evolution of the channel centerline, which has been derived from the morphological surveys. (b) Temporal evolution of the longitudinal bed elevation. Bed elevation is obtained at each channel cross-section by averaging the measured cross-sectional data over the width of the channel bed, between the channel banks.

longitudinal bed elevation for all six morphological surveys. Morphological data obtained upstream from the main study area is also included in Figure 5.7b. In both figures, the  $x$ -axis is displayed as the length along the valley centerline. Figure 5.7a clearly shows the cutoff occurred between the second and third survey, after which bend 3 started to migrate in the downstream direction. When comparing the initial and final bed levels in Figure 5.7b, it appears that sediment was deposited in the downstream part of the study area. At the upstream end of the study area erosion occurred. This caused a dramatic reduction of the channel gradient, from  $0.96 \text{ m km}^{-1}$  to  $0.20 \text{ m km}^{-1}$ . When looking into more detail, Figure 5.7b shows that bend 1 featured only minor changes throughout the survey period, with deposition of sediment between the second and third survey being most apparent. The deposition of sediment in bend 2 had already started in the second survey, which was prior to the occurrence of the chute cutoff.

Figure 5.8 shows in red the grain size distribution of the sediment samples taken from the constructed channel. The figure shows in blue and red the grain size distributions of the deposited sediment in the cutoff channel, for the upper and

## 5. Chute Cutoff

**Table 5.2** Statistical parameters (median grain size, kurtosis and skewness) of the sediment samples taken in the constructed channel (day 0) and in the cutoff channel (day 341).

	median grain size ( $\mu\text{m}$ )	kurtosis (-)	skewness (-)
constructed channel bed	218	6.9	2.3
cutoff channel (upper)	172	10.1	2.9
cutoff channel (lower)	234	9.3	2.7

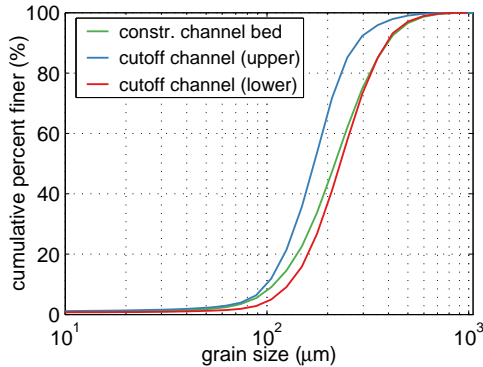
lower half of the deposited sediment layer, respectively. The figure clearly shows that the average grain size in the upper layer of the cutoff channel is finer than in the lower layer of the channel. The grain size of the constructed channel can be found in between the grain size distributions from for the upper and lower layers in the cutoff channel.

Table 5.2 shows three commonly used statistical parameters to describe grain size distributions, i.e. the median grain size, the kurtosis and the skewness. Both the kurtosis and the skewness are lower for the samples taken in the constructed channel. This indicates the sediment deposited in the cutoff channel is more uniform than the sediment present in the channel directly after construction.

Figure 5.9 shows the sediment characteristics of the sediment samples taken in the cutoff channel. Figure 5.9a shows sample locations of the 10 sediment cores. Figure 5.9b includes the morphological evolution of the channel bed elevation in the cutoff channel and shows sediment was first deposited in the upper limb of the cutoff bend. Sedimentation gradually continued in the downstream direction, until the entire cutoff channel was filled with sediment. Figure 5.9c shows in more detail the distinction between the finer upper layer and the coarser lower layer. The median grain size of the upper samples is finer than the grain size of the lower samples. Besides, the panel shows a downstream fining, where the deposited sediment is coarser in the upper limb of the cutoff channel (increased median grain sizes), both for the upper and lower samples.

### 5.4.2 Model Results

Figure 5.10 shows the results from the series of steady-state hydrodynamic model simulations, with in panel (a) the channel centerline from the first survey as a reference. Figure 5.10b shows the average cross-sectional bed shear stress within the channel banks, along the valley centerline. The panel also displays the critical



**Figure 5.8** Grain size distributions, with in green the grain size distribution from the constructed channel bed, and in blue and red the average grain size distributions of the upper and lower half of the deposited sediment in the cutoff channel, respectively.

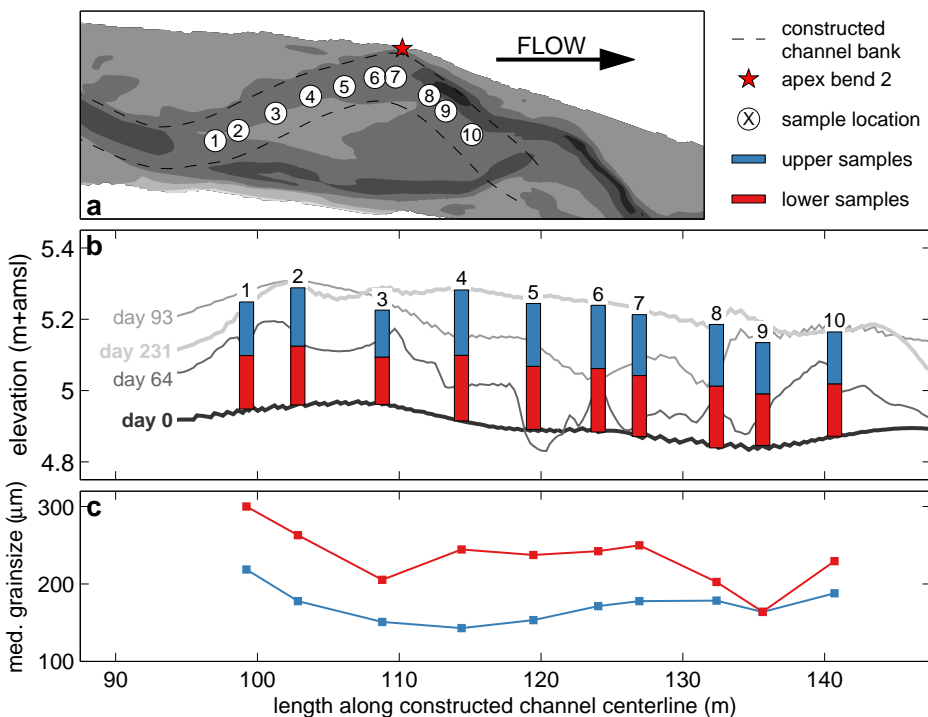


**Figure 5.9** Results of the sediment sampling taken approximately 1 year after the construction had finished: (a) plan view of the locations of the 10 sediment cores, (b) longitudinal profile along the cutoff channel showing the locations of the upper (blue) and lower (red) sediment cores and the surface level derived from four morphological surveys, and (c) median grain sizes.

## 5. Chute Cutoff

bed shear stress:

$$\tau_{\text{cr}} = \theta_{\text{cr}}(\rho_s - \rho)gd_{50} \quad (5.2)$$

where  $\theta_{\text{cr}}$  is the Shields parameter (-),  $\rho_s$  is the density of sediment,  $\rho$  is the density of water,  $g$  is the gravitational acceleration, and  $d_{50}$  is the median grain size. Attributing  $\theta_{\text{cr}} = 0.042$  (see Table 2.3 in Chapter 2),  $\rho_s = 2650 \text{ kg m}^{-3}$ ,  $\rho = 1000 \text{ kg m}^{-3}$ ,  $g = 9.81 \text{ m s}^{-2}$ ,  $d_{50} = 258 \mu\text{m}$ , this results in  $\tau_{\text{cr}} = 0.18 \text{ N m}^{-2}$ .

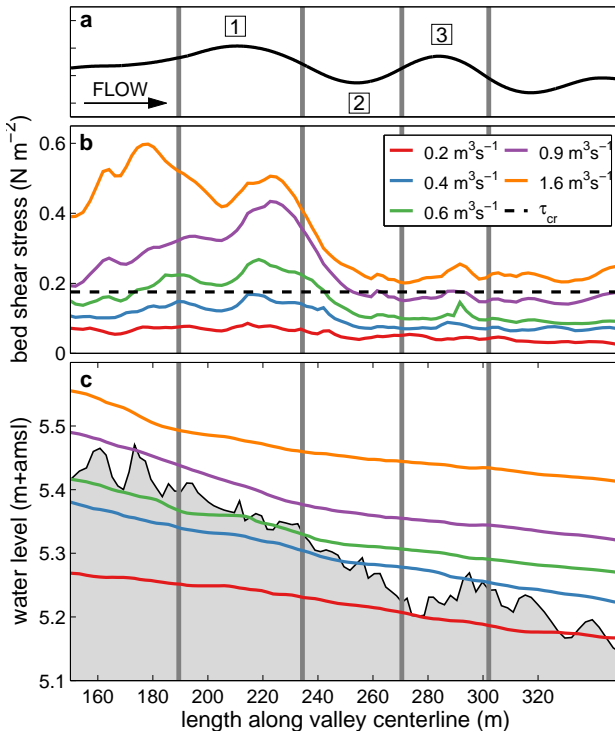
Figure 5.10b shows that the bed shear stress does not exceed its critical value in the whole study area for discharges smaller than  $0.4 \text{ m}^3\text{s}^{-1}$ . With discharges between  $0.4 \text{ m}^3\text{s}^{-1}$  and  $0.9 \text{ m}^3\text{s}^{-1}$ ,  $\tau_{\text{cr}}$  is exceeded in bend 1, but remains smaller in bend 2 and 3. For discharges exceeding  $0.9 \text{ m}^3\text{s}^{-1}$ , the bed shear stress in the channel exceeds  $\tau_{\text{cr}}$  in the whole study area.

Figure 5.10c reveals the reason for the apparent distinction between the upstream and downstream bed shear stress regimes, showing the longitudinal water level profiles from the five steady-state simulations. For the lower discharges, the water level profile is nearly linear. When discharge increases, the water level becomes bilinear, with the smallest water level slope in the downstream reach. Hence, a backwater curve appears in the upstream water level profile. This backwater curve is most likely caused by a bridge that narrows the floodplain width at the downstream end of the study reach (Figure 5.1d). Deceleration of the flow in the downstream part of the study area causes the flow velocities to decrease dramatically, and consequently, a negative gradient in bed shear stresses.

These results imply that for a range of discharges (i.e.  $0.4\text{-}0.9 \text{ m}^3\text{s}^{-1}$ ), bed material is entrained in bend 1, since bed shear stress exceeds the critical value and are increasing in downstream direction (upward gradient). Within this discharge range, bed material is likely to be deposited in bend 2, where bed shear stresses drop below the critical value and, moreover, are decreasing in downstream direction (downward gradient). In the period before the chute cutoff occurred, discharges remained for 24% of the time in this discharge range.

## 5.5 Discussion

Figure 5.11 shows a conceptual model of the main morphological processes that occurred in the period between construction and chute cutoff. Figure 5.11a shows the constructed channel planform (blue), within the lowered floodplain (yellow) and surrounded by meadow (green). The figure also indicates the location of the former straightened channel before re-meandering (brown), which was filled with sediment by the water authority following the construction of the new channel.



**Figure 5.10** Results from the hydrodynamic model: (a) Constructed channel centerline. Vertical lines indicate the inflection points for the three bends. (b) Spatial distribution of the bed shear stress for five steady state simulations, corresponding to discharges amounting to  $0.2, 0.4, 0.6, 0.9$  and  $1.6 \text{ m}^3\text{s}^{-1}$ , respectively. The dashed line indicates the critical bed shear stress  $\tau_{cr}$  (Equation 5.2). (c) The corresponding longitudinal water level profile, where the grey area indicates elevation below the channel banks.

Figure 5.11b presents a sketch of the deposition of sediment in bend 2 (red). This caused the flow to become directed across the point bar during flood events. An embayment formed at the apex of bend 2 (Figure 5.11c). The chute cutoff completed when the chute channel incised and widened into the floodplain, and more sediment was deposited in the cutoff channel. Consequently, the chute channel acted as the main channel, conveying the discharge most of the time (Figure 5.11d).

Prior to the cutoff event, a bar was deposited in the upstream limb of the cutoff bend. These bar forms are known as plug bars (Fisk, 1944). Plug bars in cutoff channels typically form in post-cutoff periods (e.g Johnson & Paynter, 1967; Hooke, 1995), when peak discharges formative for the chute channel have receded, and moderate discharges are divided over the parallel channels. Subsequently, flow is mainly concentrated in the steeper chute channel, causing channel incision and widening into the floodplain. In the cutoff channel, however, flow velocities drop

## 5. Chute Cutoff

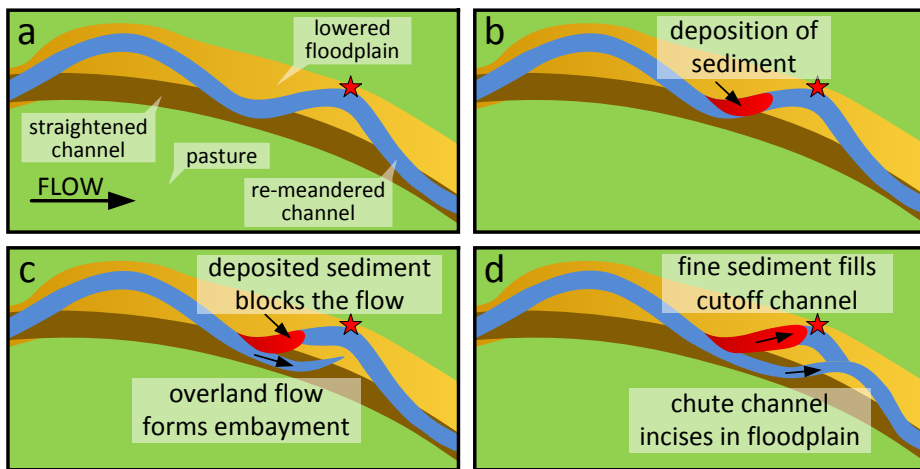


**Figure 5.11** Conceptual model of the main morphological processes, showing four stages in the development of the chute cutoff: (a) study area after construction, (b) formation of a plug bar, (c) initial embayment formation, (d) incision of the chute channel into the floodplain.

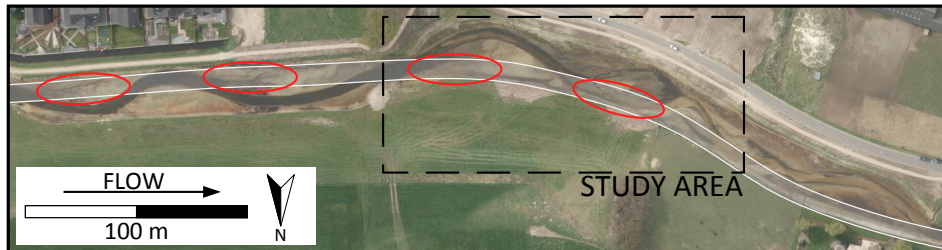


**Figure 5.12** Aerial photo taken 188 days after construction of the re-meandered channel. The shaded area indicates the former straightened channel and the red ovals the four locations along the former straightened channel where erosion is observed.

below the critical value, causing deposition of sediment in the form of a plug bar. In this case study, the plug bar can be considered the cause of the chute event, rather than a consequence. This finding confirms two recent laboratory experiments, reporting on pre-cutoff plug bar formation (Peakall *et al.*, 2007; Van Dijk *et al.*, 2012). In the experiments by Van Dijk *et al.* (2012), plug bars formed in response to an increase of overbank flow, causing deceleration of flow velocity, similar to these field observations. The numerical simulations in this study highlight the importance of backwater effects, which may be particularly relevant in restored streams, where the longitudinal water level is often influenced by downstream channel narrowing (e.g. by bridges and weirs).

The development of the plug bar must have been a very subtle process. The bed shear stress should have been sufficiently high to transport sediment from upstream. Figure 5.7 shows that erosion of the channel bed occurred at the upstream end of the study reach, hence, sediment was available from upstream. The backwater effect, caused by the floodplain narrowing near the end of the study reach, caused a downward sloping gradient in bed shear stresses in bend 2 (Figure 5.10). The combination of the available sediment from upstream and the resulting spatial variation of bed shear stresses caused by the backwater effect may explain why the plug bar formed in bend 2 (Figure 5.11b).

Figure 5.11c shows the initial chute formation coincides with a location where the former channel used to be located. The former channel was filled with sediment prior to the construction of the new channel. It is very likely that the sediment fills in the former channel were less consolidated than the rest of the floodplain. Therefore, the corresponding floodplain area was prone to erosion. The aerial photo in Figure 5.12 clarifies this observation. The photo shows that at several other locations, especially upstream from the main study area, erosion occurred in the floodplain where the former straightened channel used to be.

The deposition of sediment in the upstream limb of the bend to be cutoff and the location of the initial embayment show similarities with processes related to channel avulsions. A channel avulsion is the relatively rapid transfer of river flow out of an established section of the channel belt and into a new flow pathway on the adjacent floodplain (Mohrig *et al.*, 2000). An avulsion occurs when a new channel pathway is available which has gradient advantages over the existing channel pathway (Slingerland & Smith, 2003). The presented chute cutoff event may be interpreted as a local avulsion, which is an avulsion that forms a new channel in the adjacent floodplain, and rejoins the channel at a downstream location (Heller & Paola, 1996).

The processes that led to the chute cutoff in this case study (Figure 5.11b and 5.11c) may be related to the processes as observed in channel avulsions. Avulsions are often observed in net-depositional channels, e.g. anastomosing rivers and river deltas (Makaske *et al.*, 2002; Jerolmack & Mohrig, 2007). Besides, it has been recognized that avulsion frequency increases, with increasing upstream sediment supply (Ashworth *et al.*, 2004). In a river, net-deposition may also occur when the discharge pattern changes or when the channel gradient decreases (Slingerland & Smith, 2003). In meandering rivers, the latter may relate to sinuosity increase (due to meander migration) or base-level rise. Observations have shown that avulsion frequency increases when rivers are subject to base-level rise, eventually, resulting in channel bed aggradation (Törnqvist, 1994; Ethridge *et al.*, 2009). These findings

## 5. Chute Cutoff

show similarities with the consequences of the backwater effect in this case study. An avulsion may occur, when the channel bed level is not far below or even above the elevation of the adjacent floodplain (Mohrig *et al.*, 2000). The actual avulsion may be triggered by a flood event (Slingerland & Smith, 2003). Similar to chute cutoffs (Constantine *et al.*, 2010), the new channel is commonly located at the outer banks of meander bends, where flow velocities are high, confining levees are narrow, and flood flows impinge the banks at high angles (Slingerland & Smith, 2003). It has also been recognized that avulsions occur at locations where erodible substrate and active and abandoned floodplain channels are present (Aslan *et al.*, 2005).

Existing studies on post-cutoff morphodynamics describe the sequence of morphological developments in the chute channel following the cutoff, showing bed scour followed by a period characterized by extensive bank erosion and lateral channel migration (Hooke, 1995; Fuller *et al.*, 2003) and channel widening (Zinger *et al.*, 2013). These observations agree with the current observations. After the initial chute channel had formed, the channel gradually incised and widened into the floodplain. The channel bend migrated in the downstream direction, consistent with previous observations (Hooke, 1995; Fuller *et al.*, 2003).

This case study also presents the morphological evolution before and during the cutoff. Figure 5.13 shows the temporal evolution of the sinuosity and dimensionless wavelength over the whole study period. The cutoff occurred in bend 3, which is clearly visible from the evolution of the sinuosity. No change of sinuosity was observed between the first two morphological surveys. The chute cutoff roughly occurred between survey 2 and 3, causing a reduction of the channel sinuosity. The sinuosity reduced until survey 4, after which it increased. Bend 3 shows a reducing dimensionless wavelength over the whole study period. In bend 2, a reduction of the sinuosity is observed from survey 2 to 5 and an increase of the dimensionless wavelength. In bend 1, no significant changes were observed for the sinuosity and dimensionless wavelength.

In bend 3, the most significant difference between the constructed planform geometry and the geometry after the chute cutoff occurred is the reduced dimensionless wavelength. The channel sinuosity at survey 6 nearly equals the constructed sinuosity of this bend. Chapter 6 includes the morphological evolution of this stream restoration project in the following year after survey 6. The results of the subsequent morphological surveys show that only minor changes occurred with respect to the channel centerline. The temporal evolution of the characteristics of cutoff bend (bend 3) clearly show that the process of channel cutoff occurred in the same rate as channel recovery.

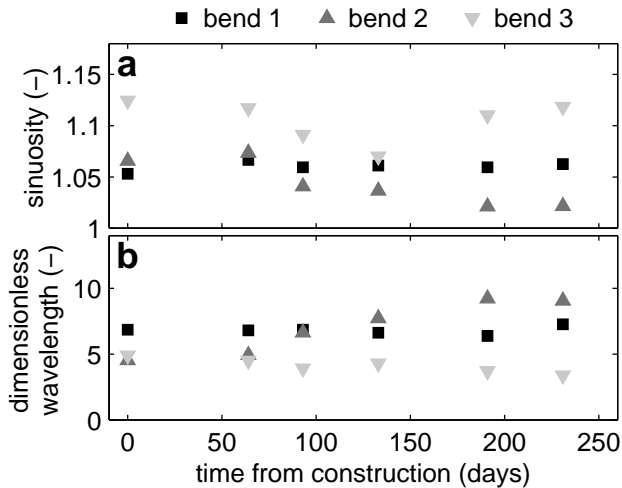


**Figure 5.13** Temporal evolution of two bend characteristics for the three bands within the study reach: (a) sinuosity (-), and (b) dimensionless wavelength (-). The dimensionless wavelength is defined as the wavelength divided by the initial channel width.

## 5.6 Conclusions

In a restored lowland stream, subject to a relatively natural, flashy discharge, a chute cutoff occurred within three months after construction of a stream restoration project. As part of a research project to establish post-project morphological changes in this stream restoration project, a detailed monitoring plan was implemented. This allowed for an unprecedented opportunity to analyse the bathymetry before, during and after the chute channel formation. The field results confirm the following inferences from previous, more indirect studies: (1) sediment was deposited in the upstream limb of the cutoff channel, prior to the cutoff event, (2) an embayment formed along the outer bank, upstream of the meander that underwent cutoff, (3) the chute channel incised and widened into the floodplain, and (4) the deposited sediment in the cutoff channel showed upward fining.

Similar to recent laboratory experiments, a plug bar formed prior to the chute cutoff. The plug bar formed in response to a backwater effect, caused by a narrowed cross-sectional shape at the downstream end of the study area. The embayment, triggering the chute cutoff, initiated at a location where the former channel was located, i.e. where the erosion resistance may expected to be low. An aerial photograph reveals that the morphological response is markedly different in the areas where the former channel was located. The main morphological process that led to

## 5. Chute Cutoff

the chute cutoff, i.e. aggradation of the channel bed, shows similarities with processes that have been observed in channel avulsions, which occur in net-depositional river systems. The results of this case study may be relevant for the initial period after the construction of a stream restoration project. Often channel slope reduction is observed in the initial period after construction, mainly due to loose sediment and an inappropriate initial channel slope. Under specific circumstances, the reduction of the channel slope may lead to chute cutoffs or other pronounced morphological changes, which potentially may be a threat for adjacent agricultural fields and structures.

# 6 | Riparian Vegetation



---

Based on: EEKHOUT, J. P. C., FRAAIJE, R. G. A., & HOITINK, A. J. F. (*under review*). Morphodynamic regime change in a restored lowland stream. Submitted to *Earth Surface Dynamics*.

## 6.1 Introduction

Riparian zones play an essential role in restoration of aquatic systems (Naiman & Décamps, 1997) and are have strong control on fluvial landforms (Corenblit *et al.*, 2007). Stream restoration in the Netherlands increasingly involves the development of riparian zones along the restored channel reaches. These riparian zones are constructed to accommodate water during flood events, and to improve the connection between aquatic and terrestrial ecology. This chapter will focus on the effect of riparian vegetation on meander morphodynamics in a restored lowland stream.

Riparian vegetation adds strength to the soil. Root mass is linearly related to soil shear strength, such that even low root densities can provide a substantial increases in shear strength of the soil matrix. Root-reinforced soils are more resistant to deformation and failure than bare soils (Abernethy & Rutherford, 2001). The stabilizing effect of riparian vegetation has an impact on meandering of rivers and streams at various spatial scales. The importance of riparian vegetation in contributing to channel bank stability is widely recognized (e.g., Simon & Collison, 2002; Pollen-Bankhead & Simon, 2009). The mechanical effect of riparian vegetation causes an increase of bank stability, through the increase of tensile strength of the soil. On the other hand, hydrological processes could cause a decrease of bank stability, including increase of pore-water pressure due to higher infiltration through macropores (Simon & Collison, 2002).

River meandering processes may induce variation in riparian vegetation biomass density (Perucca *et al.*, 2006). Perucca *et al.* (2007) constructed a process-based vegetation model, coupled with a fluid dynamics model. Their results show that riparian vegetation is potentially responsible for changes in meander planform characteristics, including wavelength and skewness. On a reach scale, riparian vegetation affects channel patterns. Recently, laboratory experiments have shown how riparian vegetation may stabilize floodplain material, causing initial braided channel patterns to shift towards single-thread (meandering) channels (Gran & Paola, 2001; Braudrick *et al.*, 2009; Tal & Paola, 2010). Van de Wiel & Darby (2004) studied morphological developments at the reach-scale in a numerical model. They showed that riparian vegetation density and root structure were the most influential parameters controlling reach-scale morphodynamics.

Details of hydrological disturbances, such as duration, intensity, frequency and extent of floods, include the most important factors influencing riparian vegetation development (Pedersen *et al.*, 2006; Merritt *et al.*, 2010). Biological and chemical processes form secondary controls on species presence and abundance (Gurnell

*et al.*, 2012). The influence of hydrological disturbances on riparian vegetation is most apparent in lowland areas, where floodplains are typically broad and flat. In these areas, species-specific responses to hydrological disturbances are related to soil moisture/oxygenation, sediment deposition, the frequency and duration of inundation, and the erosive action of flooding (Ward *et al.*, 2002). Each riparian species has a different tolerance and growth response to hydrological disturbances (Gurnell *et al.*, 2012). These differences affect the spatial distribution of species according to topography, sediment texture and landform stability within the riparian zone, both in lateral (Johnson *et al.*, 1995; Naiman *et al.*, 2005) and longitudinal direction (Bertoldi *et al.*, 2011). In a stochastic model study, Camporeale & Ridolfi (2006) showed how random variation in river discharges results in lateral variability of the distribution of riparian vegetation. Camporeale & Ridolfi (2010) extended this model with a physically-based morphodynamic model (Zolezzi & Seminara, 2001). They showed that active meander processes affect the development of riparian vegetation, especially in high-curvature bends. This chapter zooms into a low-energy stream environment, showing how riparian vegetation may have contributed to the morphodynamic developments that occur in an initial, pre-vegetation stage after construction of the channel.

Serial digital elevation models (DEMs) offer the opportunity to quantify reach-scale morphological change. Several survey techniques have been used to collect topographic data for DEM construction in fluvial environments, including total station (Fuller *et al.*, 2003), ground-based GPS (Brasington *et al.*, 2003), photogrammetry (Lane *et al.*, 2010), unmanned radio-controlled platforms (Lejot *et al.*, 2007), Terrestrial Laser Scanning (TLS; Wheaton *et al.*, 2013) and airborne LiDAR (Croke *et al.*, 2013). Temporal morphological changes could be detected when a study reach is surveyed more than once. A DEM of Difference (DoD) may quantify morphological changes when comparing two serial DEMs (Lane *et al.*, 2003). DoD in braided rivers have been extensively applied on reach-scale (e.g., Lane *et al.*, 2010; Wheaton *et al.*, 2010a, 2013). DoD analysis in meandering rivers is often restricted to bend-scale (e.g., Gautier *et al.*, 2010; Kasvi *et al.*, 2013), although there are several exceptions in meandering rivers (Fuller *et al.*, 2003; Erwin *et al.*, 2012; Croke *et al.*, 2013). Until now, DoD analyses are typically based on annual (e.g., Wheaton *et al.*, 2013) or bi-annual surveys (Fuller *et al.*, 2003; Lane *et al.*, 2010). The low temporal resolution can cause erosional and depositional patches to overlap, complicating sediment budget estimation. Besides sediment budget estimation, DoD analysis has been used to relate individual erosional and depositional patches to morphological and ecological processes (e.g., Grove *et al.*, 2013; Wheaton *et al.*, 2010b), often called DoD segregation.

## 6. Riparian Vegetation

A field study is presented, based on 14 high-resolution surveys over a period of almost two years. The study focussed on a reach-scale study site, covering three meander bends and the adjacent floodplain. Morphological and terrestrial ecological data are combined, under varying discharge conditions. The field study is performed in a stream restoration project. Stream restoration projects are rarely subject to monitoring schemes combining morphological, hydrological and ecological surveys, although there are exceptions (e.g., Gurnell *et al.*, 2006). The objective is to establish and understand the morphological response of a restored lowland stream to riparian vegetation development and varying discharge conditions.

## 6.2 Study Area

In October 2011 a stream restoration project was realized in a small lowland stream, the Lunterse Beek, located in the central part of the Netherlands ( $52^{\circ} 4' 46''$  N,  $5^{\circ} 32' 30''$  E), see Figure 6.1. A straightened channel was replaced by a new channel with a sinuous planform. The course of the new channel crosses the former channel at several locations (Figure 6.1c). The new channel was constructed with a width of 6.5 m, a depth of 0.4 m and a longitudinal slope of  $0.96 \text{ m km}^{-1}$ . A lowered floodplain surrounded the channel, with an average width of 20 m, see Figure 6.1d. The bed material mainly consists of fine sand, with a median grain size of  $258 \mu\text{m}$ .

Figure 6.1b shows the location of the study area in the catchment. The catchment has an area of  $63.6 \text{ km}^2$ . The elevation within the catchment varies between 3 to 25 m above mean sea level. The study area is located in a mildly sloping area. The subsurface of the catchment mainly consists of aeolian-sand deposits. The average yearly precipitation amounts to 793 mm (KNMI, 2014). The average daily discharge amounts to  $0.33 \text{ m}^3 \text{ s}^{-1}$  and the peak discharge during the study period was  $6.46 \text{ m}^3 \text{ s}^{-1}$ .

A chute cutoff occurred within 3 months after realization of the stream restoration project, which has been described in Chapter 5. Prior to the cutoff, a plug bar was deposited in the bend to be cutoff. Hydrodynamic model results show that the location of the plug bar coincides with the region where flow velocity drops below the threshold of sediment motion, indicating the sediment deposition was caused by a backwater effect. Upstream from the plug bar, an embayment formed in the floodplain at a location where the former channel was located. The former channel was filled with sediment prior to channel construction. The sediment fills originated from other parts of the study area, where excess sediment was available from the construction of the new channel. It is likely that the sediment at this location was less consolidated, and therefore, was prone to erosion. The chute channel continued

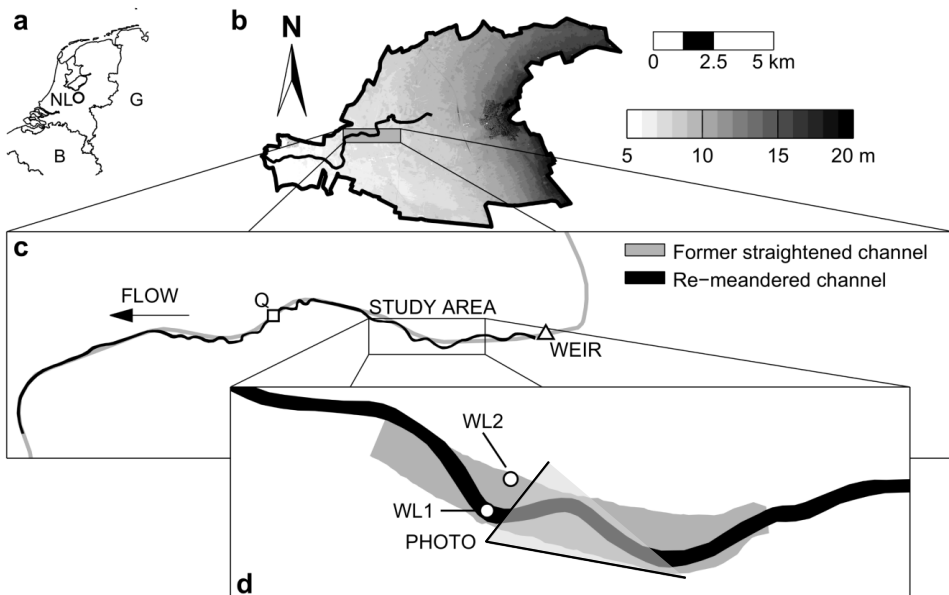


**Figure 6.1** Overview of the study area: (a) location of the study area in the Netherlands, (b) elevation model of the catchment (Actueel Hoogtebestand Nederland, AHN; Van Heerd *et al.*, 2000), (c) planform of the restored reach, with the squared marker indicating the location of the discharge station (Q), and (d) sketch of the study area, indicating the location of the water level gauges (WL1 and WL2) and the approximate extent of available terrestrial photos (grey-shaded triangle, Figure 6.8).

to incise and to widen into the floodplain and, after 6 months, acted as the main channel, conveying the discharge during the majority of time.

## 6.3 Material & Methods

### 6.3.1 Morphological Monitoring

The temporal evolution of the bathymetry has been monitored over a period of almost two years. Morphological data were collected in the area within the lowered floodplain over a length of 180 m, indicated by light grey in Figure 6.1d. Morphological data were collected with an average frequency of 52 days, using Real Time Kinematic (RTK) GPS-equipment (Leica GPS 1200+ for the surveys 1-13 and Leica Viva GS10 for survey 14) to measure surface elevation with an accuracy between 1 and 2 cm. The surface elevation data were collected along cross-sections between the two floodplain edges. The survey strategy proposed by Milan *et al.* (2011) was

**Table 6.1** Overview of all morphological measurements, with point density (PD, points m<sup>-2</sup>) and anisotropy factor (AF) as used in the interpolation routine, specified for the channel (ch.) and floodplain (fp.) areas, respectively.

Survey no.	Survey date (day)	No. data points	PD (all)	PD (ch.)	AF (ch.)	PD (fp.)	AF (fp.)
1	0	379	0.16	0.25	9.74	0.12	4.59
2	93	956	0.32	0.44	5.04	0.24	2.35
3	133	918	0.27	0.34	3.57	0.24	2.15
4	191	742	0.20	0.31	4.24	0.15	2.04
5	231	1158	0.30	0.45	4.19	0.24	2.09
6	288	1376	0.35	0.53	4.42	0.29	2.15
7	341	1296	0.32	0.50	4.04	0.26	1.86
8	377	1655	0.42	0.62	3.56	0.35	1.68
9	426	1484	0.39	0.58	3.50	0.31	1.64
10	454	1472	0.36	0.55	4.12	0.30	2.03
11	489	1420	0.35	0.51	4.08	0.29	2.05
12	525	1462	0.37	0.56	4.66	0.29	2.15
13	558	1256	0.31	0.50	4.08	0.24	1.77
14	672	1501	0.44	0.85	10.66	0.23	2.67

followed, focusing on breaks of slope. Following this strategy, the point-density was increased in the vicinity of steep slopes (e.g. channel banks), and decreased the point-density on flat surfaces (e.g. floodplains). Digital Elevation Models (DEMs) and DEMs of Difference (DoDs) of each of the fourteen datasets were constructed. The same method was used as described in Section 5.3.2. Table 6.1 lists the point density and anisotropy factors for all fourteen surveys, specified for the channel and floodplain sections.

### 6.3.2 Quantifying Morphological Activity

Morphological activity was quantified for the study area as a whole, and for isolated geomorphic zones. The study area was segregated into four geomorphic zones: channel bank, channel bed, floodplain, and cutoff channel. Figure 6.2a shows an example of the distribution of each of the four geomorphic zones in the study area, for period (4-5), day 191-231. Segregation of each of the four geomorphic zones was accomplished as follows. The channel bank mask is defined as the zone between the channel bank lines of two subsequent surveys, plus a strip of 0.5 m width on either side of the zone. The channel bed mask is defined as the zone between the two channel bank masks. The remainder of the grid domain is labelled as floodplain, with the cutoff channel considered as a separate geomorphic zone. Finally, each of the patches of morphological change was attributed to one of the geomorphic features (Figure 6.2b).

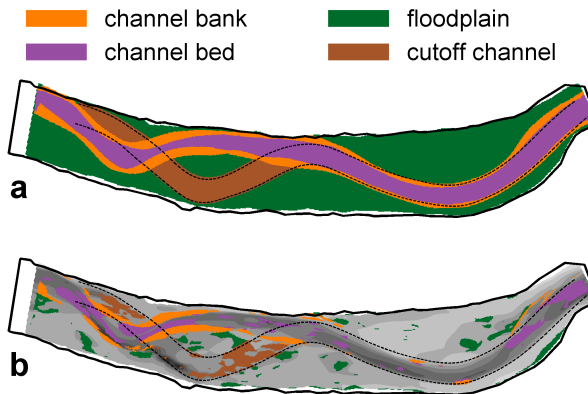


**Figure 6.2** Segregation of geomorphic zones, for period (4-5). (a) Masks of each of the four geomorphic zones, including channel bank (orange), channel bed (purple), floodplain (green), and cutoff channel (brown). (b) Resulting segregation.

Two methods were applied to quantify morphological activity. First, the volumetric change in sediment storage was determined. Volumetric change in sediment storage was determined by multiplying the elevation change by the grid cell area, distinguishing gross erosion and gross deposition. Net sediment change was determined by subtracting gross erosion from gross deposition. Second, The root-mean-square elevation difference was determined:

$$RMSD = \sqrt{\frac{\sum(z_{i,j}(new) - z_{i,j}(old))^2}{n}} \quad (6.1)$$

where  $z_{i,j}$  is the elevation in grid cell  $i,j$  of the DEM and  $n$  is the number of grid cells. The volumetric change in sediment storage and the root-mean-square elevation difference were expressed as a rate of change, by dividing both quantities by the time between two successive surveys.

### 6.3.3 Hydrological Monitoring

Discharge data were collected downstream of the study reach at a discharge measurement weir, indicated with  $Q$  in Figure 6.1c. Discharge estimates were acquired with a one-hour frequency. Water level data were collected at a water level gauge in the study area, indicated with WL1 in Figure 6.1d. The water level gauge started monitoring 103 days after construction of the channel. The water level gauge was accidentally placed in the cutoff channel. After day 288, the water level gauge was moved to a new location, on the other side of the floodplain, indicated with WL2 in Figure 6.1d. Water level data were acquired with a one-hour frequency. Longitu-

## 6. Riparian Vegetation

dinal water level profiles were measured with RTK-GPS equipment during thirteen of the fourteen morphological surveys.

### 6.3.4 Riparian Vegetation

The restored stream was constructed in bare soil. Riparian vegetation started to develop halfway the first year. The spatial distribution of the riparian vegetation was obtained from two aerial photographs, taken at day 289 (July 2012) and at day 636 (July 2013). The aerial photographs were taken with a 25 cm resolution. Figure 6.3a shows an example of the aerial photograph taken at day 289. The aerial surveys also included Colourized Infra-Red (CIR) images (Figure 6.3b), which contain data from the Near Infra-Red (NIR) wavelengths (0.78-3  $\mu\text{m}$ ). With these data the riparian vegetation development at these two dates was quantified with the Normalized Difference Vegetation Index (NDVI):

$$\text{NDVI} = \frac{\text{NIR} - \text{VIS}}{\text{NIR} + \text{VIS}} \quad (6.2)$$

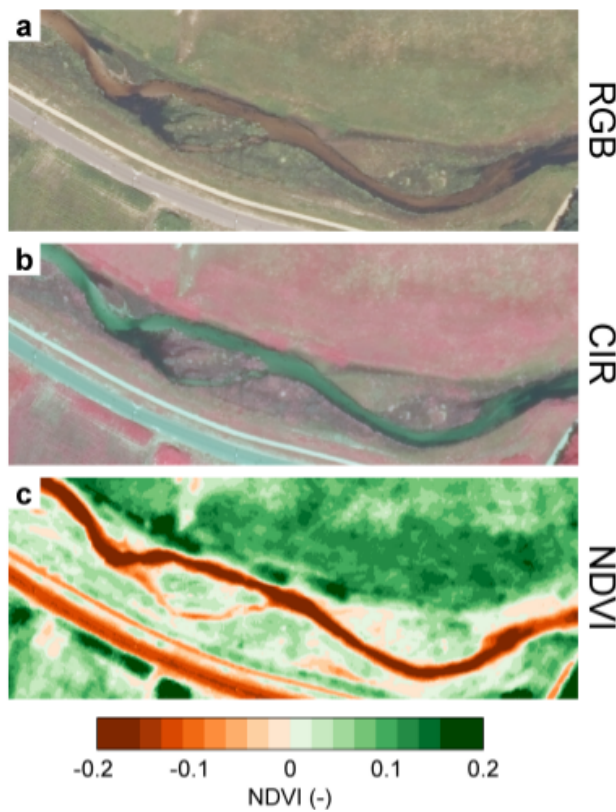
where NIR is the intensity of the Near Infra-Red wavelengths and VIS is the intensity of the VISible red wavelengths. Equation 6.2 was applied to the entire image, from which the spatial variation of the NDVI within the study area was obtained. NDVI varies between -1.0 and 1.0. Positive values generally correspond to vegetation, whereas negative values correspond to water, or other media that adsorb the infra-red wavelengths (Clevers, 1988).

Figure 6.3c shows the NDVI, from the first aerial survey, for the study area and surrounding agricultural fields and roads. The panel clearly shows positive values for the pasture area on the north-side of the study area. Negative values are obtained inside the channel and on the road, on the south-side of the study area. The obtained NDVI values within the study area are in a range of 0 to 0.2, which is associated with bare soil (Holben, 1986). Nevertheless, the aerial photo and field observations show that vegetation was present in the study area, where positive NDVI-values corresponded to vegetation. Therefore, further analysis only considers the areas where a positive NDVI-values is obtained.

## 6.4 Results

### 6.4.1 Morphodynamics

Figures 6.4 and 6.5 show the DEMs and DoDs of the fourteen morphological surveys, respectively. The first three surveys (day 0, 93 and 133) show the sequence of



**Figure 6.3** An example of the first aerial photograph from which the NDVI was determined, showing (a) the RGB-image (Red, Green, Blue), (b) the CIR-image (Colourized Infra-Red), and (c) the NDVI. In panel (c), the green coloured areas indicate positive NDVI-values and orange coloured areas indicate negative NDVI-values. All images have a 25 cm resolution.

morphological changes that capture the chute cutoff event. The first DoD (day 0-93) shows deposition of sediment on the channel bed, which is associated with the formation of a plug bar (Chapter 5). An initial embayment had formed upstream from the bend to be cutoff. The actual cutoff occurred in the second period (day 93-133), where a new channel incised into the floodplain. In the subsequent period (day 133-231), the morphological changes occurred mainly in the bend at the downstream end of the study area. During this period, in this bend both erosion of the outer bank and accretion in the inner bank were observed. Maximum bank erosion amounted to 2.5 m between day 133 and 191 (2.6 channel widths per year). Subsequently, there was a period of little morphological change (day 231-288). In the last period (day 341-672), morphological changes were restricted to

## 6. Riparian Vegetation

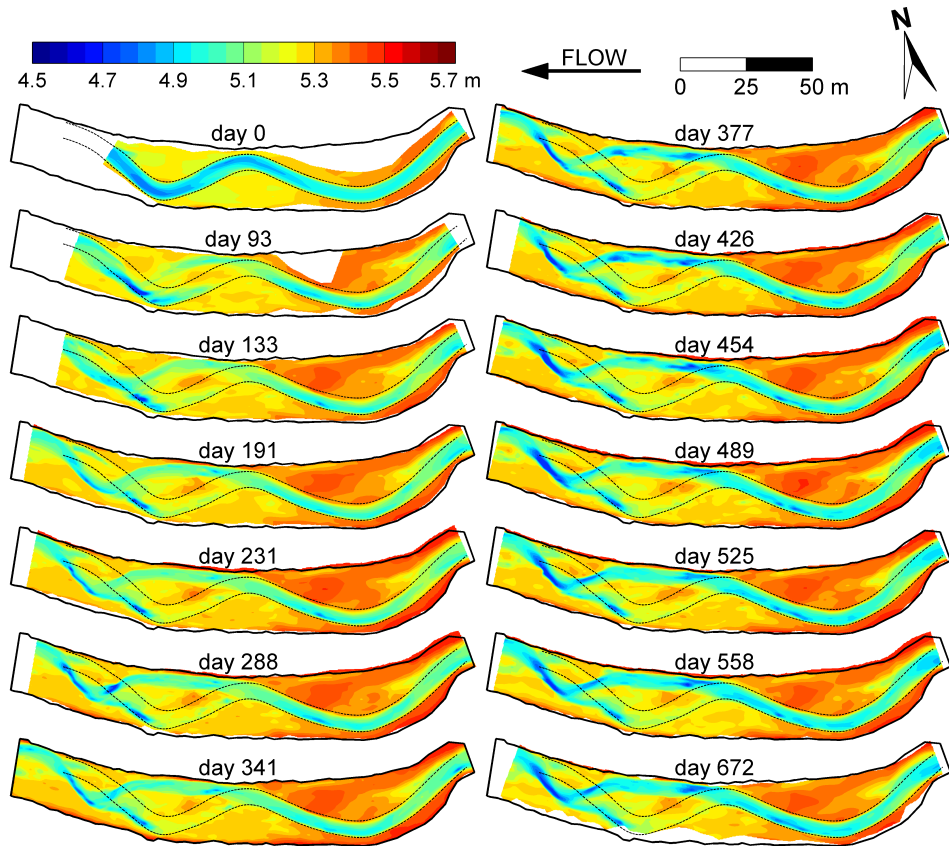
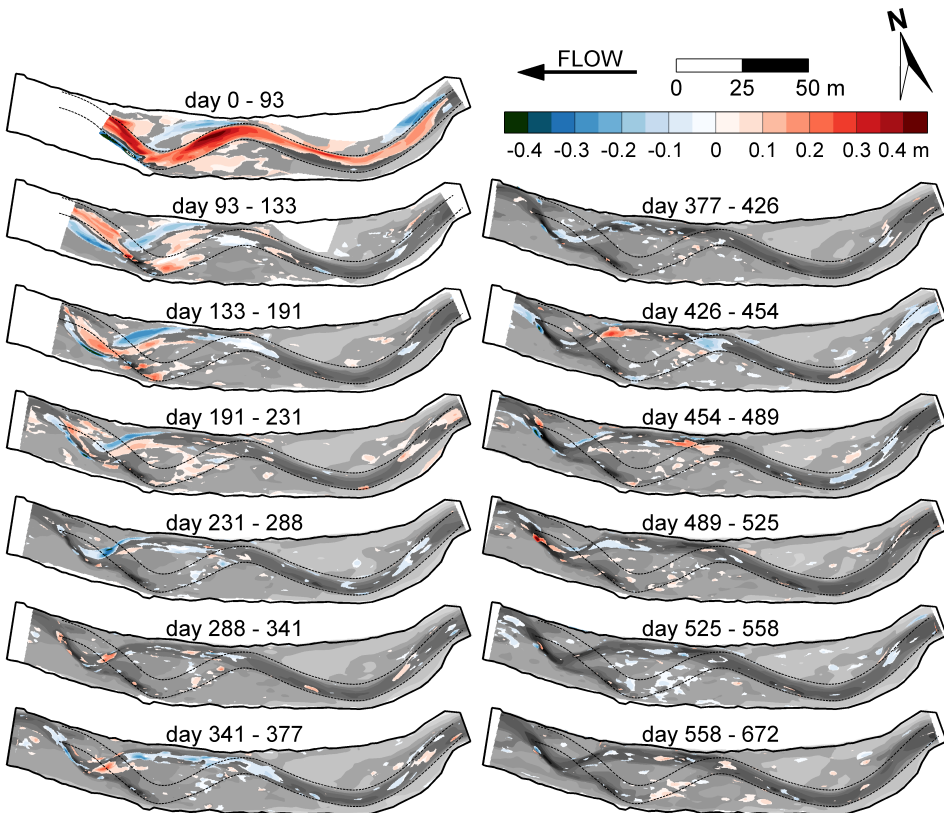


**Figure 6.4** Digital Elevation Models (DEMs) of all fourteen morphological surveys. The number of days indicates the time since construction of the channel. The dashed black lines indicate the location of the channel banks of the constructed channel. The solid black line surrounding the DEMs indicates the extent of the seventh morphological survey (day 341). Elevation is indicated in meters above mean sea level.

the channel bed and banks. Maximum bank erosion amounted to 0.7 m between day 341 and 377 (1.2 channel widths per year). At that time, little morphological change was observed in the floodplain.

Overall, dynamics of the bed level is highest in the downstream half of the study area. Figure 6.4 clearly illustrates the channel bed incision of the bend at the downstream end of the study area, in the period following the chute cutoff. The upstream half of the study area did not show pronounced morphological changes. Apart from occasional changes in the channel bed, no structural bank erosion or accretion was observed.

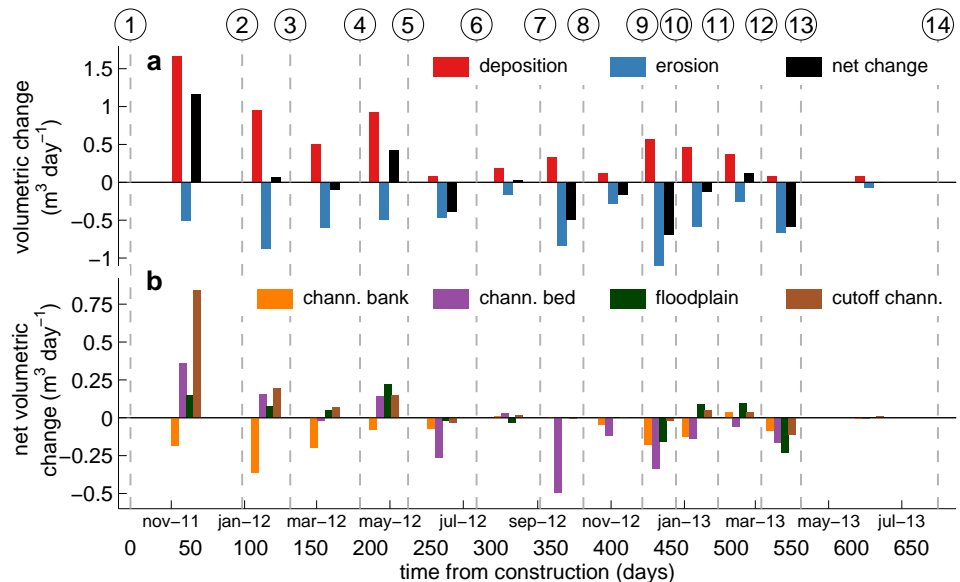
Figure 6.6 shows the sediment budget, derived from the DoDs (Figure 6.5).



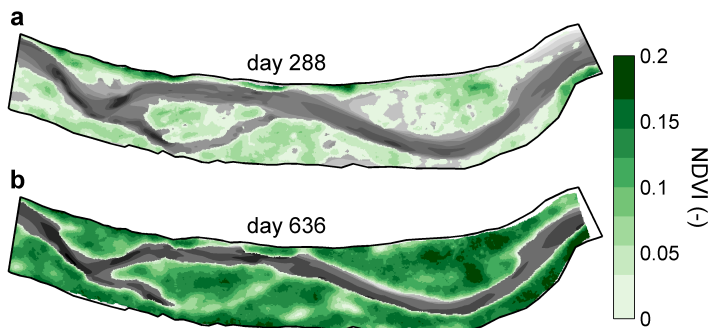
**Figure 6.5** DEMs of Difference (DoDs) of all thirteen periods between the fourteen morphological surveys. The number of days indicates the time since construction of the channel. The dashed black lines indicate the location of the channel banks of the constructed channel. The solid black line surrounding the DEMs indicates the extent of the seventh morphological survey (day 341). Erosion is indicated in blue and deposition in red. The DEM of the first of the two DEMs is shown in grey-scale.

Figure 6.6a shows volumetric change over the study area as a whole, aggregated for regions of erosion and deposition, and net change. Figure 6.6b shows the volumetric change, subdivided per geomorphic zone. Considering the study area as a whole (Figure 6.6a), a shift from net deposition to net erosion is observed. In the first period (1-2), deposition is mainly caused by the deposition of sediment in the channel bed and the cutoff channel. This is followed by a period (2-4) of limited net change, where bank erosion is balanced by net deposition in the rest of the study area. From the fifth survey onwards, the sediment balance shifts towards net erosion. Channel bed processes (channel bed incision) are the dominant contributor to the net erosion of sediment in the study area.

## 6. Riparian Vegetation



**Figure 6.6** Temporal evolution of the volumetric change in sediment storage. (a) Volumetric change in sediment storage ( $\text{m}^3 \text{ day}^{-1}$ ), for regions of deposition (red), erosion (blue), and net change (black). (b) Volumetric change in sediment storage ( $\text{m}^3 \text{ day}^{-1}$ ), specified per geomorphic feature, with channel bank (orange), channel bed (purple), floodplain (green), and cutoff channel (brown). The dashed vertical lines indicate the surveying moments, the numbers at the top of the figure correspond with the numbers in Table 6.1.



**Figure 6.7** Riparian vegetation cover derived from aerial photographs taken on (a) day 289 (July 2012) and (b) day 636 (July 2013). The two panels only show the positive NDVI values, with the DEM from survey 6 and survey 12 in grey-scale as a reference.

### 6.4.2 Riparian Vegetation Development

Figure 6.7 shows the positive values of the NDVI in the study area, obtained from the two aerial photographs. The figure clearly shows that riparian vegetation cover increased from the first to the second year. Riparian vegetation cover (observed as a positive NDVI-value) amounted to 56% of the study area in the first year and 77% of the study area in the second year. At the time of the first aerial photograph, riparian vegetation covered 33% of the channel bank zone, 3% of the channel bed zone, 80% of the floodplain zone, and 57% of the cutoff channel zone. This shows riparian vegetation did not develop as abundantly in the cutoff channel as in the rest of the floodplain. There is also a clear distinction between channel (bed and bank) and floodplain. At the time of the second aerial photographs, riparian vegetation covered 84% of the channel bank zone, 22% of the channel bed zone, 97% of the floodplain zone, and 92% of the cutoff channel zone. The cover increased in all geomorphic zones, where the channel bank, floodplain, and cutoff channel zone were almost totally covered with riparian vegetation.

Figure 6.8 shows the series of fourteen oblique terrestrial photos taken from the location indicated in Figure 6.1d. Just after construction had finished at day 0 (first photo of row one), riparian vegetation was visible on the left channel bank. Overall, riparian vegetation was absent in the floodplain. In the subsequent period, until day 161 (third photo of row one), no change in riparian vegetation coverage was observed. Riparian vegetation started to develop around day 231 (first photo of row two). Some patches of riparian vegetation were emerging in the floodplain and at the channel banks. The development of riparian vegetation continued in the following period and a maximum riparian vegetation coverage was observed at day 341 (last photo of row two). At that moment, the floodplain was almost entirely covered with riparian vegetation. Only in the cutoff channel, riparian vegetation did not develop as abundantly as in the floodplain, see also Figure 6.7a. In the period until the end of the study period, from day 377 (first photo of row three) until day 558 (the last photo of row four), the riparian vegetation cover started to decrease, approximately to a level similar to the situation between day 231 and 288. The riparian vegetation cover started to increase again from day 558 onwards. This resulted in the maximum riparian vegetation cover at the end of the survey period, at day 672 (the last photo of row five).

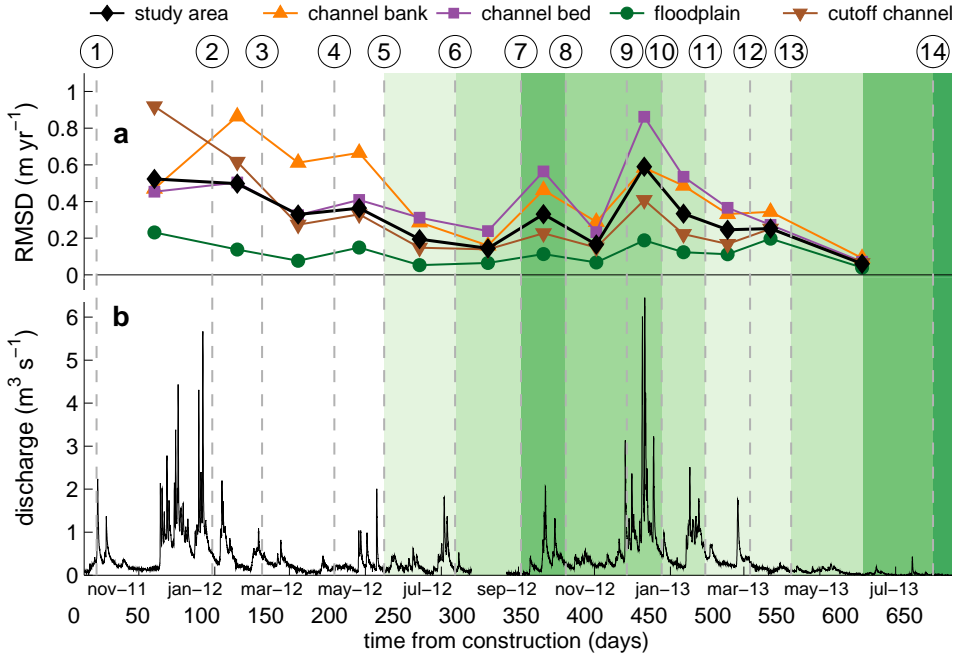
### 6.4.3 Morphodynamic Regime Change

Figure 6.9 combines the data obtained from the morphological surveys, terrestrial photos and discharge measurements. Figure 6.9a shows morphological change (m

## 6. Riparian Vegetation



**Figure 6.8** Series of fourteen oblique terrestrial photos taken from the location indicated in Figure 6.1d, except for the third photo (day 161), which was taken from the other side of the floodplain.



**Figure 6.9** Temporal evolution of: (a) the rate of morphological change ( $\text{m year}^{-1}$ ) for the study area as a whole (black diamonds), and specified per morphological feature, with channel bank (orange triangles), channel bed (purple squares), floodplain (green circles), and cutoff channel (brown triangles), and (b) discharge hydrograph ( $\text{m}^3 \text{s}^{-1}$ ). The green shaded colours indicate the riparian vegetation coverage, estimated from Figure 6.8. The dashed vertical lines indicate the surveying moments, the numbers at the top of the figure correspond to the numbers in Table 6.1.

year<sup>-1</sup>), which has been derived from Figure 6.5, with Equation 6.1. Figure 6.9b shows the discharge hydrograph, obtained from the measurement weir located 360 m downstream from the study area. The temporal evolution of the morphological change (black diamonds in Figure 6.9a) shows that the RMSD-metric of morphological change was relatively high in the first two periods (1-3). In the subsequent period, morphological changes show a decreasing trend until period (6-7). In the final period, incidental peaks are observed during periods of increased discharges, i.e. in period (7-8) and (9-10).

From Figure 6.9a it appears that the study period can be divided into two stages. The first stage can be considered an apparent morphological disequilibrium. The interval between surveys 1 and 3 is largely dominated by the chute cutoff event, which is followed by an interval until survey 5 that is dominated by channel bank processes. The second stage can be considered to be a morphodynamic equilibrium,

## 6. Riparian Vegetation

in the sense that the reach-scale morphology has stabilized. Both channel bank and channel bed processes dominate morphological change in the latter stage. During the whole study period, morphological changes in the floodplain contributed only slightly to the overall changes in the study area.

The temporal development of riparian vegetation, indicated with the green shaded colours in Figure 6.9, shows reach-scale riparian vegetation development from day 231 onwards. A maximum riparian vegetation coverage is observed in period (7-8), which corresponds with the photo taken on day 341 (Figure 6.8, last photo on row two). In the subsequent period, until the end of the study period, a decrease of riparian vegetation cover is observed. In Figure 6.9b, two periods of extremely high discharges occurred, i.e. in period (1-2) and period (9-10), from which the discharge peaks have a return period of 120 days and 180 days per year, respectively. The discharge peaks are associated with high-intensity precipitation events, which is commonly observed in regulated lowland catchments.

## 6.5 Discussion

Figure 6.9 shows an initial stage of morphological disequilibrium, when rates of morphological change are relatively high, without showing a clear response to discharge variation. In the subsequent near-equilibrium stage, a clear response to the varying discharge is evident. To investigate the degree in which morphological activity is in response to discharge variation, values of the RMSD were related to time-averaged dimensionless bed shear stress (Shields stress)  $\theta$  (-). The Shields stress is defined as:

$$\theta(t) = \frac{SR(t)}{d_{50}s} \quad (6.3)$$

where  $S$  is the longitudinal water level slope,  $R(t)$  is the hydraulic radius (m),  $d_{50}$  is the median grain size (m), and  $s = (\rho_s - \rho)/\rho$  is the relative submerged specific gravity of the sediment (-), with  $\rho = 1000 \text{ kg m}^{-3}$  the density of water and  $\rho_s = 2650 \text{ kg m}^{-3}$  the density of sediment. The average longitudinal water level slope  $S$  was used, which was calculated from the eleven last water level profiles from the GPS-surveys, excluding the two pre-cutoff water level profiles. An average water level slope of  $0.49 \text{ m km}^{-1}$  was obtained. The hydraulic radius  $R(t)$  was obtained by dividing the cross-sectional flow area  $A(t)$  by the wetted perimeter  $P(t)$ , obtained from the cross-section at the location of the water level gauge. Equation 6.3 was applied to the discharge and water level time-series and averaged between two successive morphological surveys, to obtain an estimate of the time-averaged Shields stress per period.

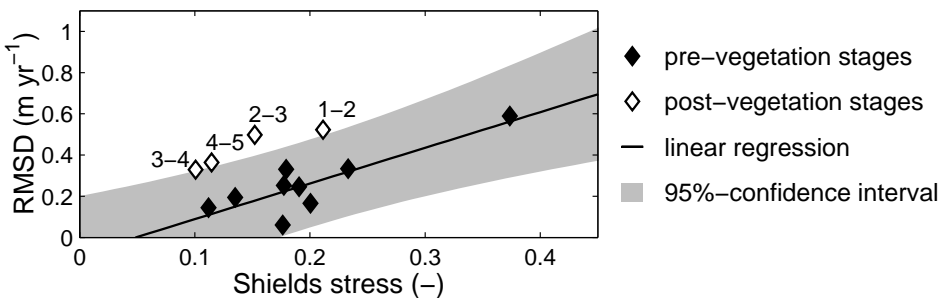


**Figure 6.10** Linear regression between time-averaged Shields stress (-) and the root-mean-square elevation difference (RMSD;  $\text{m year}^{-1}$ ) for the study area as a whole. The filled and open markers correspond to the pre-vegetation and post-vegetation stages, respectively. The solid black line denotes the linear regression curve for the period after vegetation emerged (5-14). The grey-shaded area indicates the extent of the 95%-confidence interval of the regression model.

A linear regression model was determined, relating the RMSD to time-averaged Shields stress for the study area as a whole. The linear regression model was determined for the period after vegetation emerged (5-14) only. Evaluation was based on the hypothesis that morphological activity in the period prior to vegetation growth was significantly different from the period after vegetation emerged. Additionally, the 95%-confidence interval was determined based on the Student's *t*-distribution, with the degrees of freedom corresponding to the number of periods after vegetation emerged.

Figure 6.10 shows the results from the linear regression between RMSD and time-averaged Shields stress. The RMSD in a certain period is significantly different from the linear regression model when the value is outside the 95%-confidence interval. Considering the study area as a whole, the whole period prior to vegetation growth is outside the 95%-confidence interval. These results suggest that the morphodynamic behaviour during the period prior to vegetation growth is significantly different from the period after vegetation emerged.

Chapter 5 showed that active meander processes occurred in the initial period prior to vegetation growth, including a chute cutoff and meander migration. In the subsequent period, when riparian vegetation started to emerge, the active meander processes were less pronounced, although localized bank erosion was observed. From Figure 6.6 it appears that study period can be subdivided into an initial period of net-deposition (1-5) and a latter period of net-erosion (5-14). The active meandering processes as observed in the period prior to vegetation growth may be related to an imbalance of sediment in- and output. Variation in sediment supply

## 6. Riparian Vegetation

have been related to channel patterns, where increased sediment supply in a river may result in a braiding planform, whereas reduced sediment supply in a meandering planform (Church, 2006; Kleinhans, 2010). In this case study, the difference between the two periods may be explained by the difference in sediment supply. In the initial period the channel may have acted as a meandering river due to excessive sediment supply. Data collected upstream from the study area showed channel incision in the first year (Figure 2.4, Chapter 2). Subsequently, the sediment supply decreased and the channel may have acted as a laterally stable sinuous river. The marked difference between the two periods of morphological behaviour may coincidentally corresponded with the growing season of the observed riparian vegetation. Nevertheless, riparian vegetation may have played a substantial role in the processes that led to the morphological regime change, which is discussed below.

This study was part of a multidisciplinary research project, which included aquatic and terrestrial ecological surveys. Upstream from the current study reach, riparian vegetation species were mapped in three cross-sections, respectively at 17 m, 84 m, and 120 m from the study area. In each cross-section, species cover was mapped in five rectangular plots (25 × 50 cm), located on the channel bed (1 plot), at the channel bank toe (1), in the floodplain (2) and on the floodplain edge (1). Data from two plots per cross section were used in the present study to estimate the dominant species. The two plots were located in the floodplain at 2.7–5.5 and 7.9–11.7 m from the channel banks, respectively. Coverage of the riparian vegetation species was estimated twice, at day 339 (September 2012) and 645 (July 2013), respectively.

The dominant species (average cover > 10%) in 2012 were *Juncus articulatus* (Jointed Rush) and *Juncus bufonius* (Toad Rush). *Juncus articulatus* was also among the dominant species in 2013, which also included *Juncus effusus* (Soft Rush) and *Trifolium repens* (White Clover). The observed species and their characteristics are summarized in Table 6.2. All species are classified as herbaceous vegetation and are perennial, rather than annual. The growing season of the dominant species are roughly from June to September, which explains the maximum coverage in September as observed in Figure 6.8 (last photo of row two). Root depths vary between less than 10 centimetres to 100 centimetres. The presented root depth values are valid for full grown specimens. It is likely that the root depths for the observed vegetation in this case study were shorter.

The most dominant species are all classified as herbaceous vegetation. The root structure of herbaceous vegetation differs from other vegetation types, such as shrubby and woody vegetation. Herbaceous vegetation shows a more graminoid-shaped root structure, including fibrous roots (Wynn *et al.*, 2004; Burylo *et al.*,

**Table 6.2** Characteristics of the most dominant riparian vegetation species found on the channel banks and in the floodplain, including location where the species were found, average cover (%), lifetime, growing season, and root depth. The presented characteristics were obtained from <http://www.wilde-planten.nl/> (Wilde planten in Nederland en België; Wild plants in the Netherlands and Belgium).

scientific name	cover (%)	lifetime	growing season	root depth
<b>September 2012</b>				
<i>Juncus articulatus</i>	19	perennial	Jun-Sep	10-20 cm
<i>Juncus bufonius</i>	22	annual	Jun-Sep	< 10 cm
<b>July 2013</b>				
<i>Juncus articulatus</i>	14	perennial	Jun-Sep	10-20 cm
<i>Juncus effusus</i>	14	perennial	Jun-Aug	< 100 cm
<i>Trifolium repens</i>	28	perennial	May-Oct	10-50 cm

2011). On the other hand, shrubby and woody vegetation include a tap-like root system, without fibrous roots (Burylo *et al.*, 2011). The differences in root structure cause differences in erosional resistance. Recent studies, in other geographical regions, have shown that herbaceous vegetation provides more soil reinforcement and is more efficient in improving aggregate stability than shrubby and woody vegetation (Burylo *et al.*, 2011; Fattet *et al.*, 2011). The advantages in erosion resistance for herbaceous vegetation are most effective in the top soil layer (< 30 cm; Wynn *et al.*, 2004). Previous studies have demonstrated that herbaceous vegetation types are among the first to (re)colonize the substrate, after environmental disturbance or land restoration (Cammerraat *et al.*, 2005; Burylo *et al.*, 2007). Although most of these studies were performed in different geographical regions and within different climates, these results show that herbaceous vegetation may have a significant impact on soil stability. The influence of herbaceous vegetation on bank stability may be even more relevant for lowland streams, due to their low channel depths. The temporal rate in which riparian vegetation has colonized the lowered floodplains confirms a previous study (Gurnell *et al.*, 2006). For future research, it may be worthwhile to study the rate in which riparian vegetation is able to colonize and stabilize the floodplain and channel banks after stream restoration measures are implemented.

At longer time scales, shrubby and woody vegetation will most likely colonize the channel banks in lowland streams. In September 2011, four morphologically undisturbed lowland streams were visited in central Poland (Figure 6.11). Visual observations in these morphologically undisturbed lowland streams show that the channel banks are dominated by vegetation, including herbaceous (panel (a) and (b)) and woody vegetation (panels (a), (c) and (d)). Fully grown trees are observed on the channel banks, which may infer that lateral channel development is rare.



**Figure 6.11** Photos from four morphologically undisturbed lowland streams in central Poland (Łódzkie region), with (a) Gać river ( $51^{\circ} 36' 16''$  N,  $20^{\circ} 7' 57''$  E), (b) Grabia river ( $51^{\circ} 34' 1''$  N,  $19^{\circ} 15' 46''$  E), (c) Korabiewka river ( $52^{\circ} 0' 58''$  N,  $20^{\circ} 12' 50''$  E), and (d) Słomianka river ( $51^{\circ} 29' 29''$  N,  $20^{\circ} 14' 27''$  E).

Evidence of lateral channel development was only observed in the Gracia river (panel (b)). On the lower part of the photo, emergent vegetation shows the location of several slump blocks, which are most likely a result of channel bank undercutting. These observations show that the herbaceous vegetation may affect channel bank stability of the top soil layer in lowland streams. Furthermore, the observations in the Korabiewka river and Słomianka river show that it is likely that the woody vegetation is able to stabilize the channel banks in lowland streams.

## 6.6 Conclusions

A detailed monitoring plan was implemented to monitor a restored lowland stream for a period of almost two years after channel construction. Morphological, hydrological and ecological data were combined to establish interactions between reach-scale morphodynamics, discharge dynamics and riparian vegetation development. In the initial stage after channel construction, when negligible riparian

vegetation was present, channel morphology adjusted rapidly towards an alternative, complex topography. In this period, maximum bank erosion rates amounted to 2.6 channel widths per year. Riparian vegetation emerged in the subsequent stage. The spatial distribution of the riparian vegetation is found to be governed by inundation frequency. Channel bed incision and localized bank erosion dominate the morphodynamic developments after riparian vegetation developed, with maximum bank erosion rates amounting to 1.2 channel widths per year. Linear regression analysis shows that the morphological response to Shields stress is significantly different between the pre-vegetation and post-vegetation stages, hence, a morphological regime change had occurred.

The two stages of morphological adjustments reveal the rate in which a lowland stream adjusts to a new morphological equilibrium. From the obtained field evidence, it can not indisputably be concluded that riparian vegetation is responsible for the morphological regime change. Nevertheless, the characteristics of the herbaceous vegetation and channel dimensions of lowland streams suggest that the initial riparian vegetation may have a strong control on the stability of the channel banks. Consequently, it may be worthwhile to minimize the duration of the initial stage of morphological adaptations after a lowland stream restoration project is realized. To some extent this duration can be manipulated by changing the season when the new channel is constructed, which has an impact on the duration of the pre-vegetation period and time channel forming discharges cause morphological changes. Future research is needed to substantiate these hypotheses.



# 7 | Synthesis



## 7. Synthesis

In the previous five chapters, the results from the field campaigns have been presented. Historical evidence and field data were obtained at five study sites, in the context of four stream restoration projects (three re-meandered reaches and one straight experimental reach) and a 240 year old man-made canal, all located in the Netherlands.

Over a period of 2-3 years, morphological and hydrological data were obtained from the stream restoration projects. Adjustment of the longitudinal bed profile was observed at each of the four sites. Structures (e.g. bridges and weirs), channel width variation and heterogeneity of the channel substrate affected the water level slope and the transport of sediment. In three of the four cases this resulted in a declining channel slope. Lateral development was only observed in a limited number of locations along the studied streams. These locations mainly relate to the absence of riparian vegetation and the presence of floodplain heterogeneity. At one field site, a chute cutoff and extensive bank erosion and accretion occurred in the initial period prior to vegetation growth. A shift was observed from channel bank to channel bed processes, coinciding with a period when riparian vegetation started to develop. This shift may be related to stabilisation of the channel banks by riparian vegetation, although the field evidence was insufficient to substantiate these findings, and further research is needed. Other cases of bank erosion were related to floodplain heterogeneity (i.e. unconsolidated floodplain material and a sand layer overlain by established riparian vegetation).

Large-scale morphological developments are exceptional and only occurred during the initial phase, after construction. Nevertheless, due to the fine sediment characteristics (median grain size 125-250 µm), sediment is transported throughout the year, where critical flow velocities are exceeded during the majority of time. At the experimental field site, this characteristic led to the formation of alternate bars on the channel bed. The alternate bars showed a dynamic morphological development. A declining channel slope and possible other external controls caused the regular bar pattern to disappear, resulting in a more complex, but still dynamic channel morphology.

Historical evidence shows that floodplain heterogeneity influenced initiation of meandering in a man-made canal. Meandering had initiated at three locations where traces of seepage were found in the subsoil. In the upstream half of the channel, where the channel dimensions correspond to those of lowland streams, meander activity ceased after the initial bend had formed. Historical maps of two out of three re-meandered channels show negligible change of the channel planform in the 30-year period before straightening. The studied lowland streams lack the ability to develop active meandering processes on geological time scales.

The results presented in this thesis, as summarized above, are synthesized in the current chapter. The research questions from Chapter 1 are answered and an outlook is provided proposing future research in lowland streams.

## 7.1 Meander Processes in Lowland Streams

*How can the archetypical channel planform of a lowland stream be characterized?*

Water authorities in the Netherlands use the term *re-meandering* for the construction of a sinuous channel in stream restoration projects. The term *re-meandering* may suggest that lowland streams are characterized by a meandering planform. Meandering may be interpreted as a temporal phenomenon associated with the process of bank erosion and accretion, that eventually leads to meander migration and an increase of channel sinuosity. The sinuosity decreases through neck or chute cutoffs, after which these processes repeat themselves. Water authorities in the Netherlands fear morphological developments related to meandering, including bank erosion and channel migration. This thesis focussed on meandering processes and showed that in lowland streams, these processes may only occur under specific conditions, in the initial period after realization of a stream restoration project.

Initiation of meandering has been attributed to bar and bend instability Blondeaux & Seminara (1985), which have been studied in Chapters 3 and 4, respectively. In the Hooge Raam (Chapter 3) alternate bars formed under channel conditions that do not agree with typical lowland stream characteristics (channel slope  $> 1 \text{ m km}^{-1}$ ). The evolution of the bar pattern involved an increase of bar wavelength and bar amplitude, and within one and a half years a more or less sinuous thalweg appeared on the channel bed. The regular alternate bar pattern and sinuous thalweg disappeared after the channel slope declined to less than  $1 \text{ m km}^{-1}$ . Two bar models predicted a decreasing likelihood for alternate bars to form, in response to the declining channel slope. This case study, representing a relatively large bed slope, suggests that the channel slope of lowland streams may generally be too low for alternate bars to form. Therefore, exogenous influences offer a more plausible explanation for the initiation of the sinuous planform, rather than autogenous processes. An initial perturbation of the channel centerline (bend instability) is most likely responsible for the initiation of meandering in the Gelderns-Nierskanaal (Chapter 3). The initial perturbation was caused by local seepage. In lowland streams other causes for floodplain heterogeneity (e.g. gravel layers and peat deposits), may also be related to the initial perturbation of the channel centerline. Subsequently, autoge-

## 7. Synthesis

nous meandering processes may have formed the typical sinuous channel planform. These findings are based on two case studies, which limit the applicability in a wider context. Further research is needed to better explain the initiation of meandering in lowland streams, which may focus on long-term numerical meander modelling, on detailed historical reconstructions and on characterization of morphologically undisturbed lowland streams.

In the Gelderns-Nierskanaal (Chapters 3), historical sources also show evidence of an active meandering channel, including meander migration and bend cutoffs. These processes mainly occurred in the downstream section of the channel, which is characterized by a steep channel slope ( $> 1 \text{ m km}^{-1}$ ) and coarse channel bed substrate (gravel). The processes that occurred in the upstream section may be most relevant for lowland streams, where the channel slope ( $< 1 \text{ m km}^{-1}$ ) and the channel bed substrate (coarse sand) are more closely related to lowland stream conditions. In this section of the channel, the observed meandering processes were less evident. Meander migration only occurred in the first stages after meander initiation. In the subsequent period, the channel centerline stabilised. Stabilisation of the channel centerline may be related to anthropogenic influences, some remainders of bank revetments are still visible. Stabilisation of the channel centerline was also observed from historical sources of lowland streams before channelisation (Chapter 2). The stability of the channel planforms at geological time scales may be surprising, considering the fine sediment characteristics of lowland streams (median grain size 125–250  $\mu\text{m}$ ). At shorter time scales, morphological changes of the channel bed did occur in the studied lowland streams and sediment is almost constantly being transported (Chapters 2, 3, 5, and 6). Consequently, the stable sinuous channel planform is most likely a result of stabilization of the channel banks. Visual observations in morphologically undisturbed lowland streams in Poland show that the channel bank zone is dominated by herbaceous and woody vegetation (Chapter 6), which both have the potential to stabilize channel banks (Wynn *et al.*, 2004; Fattet *et al.*, 2011). These observations show that morphologically undisturbed lowland streams consist of a stable sinuous channel planform over longer (geological) time scales, which is most likely stabilized by riparian vegetation.

*Can post-project appraisals in lowland stream restoration bridge the gap between laboratory studies and rivers with a mild slope?*

Recently, two special issues on river meandering have been published, in *Earth Surface Processes and Landforms* (Hooke *et al.*, 2011) and in *Geomorphology* (Güneralp *et al.*, 2012). Both editorial commentaries acknowledge the need for field

evidence to validate and test existing models and future refinements of these models. Until now, the natural variability, dynamics and complexity of real rivers are not incorporated into meander models, which may have practical application in the design of re-meandered streams and rivers. Post-project appraisals of re-meandered streams and rivers add to the knowledge of meandering rivers and will directly find their practical application in stream restoration when such projects are subject to frequent morphological surveys. The field cases described in this thesis were all performed in a lowland setting, which may imply only limited morphological changes would occur. Nevertheless, substantial morphological development has been observed in the studied streams. Furthermore, the presented case studies in Chapters 3 - 6 are among the few field studies presented in the literature within their specific focus area and have subsequently added to the knowledge on meandering processes that occur under field conditions.

Lowland streams have a few advantages over other river systems, as case study areas for studying meandering processes. These advantages mainly relate to the small spatial and short temporal scales involved in lowland streams. Lowland streams are wadeable during the majority of the year, which makes it possible to do frequent field surveys in study reaches consisting of several meander loops. Due to a flashy discharge, typical for regulated lowland catchments, channel forming discharges occur frequently. The fine sediment characteristics of the channel bed cause sediment to be transported during the majority of the year. Eventually, the discharge and sediment characteristics result in frequent morphological changes and may relate to morphological processes that occur in meandering rivers, e.g. alternate bar formation, bend migration and the occurrence of chute cutoffs. In the presented case studies, these processes ceased when the bed topography tended towards a stable equilibrium. Therefore, lowland stream restoration projects may only be valuable case study areas for studying river meandering in the initial period, although consideration should be made for the causes for the initial disequilibrium.

## 7.2 Implications for Lowland Stream Restoration

*How do the morphological developments relate to the needs to improve the ecological status?*

The main objective of stream restoration in the Netherlands is to improve the

## 7. Synthesis

ecological status of the channel (benthic ecology) and floodplain (terrestrial ecology). In the design procedure, the terrestrial ecology is only accounted for in terms of an increase of moisture content of the channel banks, without verifiable estimates for moisture content or ground water levels. The design process mainly focusses on the improvement of the abiotic conditions for in-channel benthic ecology, by applying ranges for depth-averaged flow velocity and water depth. These ranges are used to find the most suitable dimensions of the channel cross-section (channel width and depth). It is likely that these constraints are too much of a simplification of the conditions that best suit the benthic ecology in lowland streams.

The habitat of the benthic ecology is limited to a few centimetres above and below the channel bed. At this scale their habitat and mobility can be explained in relation to life resources, including oxygen, food and protection against forces of shear stress (Lancaster & Belyea, 2006). At larger spatial scales, the distribution of benthic ecological communities relate to habitat patchiness (Fonseca & Hart, 2001), where each habitat (e.g. sand, gravel, leaves, woody debris) forms under different abiotic conditions. Hydraulic conditions play an important role in the formation of each habitat type. Due to their physical characteristics, each habitat type forms under different hydraulic conditions.

The hydraulic conditions also cause micro-topography of the channel bed, which affects the mobility and distribution of benthic ecology (Buffin-Bélanger *et al.*, 2003). The majority of the presented morphological developments in the four stream restoration projects focussed on width to bend scale developments, such as bank erosion and longitudinal channel bed adjustments. In Chapters 3 and 6 an increase of the spatial resolution of the morphological measurements resulted in high-resolution DEMs, which reveal a patchiness of the channel bed topography. Chapter 2 shows a dynamic habitat pattern in the three re-meandered streams, similar to previous studies (Tolkamp, 1980; Wolfert, 2001). These findings suggest that small-scale channel bed adjustments occur in restored lowland streams. The small-scale channel bed adjustments may have a positive impact on the habitat distribution and, consequently, the ecological status of the restored streams.

Habitat scale changes occurred in the studied lowland streams, although no special attention was paid to these processes in the design procedure. What really matters for benthic ecology is the balance between the occurrence of a continuously changing mosaic of habitat patches in space and the stability of individual habitat patches in time (Tolkamp, 1980). Currently, the design procedure focusses on ranges of cross-sectional averaged flow velocities and water depths. These estimates may have a physical meaning for benthic ecology at larger spatial and temporal scales, however, they do not capture the processes at the scale of the benthic ecology.

Recently, there have been several attempts in this direction, mainly by introducing large woody debris. The introduction of large woody debris may be particularly successful in lowland streams. Trees are large in comparison to the dimensions of lowland streams, and are therefore able to provide important structures to increase the temporal and spatial flow variability (Gurnell *et al.*, 2002). In future stream restoration projects it may be worthwhile to focus on habitat scale processes and to assess the abiotic conditions favourable for typical lowland ecology.

*What is the role of longitudinal connectivity in the morphological development of restored lowland streams?*

It has been widely acknowledged that connectivity is a fundamental property of all ecosystems (Kondolf *et al.*, 2006). In riverine ecosystems, this is mainly related to hydrological connectivity. Pringle (2001) defined hydrological connectivity as: “an ecological sense to refer to water-mediated transfer of matter, energy, and/or organisms within or between elements of the hydrological cycle”. Hydrological connectivity is expressed in four dimensions (Ward, 1989), i.e. longitudinal, lateral, vertical and temporal, and covers the whole catchment. The three spatial dimensions apply to different linkages within a catchment: the longitudinal dimension to upstream-downstream linkages, the lateral dimension to channel-floodplain linkages, and the vertical dimension to channel bed-water-air linkages. The temporal dimension applies to changes over time for each spatial dimension.

These linkages have been conceptualized in the *River Continuum Concept* (Vannote *et al.*, 1980), which stresses the importance of a river without discontinuities, and implies a gradual shift in abiotic stream characteristics and species composition along the channel gradient. From a fluvial geomorphological point of view, connectivity within a catchment has been expressed as a continuum from upstream to downstream, where sediment is produced in the headwater zone (erosional zone), transported in the midzone (transportation zone) and deposited in the floodplains and delta (depositional zone) (Schumm, 1977). This continuum of erosion, transport and deposition of sediment occurs in any segment of a river, and works also in the lateral, vertical and temporal dimension. In each segment, distinct geomorphic processes and disturbance regimes are created, affecting aquatic and riparian ecosystems (Montgomery, 1999).

It has been recognized that successful stream restoration requires an increase of connectivity (Verdonschot & Nijboer, 2002; Wohl *et al.*, 2005; Kondolf *et al.*, 2006). Most restoration projects focus on single, isolated channel reaches and therefore lack connectivity, which is vital for improving the ecosystem. From the four stream

## 7. Synthesis

restoration projects evaluated in this thesis, only one project (Tungelroyse beek) involved restoration of the whole stream. The other projects were realized in isolated channel reaches. This has caused a lack of longitudinal connectivity, mainly affecting the temporal evolution of the longitudinal channel bed profile. The longitudinal channel bed profile was mainly influenced by backwater effects, caused by narrowing of the channel width downstream of the study reaches (Chapters 3 and 5), and by a lack of upstream sediment input (Chapter 2). Eventually, these exogenous influences caused a decrease of channel slope in three of the studied streams (viz. Hooge Raam, Lunterse beek and Tungelroyse beek). Similar morphological adjustments have been observed in isolated restored channel reaches of lowland streams in the UK (Sear *et al.*, 1998).

Longitudinal channel bed adjustments were the most significant morphological responses that occurred in the stream restoration projects subjected to study. In most cases, the lack of longitudinal connectivity was the main cause explaining these changes. These results show that the basic principles of the sediment transport continuum (Schumm, 1977) is not applicable in these streams. In future stream restoration projects it may be worthwhile to aim at increasing the longitudinal connectivity by removing weirs and to anticipate on causes of backwater effects. Special attention should be paid to the introduction of large woody debris, which is increasingly used as a stream restoration measure in lowland streams. Since the size of the woody debris are often exceeding the channel width, debris jams may develop, causing backwater effects (Piégay & Gurnell, 1997).

Stream restoration projects should not be limited to isolated channel reaches, but it may be worthwhile to consider the stream as a whole. Recently, related concepts have been presented in literature, such as the '*erodible corridor*' (Piégay *et al.*, 2005) and '*espace de liberté*' (Kondolf, 2012). These concepts involve the development of a zone along a river or stream, where the active channel can naturally move in order to maintain sediment supply, which is essential for optimal terrestrial and aquatic ecosystem functioning. This will not only improve the longitudinal connectivity in the processes related to channel bed adjustments, but will also induce an increase of ecological connectivity, which may be essential for reaching the main goal of stream restoration.

*Which are the main controls on the lateral development in restored lowland streams?*

Lateral development in meandering rivers mainly occurs in channel bends, where erosion of the outer bank and accretion of the opposing inner bank causes a shift of the channel centerline. These meandering processes are controlled by the

interaction of the secondary flow and sediment transport in curved channel bends. Channel bank characteristics influence the rate at which these autogenous processes cause erosion of the outer bank, which include channel bank composition (Midgley *et al.*, 2012), hydrological conditions (Casagli *et al.*, 1999; Fox *et al.*, 2006), and the presence of riparian vegetation (Simon & Collison, 2002; Pollen-Bankhead & Simon, 2009). These channel bank characteristics are all represented by floodplain heterogeneity, and may impose an exogenous influence on the processes related to lateral channel development.

Spatial variation of lateral channel development has been related to floodplain heterogeneity. Recently, the importance of floodplain heterogeneity on meander planform dynamics has been recognized and studied in meander models (Güneralp & Rhoads, 2011; Motta *et al.*, 2012a). In Chapters 4 and 2, hydrological conditions (local seepage) and channel bank composition (gravel and former channel fills) were a cause for floodplain heterogeneity, and, hence, resulted in spatial variation of the observed lateral development. In future stream restoration projects it may be worthwhile to involve a field reconnaissance to map possible causes of floodplain heterogeneity, such as local seepage, gravel and peat deposits, and former channel fills. Such field reconnaissances may assist in assessing the causes of lateral channel development, and may help to prevent unwanted changes to the new channel topography.

Lowland streams consist of a sinuous planform, which is most likely stabilized by vegetation. The time scale of the field observations in the four stream restoration projects under consideration was too short to establish the role of the riparian vegetation in the morphodynamics of lowland streams. Chapter 6 discusses the growing season and root characteristics of the dominant riparian vegetation types found in the Lunterse beek. The observed riparian vegetation characteristics suggest that the (mainly) herbaceous vegetation may influence channel bank stabilization, although further research is needed to substantiate these findings. Nevertheless, it may be worthwhile to minimize the duration of the initial stage of morphological adaptations after a lowland stream restoration project is realized. To some extent, this duration can be manipulated by considering the season when the channel is constructed, which has an impact on the growth of vegetation to be expected, and the time that channel forming discharges cause morphological changes.

## 7.3 Outlook

### 7.3.1 Flow Processes at the Scale of Benthic Ecology

In this thesis morphological processes of lowland streams have been established. The focus was mainly on the spatial and temporal scales that matter most for water authorities, i.e. the reach and engineering scale. Lateral channel migration and longitudinal channel bed adjustments may affect structures and adjacent agricultural fields. These morphological adjustments are potentially a cause for channel maintenance, and are therefore of interest for the water authorities.

The current design procedures for lowland streams in the Netherlands aim to optimize the abiotic conditions for benthic ecology typical in lowlands. From a hydrological point-of-view, the benthic ecology is affected by processes at several spatial and temporal scales. At the catchment scale, the distribution of water through the subsoil and drainage network affects the discharge dynamics at the reach scale. The discharge dynamics causes variation of channel forming discharges, affecting the cross-sectional shape and the channel bed composition. The dynamics of the channel morphology will eventually influence the flow velocity and habitat conditions at the smallest spatial and temporal scales, which are most relevant for benthic ecological processes.

The typical benthic ecology found in natural lowland streams occur under low to moderate dynamic conditions. The streams studied in this thesis are characterized by flashy discharge dynamics, which may result in rapidly increasing flow velocities. Consequently, under these conditions, the benthic ecology and their habitat are washed away during recurring flood events. When these flashy discharge conditions persist, the benthic ecology may not establish after restoration measures are implemented. The flashy discharge dynamics are most likely detrimental for the benthic ecology and may interfere with the main goal of lowland stream restoration, i.e. to improve the ecological status of lowland streams.

The construction of a lowered floodplain aims at storing water during flood events, however, it may also reduce the flow dynamics during such events. For future research it may be worthwhile to focus on understanding the impact of the flashy discharge on the abiotic conditions relevant for benthic ecology. These may include laboratory studies focussing on detailed flow processes near lowland habitat, such as leaf patches, woody debris, and coarse organic matter. Research may also focus on the effect of restoration measures such as a floodplain lowering and adjusting the width-to-depth ratio of a channel. Field studies may focus on the spatial and temporal dynamics of flow velocity and sediment transport. These

studies could potentially reveal the abiotic conditions needed for typical lowland benthic ecology to flourish.

The results of these studies may help to improve restoration design of lowland streams. Until now, the ecological constraints include ranges of cross-sectional averaged flow velocities. These constraints are too much of a simplification of the abiotic conditions, relevant for benthic ecology. The design may involve an assessment of the prospective temporal dynamics of flow velocity, and constrain the abiotic conditions needed for improved benthic ecological conditions. Measures should not only focus at the reach scale, where stream restoration projects are implemented. The causes of the flashy discharge dynamics are found at the catchment scale. Until now, stream restoration often only involves the construction of a new channel in isolated sections of the stream. In future restoration projects, it may be worthwhile to involve measures at the catchment scale, aiming at reducing the flashy discharge dynamics.

### 7.3.2 Riparian Vegetation Control on Stream Morphology

One of the main conclusions of this thesis is that morphologically undisturbed lowland streams exhibit a stable sinuous planform. The sediment characteristics (fine sands, median grain size between 125 and 250 µm) cause sediment to be transported virtually all throughout the year. Observations have shown that morphological development at the habitat scale occurred during the majority of the year as well. Nevertheless, at geological time scales, lateral development is rarely observed. The lack of lateral development has been related to riparian vegetation, which may stabilize the channel banks. However, the evidence used to substantiate these findings was only based on visual observations and not on actual field measurements.

This yields an opportunity for future research. The field observations have shown that herbaceous vegetation is the most dominant vegetation type in the first few years after construction. Previous studies, in other geographical regions, have shown how herbaceous vegetation is able to stabilize the top soil. Due to their root depth, herbaceous vegetation may subsequently fix the channel banks in lowland streams, as soon as the roots have developed sufficiently. The characteristics of the roots are essential when evaluating the stabilizing potential of a species. These characteristics may include root depth, growth rate and root biomass. When species and their characteristics are known, an assessment can be made estimating the rate at which vegetation controls the lateral development of a channel. This may potentially be relevant for stream restoration planning and maintenance, leading to a reduction of the costs of stream restoration.



# Bibliography

- ABAD, J. D., & GARCÍA, M. H. 2006. RVR Meander: A toolbox for re-meandering of channelized streams. *Journal of Computers and Geosciences*, **31**, 91–101.
- ABERNETHY, B., & RUTHERFURD, I. D. 2001. The distribution and strength of riparian tree roots in relation to riverbank reinforcement. *Hydrological Processes*, **15**, 63–79.
- ALTERRA. 2006. *Grondsoortenkaart 2006 - Simplified soil map of the Netherlands*. <http://www.geodata.alterra.nl/Grondsoorten.htm> (accessed 13-01-2014).
- ANDERSON, D. W. 1988. The effect of parent material and soil development on nutrient cycling in temperate ecosystems. *Biogeochemistry*, **5**, 71–97.
- ASAHI, K., SHIMIZU, Y., NELSON, J. M., & PARKER, G. 2013. Numerical simulation of river meandering with self-evolving banks. *Journal of Geophysical Research - Earth Surface*, **118**, 2208–2229.
- ASCE. 1998. River width adjustment. I: Processes and mechanisms. *Journal of Hydraulic Engineering*, **124**, 881–902.
- ASHWORTH, P. J., BEST, J. L., & JONES, M. 2004. Relationship between sediment supply and avulsion frequency in braided rivers. *Geology*, **32**, 21–24.
- ASLAN, A., AUTIN, W. J., & BLUM, M. D. 2005. Causes of river avulsion: Insights from the late Holocene avulsion history of the Mississippi River, U.S.A. *Journal of Sedimentary Research*, **75**, 650–664.
- BAAIJENS, G. J., & DAUVELLIER, P. 2011. *Stromend landschap: vloeiweidenstelsels in Nederland*. KNNV Uitgeverij, Zeist.
- BAATTRUP-PEDERSEN, A., RIIS, T., HANSEN, H. OLE, & FRIBERG, N. 2000. Restoration of a Danish headwater stream: short-term changes in plant species abundance and composition. *Aquatic Conservation: Marine and Freshwater Ecosystems*, **10**, 13–23.
- BANGEN, S. G., WHEATON, J. M., BOUWES, N., BOUWES, B., & JORDAN, C. 2014. Amethodological intercomparison of topographic survey techniques for characterizing wadeable streams and rivers. *Geomorphology*, **206**, 343–361.
- BARTLEY, R., KEEN, R. J., HAWDON, A. A., HAIRSINE, P. B., DISHER, M. G., & KINSEY-HENDERSON, A. E. 2008. Bank erosion and channel width change in a tropical catchment. *Earth Surface Processes and Landforms*, **33**, 2174–2200.

## Bibliography

- BERTOLDI, W., DRAKE, N. A., & GURNELL, A. M. 2011. Interactions between river flows and colonizing vegetation on a braided river: exploring spatial and temporal dynamics in riparian vegetation cover using satellite data. *Earth Surface Processes and Landforms*, **36**, 1474–1486.
- BLONDEAUX, P., & SEMINARA, G. 1985. A unified bar-bend theory of river meanders. *Journal of Fluid Mechanics*, **157**, 449–470.
- BRASINGTON, J., LANGHAM, J., & RUMSBY, B. 2003. Methodological sensitivity of morphometric estimates of coarse fluvial sediment transport. *Geomorphology*, **53**, 299–316.
- BRAUDRICK, C. A., DIETRICH, W. E., LEVERICH, G. T., & SKLAR, L. S. 2009. Experimental evidence for the conditions necessary to sustain meandering in coarse-bedded rivers. *Proceedings of the National Academy of Science of the United States of America*, **106**, 16936–16941.
- BROOKES, A. 1987. Restoring the sinuosity of artificially straightened stream channels. *Environmental Geology and Water Sciences*, **10**, 33–41.
- BROOKES, A., & GREGORY, K. 1988. *Channelized rivers: Perspectives for environmental management*. Wiley, Chichester. 326 pp.
- BROOKES, A., & LONG, A. J. 1990. *Chart catchment morphological survey: Appraisal report and watercourse summaries*. Tech. rept. National Rivers Authority Reading.
- BRUSH, L. M., & WOLMAN, M. G. 1960. Knickpoint behaviour in noncohesive material: A laboratory study. *Geological Society of America Bulletin*, **71**, 59–73.
- BUCHANAN, B. P., NAGLE, G. N., & WALER, M. T. 2014. Long-term monitoring and assessment of a stream restoration project in Central New York. *River Research and Applications*, **30**, 245–258.
- BUFFIN-BÉLANGER, T., REID, I., RICE, S. P., CHANDLER, J. H., & LANCASTER, J. 2003. A casting procedure for reproducing coarse-grained sedimentary surfaces. *Earth Surface Processes and Landforms*, **28**, 787–796.
- BURYLO, M., REY, F., & DELCROS, P. 2007. Abiotic and biotic factors influencing the early stages of vegetation colonization in restored marly gullies (Southern Alps, France). *Ecological Engineering*, **30**, 231–239.
- BURYLO, M., HUDEK, C., & REY, F. 2011. Soil reinforcement by the roots of six dominant species on eroded mountainous marly slopes (Southern Alps, France). *Catena*, **84**, 70–78.
- CALLANDER, R. A. 1969. Instability of river channels. *Journal of Fluid Mechanics*, **36**, 465–480.
- CAMMERAAT, E., VAN BEEK, R., & KOOIJMAN, A. 2005. Vegetation succession and its consequences for slope stability in SE Spain. *Plant and Soil*, **278**, 135–147.
- CAMPOREALE, C., & RIDOLFI, L. 2006. Riparian vegetation distribution induced by river flow variability: A stochastic approach. *Water Resources Research*, **42**, W10415.
- CAMPOREALE, C., & RIDOLFI, L. 2010. Interplay among river meandering, discharge stochasticity and riparian vegetation. *Journal of Hydrology*, **382**, 138–144.

- CASAGLI, N., RINALDI, M., GARGINI, A., & CURINI, A. 1999. Pore water pressure and streambank stability: results from a monitoring site on the Sieve River, Italy. *Earth Surface Processes and Landforms*, **24**, 1095–1114.
- CHARLTON, M. E., LARGE, A. R. G., & FULLER, I. C. 2003. Application of airborne LiDAR in river environments: The River Coquet, Northumberland, UK. *Earth Surface Processes and Landforms*, **28**, 299–306.
- CHURCH, M. 2006. Bed material transport and the morphology of alluvial river channels. *Annual Review of Earth and Planetary Sciences*, **34**, 325–354.
- CHURCH, M., & RICE, S. P. 2009. Form and growth of bars in a wandering gravel-bed river. *Earth Surface Processes and Landforms*, **34**, 1422–1432.
- CHURCH, M. A., & ROAD, K. 1983. *Catalogue of alluvial river channel regime data*. Tech. rept. Department of Geography, University of British Columbia, Vancouver, B.C.
- CLEVERS, J. G. P. W. 1988. The derivation of a simplified reflectance model for the estimation of leaf area index. *Remote Sensing of Environment*, **25**, 53–69.
- COLOMBINI, M., & TUBINO, M. 1990. Finite amplitude multiple row bars: a fully non-linear spectral solution. In: SOULSBY, R., & BETTESS, R. (eds), *Proceedings of Euromech 262*. 162–169.
- COLOMBINI, M., SEMINARA, G., & TUBINO, M. 1987. Finite-amplitude Alternate Bars. *Journal of Fluid Mechanics*, **181**, 213–232.
- CONSTANTINE, J. A., MCLEAN, S. R., & DUNNE, T. 2010. A mechanism of chute cutoff along large meandering rivers with uniform floodplain topography. *Geological Society of America Bulletin*, **122**, 855–869.
- COPELAND, R. R., MCCOMAS, D. N., THORNE, C. R., SOAR, P. J., JONAS, M. M., & FRIPP, J. B. 2001. *Hydraulic Design of Stream Restoration Projects*. Tech. rept. US Army Corps of Engineers, Washington, DC.
- CORENBLIT, D., TABACCHI, E., STEIGER, J., & GURNELL, A. M. 2007. Reciprocal interactions and adjustments between fluvial landforms and vegetation dynamics in river corridors: A review of complementary approaches. *Earth-Science Reviews*, **84**, 56–86.
- COULTHARD, T. M., & VAN DE WIEL, M. J. 2006. A cellular model of river meandering. *Earth Surface Processes and Landforms*, **31**, 123–132.
- COUNCIL OF THE EUROPEAN COMMUNITIES. 2000. Directive 2000/60/EC of the European Parliament and of the Council of 23 October 2000 establishing a framework for Community action in the field of water policy. *Official Journal of the European Communities*, L327, 1–73.
- CROKE, J., TODD, P., THOMPSON, C., WATSON, F., DENHAM, R., & KHANAL, G. 2013. The use of multi temporal LiDAR to assess basin-scale erosion and deposition following the catastrophic January 2011 Lockyer flood, SE Queensland, Australia. *Geomorphology*, **184**, 111–126.
- CROSATO, A. 1987. Simulation model of meandering processes of rivers. Pages 158–161 of: *Extended Abstracts of the International Conference: Euromech 215-Mechanics of Sediment Transport in Fluvial and Marine Environments*. European Mechanics Society, Santa Margherita Ligure-Genoa, Italy.

## Bibliography

- CROSATO, A. 2007. Effects of smoothing and regridding in numerical meander migration models. *Water Resources Research*, **43**, W01401.
- CROSATO, A., & MOSELMAN, E. 2009. Simple physics-based predictor for the number of river bars and the transition between meandering and braiding. *Water Resources Research*, **45**, W03424.
- CROSATO, A., MOSELMAN, E., DESTA, F., BEIDMARIAM, & UIJTEWAAL, W. S. J. 2011. Experimental and numerical evidence for intrinsic nonmigrating bars in alluvial channels. *Water Resources Research*, **47**, W03511.
- DE MOOR, J. J. W., & VERSTRAETEN, G. 2008. Alluvial and colluvial sediment storage in the Geul River catchment (The Netherlands) - Combining field and modelling data to construct a Late Holocene sediment budget. *Geomorphology*, **95**, 487–503.
- DE MOOR, J. J. W., KASSE, C., VAN BALEN, R., VANDENBERGHE, J., & WALLINGA, J. 2008. Human and climate impact on catchment development during the Holocene - Geul River, the Netherlands. *Geomorphology*, **98**, 316–339.
- DE VRIES, M. 1975. A morphological time scale for rivers. Pages 17–23 of: *Proceedings of the 16th Congress IAHR*, vol. 2.
- DEFINA, A. 2003. Numerical Experiments on Bar Growth. *Water Resources Research*, **39**, 1092.
- DELTARES. 2011. *SOBEK 2.12 user manual*. Deltires, Delft, the Netherlands.
- DIERAS, P. L., J. A. CONSTANTINE, J. A., HALES, T. C., PIÉGAY, H., & RIQUIER, J. 2013. The role of oxbow lakes in the off-channel storage of bed material along the Ain River, France. *Geomorphology*, **188**, 110–119.
- EATON, B. C., CHURCH, M., & MILLAR, R. G. 2004. Rational regime model of alluvial channel morphology and response. *Earth Surface Processes and Landforms*, **29**, 511–529.
- ENGELUND, F. 1970. Instability of erodible beds. *Journal of Fluid*, **42**, 225–244.
- ENGELUND, F., & HANSEN, E. 1967. *A monograph on sediment transport in alluvial streams*. Teknisk Forlag.
- ENGLAND, J., SKINNER, K. S., & CARTER, M. G. 2008. Monitoring, river restoration and the Water Framework Directive. *Water and Environment Journal*, **22**, 227–234.
- ERSKINE, W., MCFADDEN, C., & BISHOP, P. 1992. Alluvial cutoffs as indicators of former channel conditions. *Earth Surface Processes and Landforms*, **17**, 23–37.
- ERWIN, S. O., SCHMIDT, J. C., WHEATON, J. M., & WILCOCK, P. R. 2012. Closing a sediment budget for a reconfigured reach of the Provo River, Utah, United States. *Water Resources Research*, **48**, W10512.
- ETHRIDGE, F. G., SKELLY, R. L., & BRISTOW, C. S. 2009. *Fluvial Sedimentology VI*. Blackwell Publishing Ltd., Oxford, UK. Chap. Avulsion and crevassing in the sandy, braided Niobrara River: Complex response to base-level rise and aggradation.
- FATTET, M., FU, Y., GHESTEM, M., MA, W., FOULONNEAU, M., NESPOULOUS, J., LE BISSONNAIS, Y., & STOKES, A. 2011. Effects of vegetation type on soil resistance to erosion: Relationship between aggregate stability and shear strength. *Catena*, **87**, 60–69.

- FEDERICI, B., & PAOLA, C. 2003. Dynamics of channel bifurcations in noncohesive sediments. *Water Resources Research*, **39**, 1162.
- FEDERICI, B., & SEMINARA, G. 2003. On the convective nature of bar instability. *Journal of Fluid Mechanics*, **487**, 125–145.
- FISK, H. N. 1944. *Geological investigation of the alluvial valley of the lower Mississippi river*. U.S. Department of the Army, Mississippi River Commission. 78 pp.
- FONSECA, D. M., & HART, D. D. 2001. Colonization history masks habitat preferences in local distributions of stream insects. *Ecology*, **82**, 2897–2910.
- FOX, G. A., & WILSON, G. V. 2010. The role of subsurface flow in hillslope and stream bank erosion: A review. *Soil Science Society of America Journal*, **74**, 717–733.
- FOX, G. A., WILSON, G. V., PERIKETI, R. K., & CULLUM, R. F. 2006. Sediment transport model for seepage erosion of streambank sediment. *Journal of Hydrologic Engineering*, **11**, 603–611.
- FOX, G. A., WILSON, G. V., SIMON, A., LANGENDOEN, E. J., AKAY, O., & FUCHS, J. W. 2007. Measuring streambank erosion due to ground water seepage: Correlation to bank pore water pressure, precipitation and stream stage. *Earth Surface Processes and Landforms*, **32**, 1558–1573.
- FRIEDKIN, J. F. 1945. *A Laboratory Study of the Meandering of Alluvial Rivers*. U.S. Army Corps of Engineers Waterways Experiment Stations, Vicksburg, MS, USA. 61 pp.
- FULLER, I. C., LARGE, A. R. G., & MILAN, D. J. 2003. Quantifying channel development and sediment transfer following chute cutoff in a wandering gravel-bed river. *Geomorphology*, **54**, 307–323.
- GAUTIER, E., BRUNSTAIN, D., VAUCHEL, P., JOUANNEAU, J., ROULET, M., GAR-CIA, C., GUYOL, J., & CASTRO, M. 2010. Channel and floodplain sediment dynamics in a reach of the tropical meandering Rio Beni (Bolivian Amazonia). *Earth Surface Processes and Landforms*, **35**, 1838–1853.
- GAY, G. R., GAY, H. H., GAY, W. H., MARTINSON, H. A., MEADE, R. H., & MOODY, J. A. 1998. Evolution of cutoffs across meander necks in Powder River, Montana, USA. *Earth Surface Processes and Landforms*, **23**, 651–662.
- GERMANOSKI, D., & SCHUMM, S. A. 1993. Changes in braided river morphology resulting from aggradation and degradation. *Journal of Geology*, **101**, 451–466.
- GHINASSI, M. 2011. Chute channels in the Holocene high-sinuosity river deposits of the Firenze plain, Tuscany, Italy. *Sedimentology*, **58**, 618–642.
- GRAN, K., & PAOLA, C. 2001. Riparian vegetation controls on braided stream dynamics. *Water Resources Research*, **37**, 3275–3284.
- GRENFELL, M., AALTO, R., & NICHOLAS, A. 2012. Chute channel dynamics in large, sand-bed meandering rivers. *Earth Surface Processes and Landforms*, **37**, 315–331.
- GROVE, J.R., CROKE, J., & THOMPSON, C. 2013. Quantifying different riverbank erosion processes during an extreme flood event. *Earth Surface Processes and Landforms*, **38**, 1393–1406.

## Bibliography

- GÜNERALP, I., & RHOADS, B. L. 2011. Influence of floodplain erosional heterogeneity on planform complexity of meandering rivers. *Geophysical Research Letters*, **38**, L14401.
- GÜNERALP, I., ABAD, J. D., ZOLEZZI, G., & HOOKE, J. 2012. Advances and challenges in meandering channels research. *Geomorphology*, **163-164**, 1–9.
- GURNELL, A. M., PIÉGAY, H., SWANSON, F. J., & GREGORY, S. V. 2002. Large wood and fluvial processes. *Freshwater Biology*, **47**, 601–619.
- GURNELL, A. M., MORRISSEY, I. P., BOITSIDIS, A. J., BARK, T., CLIFFORD, N. J., PETTS, G. E., & THOMPSON, K. 2006. Initial Adjustments Within a New River Channel: Interactions Between Fluvial Processes, Colonizing Vegetation, and Bank Profile Development. *Environmental Management*, **38**, 580–596.
- GURNELL, A. M., BERTOLDI, W., & CORENBLIT, D. 2012. Changing river channels: The roles of hydrological processes, plants and pioneer fluvial landforms in humid temperate, mixed load, gravel bed rivers. *Earth-Science Reviews*, **111**, 129–141.
- HANSEN, E. 1967. *On the formation of meanders as a stability problem*. Prog. Rep. 13. Coastal Eng. Lab., Tech. Univ. of Denmark.
- HELLER, P. L., & PAOLA, C. 1996. Downstream changes in alluvial architecture; an exploration of controls on channel-stacking patterns. *Journal of Sedimentary Research*, **66**, 297–306.
- HERITAGE, G. L., MILAN, D. J., LARGE, A. R. G., & FULLER, I. C. 2009. Influence of survey strategy and interpolation model on DEM quality. *Geomorphology*, **112**, 334–344.
- HEY, R. D., & THORNE, C. R. 1986. Stable Channels with Mobile Gravel Beds. *Journal of Hydraulic Engineering*, **112**, 671–689.
- HOGARTH, W. 1753. *The analysis of beauty*. Reprinted in 1997 by Yale University Press, New Haven, Connecticut, USA.
- HOLBEN, B. N. 1986. Characteristics of maximum-value composite images from temporal AVHRR data. *International Journal of Remote Sensing*, **7**, 1417–1434.
- HOOKE, J. M. 1995. River channel adjustment to meander cutoffs on the River Bollin and River Dane, northwest England. *Geomorphology*, **14**, 235–253.
- HOOKE, J. M., & YORKE, L. 2010. Rates, distributions and mechanisms of change in meander morphology over decadal timescales, River Dane, UK. *Earth Surface Processes and Landforms*, **35**, 1601–1614.
- HOOKE, J. M., GAUTIER, E., & ZOLEZZI, G. 2011. River meander dynamics: developments in modelling and empirical analyses. *Earth Surface Processes and Landforms*, **36**, 1550–1553.
- HOWARD, A. D. 1996. *Floodplain Processes*. John Wiley & Sons. Chap. Modelling channel evolution and floodplain morphology, pages 15–62.
- HOWARD, A. D., & KNUTSON, T. R. 1984. Sufficient conditions for river meandering: a simulation approach. *Water Resources Research*, **20**, 1659–1667.
- HOWARD, A. D., & McLANE, C. F. 1988. Erosion of cohesionless sediment by groundwater seepage. *Water Resources Research*, **24**, 1659–1674.

- IKEDA, S., PARKER, G., & SAWAI, K. 1981. Bend theory of river meanders. Part 1. Linear development. *Journal of Fluid Mechanics*, **112**, 363–377.
- IVERSEN, T. M., KRONVANG, B., MADSEN, B. L., MARKMANN, P., & NIELSEN, M. 1993. Re-establishment of Danish streams: restoration and maintenance measures. *Aquatic Conservation: Marine and Freshwater Ecosystems*, **3**, 73–92.
- JÄHNIG, S. C., BRABEC, K., BUFFAGNI, A., ERBA, S., LORENZ, A. W., OFENBÖCK, T., VERDONSCHOT, P. F. M., & HERINGK, D. 2010. A comparative analysis of restoration measures and their effects on hydromorphology and benthic invertebrates in 26 central and southern European rivers. *Journal of Applied Ecology*, **47**, 671–680.
- JEROLMACK, D. H., & MOHRIG, D. 2007. Conditions for branching in depositional rivers. *Geology*, **35**, 463–466.
- JIN, D., & SCHUMM, S. A. 1987. *International Geomorphology, Part I*. Chichester, U.K.: John Wiley & Sons. Chap. A new technique for modeling river morphology, pages 681–690.
- JOHANNESSON, H., & PARKER, G. 1989. *River Meandering*. Water Resources Monograph, vol. 12. American Geophysical Union, Washington, D.C. Chap. Linear Theory of River Meanders, pages 181–214.
- JOHNSON, R. H., & PAYNTER, J. 1967. Development of a cutoff on the River Irk at Chadderton, Lancashire. *Geography*, **52**, 41–49.
- JOHNSON, W. C., DIXON, M. D., SIMONS, R., JENSON, S., & LARSON, K. 1995. Mapping the response of riparian vegetation to possible flow reductions in the Snake River, Idaho. *Geomorphology*, **13**, 159–173.
- KASSE, C., HOEK, W. Z., BOHNCKE, S. J. P., KONERT, M., WEIJERS, J. W. H., CASSEE, M. L., & VAN DER ZEE, R. M. 2005. Late Glacial fluvial response of the Niers-Rhine (western Germany) to climate and vegetation change. *Journal of Quaternary Science*, **20**, 377–394.
- KASVI, E., VAAJA, M., ALHO, P., HYYPÄ, J., KAARTINEN, H., & KUKKO, A. 2013. Morphological changes on meander point bars associated with flow structure at different discharges. *Earth Surface Processes and Landforms*, **38**, 577–590.
- KLEINHANS, M. G. 2010. Sorting out river channel patterns. *Progress in Physical Geography*, **34**, 287–326.
- KLEINHANS, M. G., & VAN DEN BERG, J. H. 2011. River channel and bar patterns explained and predicted by an empirical and a physics-based method. *Earth Surface Processes and Landforms*, **36**, 721–738.
- KNMI. 2014. *Langjarige gemiddelden en extremen, tijdvak 1971-2000*. <http://www.knmi.nl/klimatologie/normalen1971-2000/index.html> (accessed 26-01-2014).
- KOCHEL, R. C., & PIPER, J. F. 1986. Morphology of large valleys on Hawaii: Evidence for groundwater sapping and comparisons with Martian valleys. *Journal of Geophysical Research*, **91**, 175–192.
- KONDOLF, G. M. 2006. River restoration and meanders. *Ecology and Society*, **11**, 42.

## Bibliography

- KONDOLF, G. M. 2012. *River Conservation and Management*. John Wiley & Sons. Chap. The Espace de Liberté and Restoration of Fluvial Process: When Can the River Restore Itself and When Must we Intervene, pages 225–241.
- KONDOLF, G. M., BOULTON, A. J., O'DANIEL, S., POOLE, G. C., RAHEL, F. J., STANLEY, E. H., WOHL, E., BÅNG, A., CARLSTROM, J., CRISTONI, C., HUBER, H., KOLJONEN, S., & LOUHI, P. NAKAMURA, K. 2006. Process-based ecological river restoration: Visualizing three-dimensional connectivity and dynamic vectors to recover lost linkages. *Ecology and Society*, **11**, 5.
- KUENEN, P. H. 1944. *Gedenkboek van Dr. Ir. P. Tesch. Geologische Serie XIV, Verhandelingen van het Geologisch-Mijnbouwkundig Genootschap voor Nederland en koloniën*. Chap. De Drentsche riviertjes en het meandervraagstuk, pages 313–336.
- LANCASTER, J., & BELYEA, L. R. 2006. Defining the limits to local density: Alternative views of abundance-environment relationships. *Freshwater Biology*, **51**, 783–796.
- LANE, S. N., WESTAWAY, R. M., & HICKS, D. M. 2003. Estimation of erosion and deposition volumes in a large, gravel-bed, braided river using synoptic remote sensing. *Earth Surface Processes and Landforms*, **28**, 249–271.
- LANE, S. N., WIDDISON, P. E., THOMAS, R. E. ANS ASHWORTH, P. J., BEST, J. L., LUNT, I. A., SAMBROOK SMITH, G. H., & SIMPSON, C. J. 2010. Quantification of braided river channel change using archival digital image analysis. *Earth Surface Processes and Landforms*, **35**, 971–985.
- LANGENDOEN, E. J., & ALONSO, C. V. 2008. Modeling the evolution of incised streams. I: Model formulation and validation of flow and streambed evolution components. *Journal of Hydraulic Engineering*, **134**, 749–762.
- LANGENDOEN, E. J., & SIMON, A. 2008. Modeling the Evolution of Incised Streams. II: Streambank Erosion. *Journal of Hydraulic Engineering*, **134**, 905–915.
- LANZONI, S. 2000. Experiments on bar formation in a straight flume 1. Uniform sediment. *Water Resources Research*, **36**, 3337–3349.
- LEGLEITER, C. J., & KYRIAKIDIS, P. C. 2007. Forward and inverse transformations between cartesian and channel-fitted coordinate systems for meandering rivers. *Mathematical Geology*, **38**, 927–958.
- LEJOT, J., DELACOURT, C., PIÉGAY, H., FOURNIER, T., TRÉMÉLO, M-L., & ALLEMAND, P. 2007. Very high spatial resolution imagery for channel bathymetry and topography from an unmanned mapping controlled platform. *Earth Surface Processes and Landforms*, **32**, 1705–1725.
- LEOPOLD, L. B., & WOLMAN, M. G. 1957. *River Channel Patterns - Braided, Meandering and Straight*. Tech. rept. 282-B. US Geological Survey Professional Paper.
- LEWIN, J. 1976. Initiation of bed forms and meanders in coarse-grained sediment. *GSA Bulletin*, **87**, 281–285.
- LEWIS, G. W., & LEWIN, J. 1983. *Modern and Ancient Fluvial Systems*. Blackwell Publishing Ltd. Chap. Alluvial Cutoffs in Wales and the Borderlands, pages 145–154.
- LINDOW, N., EVANS, R. O., & BASS, K. 2007. Channel evolution and sediment transport in a restored sand bed stream. *Pages 1–10 of: Restoring Our Natural Habitat - Proceedings of the 2007 World Environmental and Water Resources Congress*.

- LINDOW, N., FOX, G. A., & EVANS, R. O. 2009. Seepage erosion in layered stream bank material. *Earth Surface Processes and Landforms*, **34**, 1693–1701.
- LISLE, T. E., IKEDA, H., & ISEYA, G. 1991. Formation of stationary alternate bars in a steep channel with mixed-size sediment: A flume experiment. *Earth Surface Processes and Landforms*, **16**, 463–469.
- LORENZ, A. W., HERING, D., FELD, C. K., & ROLAUFFS, P. 2004. A new method for assessing the impact of hydromorphological degradation on the macroinvertebrate fauna of five German stream types. *Hydrobiologia*, **516**, 107–127.
- LORENZ, A. W., JÄHNIG, S. C., & HERING, D. 2009. Re-meandering german lowland streams: Qualitative and quantitative effects of restoration measures on hydromorphology and macroinvertebrates. *Environmental Management*, **44**, 745–754.
- MAKASKE, B., SMITH, D. G., & BERENDSEN, H. J. A. 2002. Avulsions, channel evolution and floodplain sedimentation rates of the anastomosing upper Columbia River, British Columbia. *Sedimentology*, **49**, 1049–1071.
- MCGOWEN, J. H., & GARNER, L. E. 1970. Physiographic Features and Stratification Types of Coarse-Grained Point Bars: Modern and Ancient Examples. *Sedimentology*, **14**, 77–111.
- MCMILLAN, S. K., & VIDON, P. G. 2014. Taking the pulse of stream restoration practices: Moving towards healthier streams. *Hydrological Processes*, **28**, 398–400.
- MEIJLES, E. W., & WILLIAMS, A. 2012. Observation of regional hydrological response during time periods of shifting policy. *Applied Geography*, **34**, 456–470.
- MERRITT, D. M., SCOTT, M. L., POFF, N. L., AUBLE, G. T., & LYTLE, D. A. 2010. Theory, methods and tools for determining environmental flows for riparian vegetation: Riparian vegetation-flow response guilds. *Freshwater Biology*, **55**, 206–225.
- MICHELI, E. R., & LARSEN, E. W. 2011. River channel cutoff dynamics, Sacramento River, California, USA. *River Research and Applications*, **27**, 328–344.
- MIDGLEY, T. L., FOX, G. A., & HEEREN, D. M. 2012. Evaluation of the bank stability and toe erosion model (BSTEM) for predicting lateral retreat on composite streambanks. *Geomorphology*, **145-146**, 107–114.
- MILAN, D. J., HERITAGE, G. L., LARGE, A. R. G., & FULLER, I. C. 2011. Filtering spatial error from DEMs: Implications for morphological change estimation. *Geomorphology*, **125**, 160–171.
- MINISTERIE VAN VERKEER EN WATERSTAAT. 2000. *Anders omgaan met water; Waterbeleid in de 21ste eeuw*. Tech. rept. Ministerie van Verkeer en Waterstaat, Den Haag.
- MOHRIG, D., HELLER, P. L., PAOLA, C., & LYONS, W. J. 2000. Interpreting avulsion process from ancient alluvial sequences: Guadalupe-Matarranya system (Northern Spain) and Wasatch Formation (Western Colorado). *Geological Society of America Bulletin*, **112**, 1787–1803.
- MONTGOMERY, D. R. 1999. Process domains and the River Continuum. *Journal of the American Water Resources Association*, **35**, 397–410.

## Bibliography

- MOTTA, D., ABAD, J. D., LANGENDOEN, E. J., & GARCÍA, M. H. 2012a. A simplified 2D model for meander migration with physically-based bank evolution. *Geomorphology*, **163-164**, 10–25.
- MOTTA, D., ABAD, J. D., LANGENDOEN, E. J., & GARCÍA, M. H. 2012b. The effects of floodplain soil heterogeneity on meander planform shape. *Water Resources Research*, **48**, W09518.
- NAIMAN, R. J., & DÉCamps, H. 1997. The ecology of interfaces: Riparian zones. *Annual Review of Ecology and Systematics*, **28**, 621–658.
- NAIMAN, R. J., DÉCamps, H., & MCCLAIN, M. E. 2005. *Riparia*. Elsevier. 448 pp.
- NAKANO, D., & NAKAMURA, F. 2008. The significance of meandering channel morphology on the diversity and abundance of macroinvertebrates in a lowland river in Japan. *Aquatic Conservation: Marine and Freshwater Ecosystems*, **18**, 780–798.
- NEWBURY, R. W., & GABOURY, M. N. 1993. *Stream analysis and fish habitat design: A field manual*. Tech. rept. Newbury Hydraulics, Ltd, Gibsons, B.C.
- NIENHUIS, P. H. 2008. *Environmental History of the Rhine-Meuse Delta: An ecological story on evolving human-environmental relations coping with climate change and sea-level rise*. Springer. 642 pp.
- NIENHUIS, P. H., BAKKER, J. P., GROOTJANS, A. P., GULATI, R. D., & DE JONGE, V. N. 2002. The state of the art of aquatic and semi-aquatic ecological restoration projects in the Netherlands. *Hydrobiologia*, **478**, 219–233.
- NOTEBAERT, B., VERSTRAETEN, G., GOVERS, G., & POESEN, J. 2009. Qualitative and quantitative applications of LiDAR imagery in fluvial geomorphology. *Earth Surface Processes and Landforms*, **34**, 217–231.
- OLESEN, K. W. 1984. *River Meandering, Proc. Conf. Rivers 1983*. New York: ASCE. Chap. Alternate bars in and meandering of alluvial rivers, pages 873–884.
- OSBORNE, L. L., BAYLEY, P. B., HIGLER, L. W. G., STATZNER, B., TRISKA, F., & IVERSEN, T. MOTH. 1993. Restoration of lowland streams: An introduction. *Freshwater Biology*, **29**, 187–194.
- PARKER, G. 1976. On the cause and characteristic scales of meandering and braiding in rivers. *Journal of Fluid Mechanics*, **76**, 457–480.
- PARKER, G., & JOHANNESSEN, H. 1989. *River Meandering*. Water Resources Monograph, vol. 12. AGU. Chap. Observations on several recent theories of resonance and overdeepening in meandering channels, pages 379–415.
- PARKER, G., SHIMIZU, Y., WILKERSON, G. V., EKE, E. C., ABAD, J. D., LAUER, J. W., PAOLA, C., DIETRICH, W. E., & VOLLE, V. R. 2011. A new framework for modeling the migration of meandering rivers. *Earth Surface Processes and Landforms*, **36**, 70–86.
- PEAKALL, J., ASHWORTH, P. J., & BEST, J. L. 2007. Meander-bend evolution, alluvial architecture, and the role of cohesion in sinuous river channels: A flume study. *Journal of Sedimentary Research*, **77**, 197–212.

- PEDERSEN, T. C. M., BAATTRUP-PEDERSEN, A., & MADSEN, T. V. 2006. Effects of stream restoration and management on plant communities in lowland streams. *Freshwater Biology*, **51**, 161–179.
- PERUCCA, E., CAMPOREALE, C., & RIDOLFI, L. 2006. Influence of river meandering dynamics on riparian vegetation pattern formation. *Journal of Geophysical Research*, **111**, G01001.
- PERUCCA, E., CAMPOREALE, C., & RIDOLFI, L. 2007. Significance of the riparian vegetation dynamics on meandering river morphodynamics. *Water Resources Research*, **43**, W03430.
- PIÉGAY, H., & GURNELL, A. M. 1997. Large woody debris and river geomorphological pattern: examples from S.E. France and S. England. *Geomorphology*, **19**, 99–116.
- PIÉGAY, H., DARBY, S. E., MOSELMAN, E., & SURIAN, N. 2005. A review of techniques available for delimiting the erodible river corridor: A sustainable approach to managing bank erosion. *River Research and Applications*, **21**, 773–789.
- PIŠÚT, P. 2002. Channel evolution of the pre-channelized Danube River in Bratislava, Slovakia (1712–1886). *Earth Surface Processes and Landforms*, **27**, 369–390.
- POFF, N. L., & WARD, J. V. 1989. Implications of streamflow variability and predictability for lotic community structure: A regional analysis of streamflow patterns. *Canadian Journal of Fisheries and Aquatic Sciences*, **46**, 1805–1818.
- POLLEN-BANKHEAD, N., & SIMON, A. 2009. Enhanced application of root-reinforcement algorithms for bank-stability modeling. *Earth Surface Processes and Landforms*, **34**, 471–480.
- PRINGLE, C. M. 2001. Hydrologic connectivity and the management of biological reserves: A global perspective. *Ecological Applications*, **11**, 981–998.
- RICHARDSON, W. R. 2002. Simplified model for assessing meander bend migration rates. *Journal of Hydraulic Engineering*, **128**, 1094–1097.
- RODRIGUES, S., CLAUDE, N., JUGÉ, PH., & BRÉHERET, J. G. 2012. An opportunity to connect the morphodynamics of alternate bars with their sedimentary products. *Earth Surface Processes and Landforms*, **37**, 240–248.
- ROSGEN, D. L. 1994. A classification of natural rivers. *Catena*, **22**, 169–199.
- SCHIELEN, R., DOELMAN, A., & DE SWART, H. E. 1993. On the nonlinear dynamics of free bars in straight channels. *Journal of Fluid Mechanics*, **252**, 325–356.
- SCHUMM, S. A. 1977. *The Fluvial System*. Wiley-Interscience, New York. 338 pp.
- SCHUMM, S. A., & KHAN, H. R. 1971. Experimental study of channel patterns. *Nature*, **233**, 407–409.
- SCHUMM, S. A., WINKLEY, B. R., ROBBINS, L. G., & KHAN, H. R. 1972. Variability of river patterns. *Natural Physical Science*, **237**, 75–76.
- SCHUMM, S. A., BOYD, K. F., WOLFF, C. G., & SPITZ, W. J. 1995. A ground-water sapping landscape in the Florida Panhandle. *Geomorphology*, **12**, 281–297.

## Bibliography

- SEAR, D. A. 1994. River restoration and geomorphology. *Aquatic Conservation: Marine and Freshwater Ecosystems*, **4**, 169–177.
- SEAR, D. A., BRIGGS, & BROOKES, A. 1998. A preliminary analysis of the morphological adjustment within and downstream of a lowland river subject to river restoration. *Aquatic Conservation: Marine and Freshwater Ecosystems*, **8**, 167–183.
- SEKER, D. Z., KAYA, S., MUSAOGLU, N., KABDASLI, S., YUASA, A., & DURAN, Z. 2005. Investigation of meandering in Filyos River by means of satellite sensor data. *Hydrological Processes*, **19**, 1497–1508.
- SEMINARA, G., & TUBINO, M. 1989. *River Meandering*. Water Resources Monograph, vol. 12. AGU. Chap. Alternate bars and meandering: free, forced and mixed interactions, pages 267–320.
- SHIELDS, F. D., COPELAND, R. R., KLINGEMAN, P. C., DOYLE, M. W., & SIMON, A. 2003. Design for stream restoration. *Journal of Hydraulic Engineering*, **129**, 575–584.
- SIMON, A., & COLLISON, A. J. C. 2002. Quantifying the mechanical and hydrologic effects of riparian vegetation on streambank stability. *Earth Surface Processes and Landforms*, **27**, 527–546.
- SLINGERLAND, R., & SMITH, N. D. 2003. River avulsions and their deposits. *Annual Review of Earth and Planetary Sciences*, **32**, 257–285.
- SMITH, C. E. 1998. Modeling high sinuosity meanders in a small flume. *Geomorphology*, **25**, 19–30.
- STIBOKA. 1975. *Bodemkaart van Nederland, Schaal 1:50000*. Tech. rept. Stichting voor Bodemkartering, Wageningen. 200 pp.
- STØLUM, H. H. 1996. River meandering as a self-organized process. *Science*, **271**, 1710–1713.
- STRUIKSMA, N., OLESEN, K. W., FLOKSTRA, C., & DE VRIEND, H. J. 1985. Bed deformation in curved alluvial channels. *Journal of Hydraulic Research*, **23**, 57–79.
- SUDDUTH, E. B., MEYER, J. L., & BERNHARDT, E. S. 2007. Stream restoration practices in the Southeastern United States. *Restoration Ecology*, **15**, 573–583.
- SUN, T., MEAKIN, P., JØSSANG, T., & SCHWARZ, K. 1996. A simulation model for meandering rivers. *Water Resources Research*, **32**, 2937–2954.
- SUN, T., MEAKIN, P., & JØSSANG, T. 2001. A computer model for meandering rivers with multiple bed load sediment sizes. *Water Resources Research*, **37**, 2227–2241.
- TAL, M., & PAOLA, C. 2007. Dynamic single-thread channels maintained by the interaction of flow and vegetation. *Geology*, **35**, 347–350.
- TAL, M., & PAOLA, C. 2010. Effects of vegetation on channel morphodynamics: Results and insights from laboratory experiments. *Earth Surface Processes and Landforms*, **35**, 1014–1028.
- TALMON, A. M., STRUIKSMA, N., & VAN MIERLO, M. C. L. M. 1995. Laboratory measurements of the direction of sediment transport on transverse alluvial-bed slopes. *Journal of Hydraulic Research*, **33**, 495–517.

- TATE, N. J., BRUNSDON, C., CHARLTON, M., FOTHERINGHAM, A. S., & JARVIS, C. H. 2005. Smoothing/filtering LiDAR digital surface models. Experiments with loess regression and discrete wavelets. *Journal of Geographical Systems*, **7**, 273–290.
- THOMPSON, A. 1984. *Long and short-term channel change in gravel-bed rivers*. Ph.D. thesis, University of Liverpool, United Kingdom. 543 p.
- TIMÁR, G., SZÉKELY, B., MOLNÁR, G., FERENCZ, C., KERN, A., GALAMBOS, C., GERCSÁK, G., & ZENTAI, L. 2008. Combination of historical maps and satellite images of the Banat region - Re-appearance of an old wetland area. *Global and Planetary Change*, **62**, 29–38.
- TOLKAMP, H. 1980. *Organism-substrate relationships in lowland streams*. Ph.D. thesis, Wageningen University, The Netherlands. 211 p.
- TOONEN, W. H. J., KLEINHANS, M. G., & COHEN, K. M. 2012. Sedimentary architecture of abandoned channel fills. *Earth Surface Processes and Landforms*, **37**, 459–472.
- TÖRNQVIST, T. E. 1994. Middle and late Holocene avulsion history of the River Rhine (Rhine-Meuse delta, Netherlands). *Geology*, **22**, 711–714.
- TUBINO, M. 1991. Growth of alternate bars in unsteady flow. *Water Resources Research*, **27**, 37–52.
- TUBINO, M., REPETTO, R., & ZOLEZZI, G. 1999. Free bars in rivers. *Journal of Hydraulic Research*, **37**, 759–775.
- URIBELARREA, D., PÉREZ-GONZÁLEZ, A., & BENITO, G. 2003. Channel changes in the Jarama and Tagus rivers (central Spain) over the past 500 years. *Quaternary Science Reviews*, **22**, 2209–2221.
- VAN BALEN, R. T., KASSE, C., & DE MOOR, J. 2008. Impact of groundwater flow on meandering; example from the Geul River, The Netherlands. *Earth Surface Processes and Landforms*, **33**, 2010–2028.
- VAN DE WIEL, M. J., & DARBY, S. E. 2004. *Riparian Vegetation and Fluvial Geomorphology*. Water Science and Application Series 8. Washington, DC: American Geophysical Union. Chap. Numerical modeling of bed topography and bank erosion along tree-lined meandering rivers, pages 267–282.
- VAN DEN BERG, M. W. 1996. *Fluvial sequences of the Maas: A 10 Ma record of neotectonics and climate change at various time-scales*. Ph.D. thesis, Wageningen University, The Netherlands. 181 pp.
- VAN DER MOLEN, D. T., POT, R., EVERS, C. H. M., & VAN NIEUWERBURGH, L. L. J. 2012. *Referenties en maatlatten voor natuurlijke watertypen voor de Kaderrichtlijn water 2015-2021*. Tech. rept. 2012-31. STOWA.
- VAN DIJK, W. M., VAN DE LAGEWEG, W. I., & KLEINHANS, M. G. 2012. Experimental meandering river with chute cutoffs. *Journal of Geophysical Research*, **117**, F03023.
- VAN DONGEN, B., & MEIJER, D. 2008. *Zomerbedbodemveranderingen van de Maas (1889-2007)*. Tech. rept. Rijkswaterstaat Dienst Limburg.

## Bibliography

- VAN HEERD, R. M., KUIJLAARS, E. A. C., TEEUW, M. P., & VAN 'T ZAND, R. J. 2000. *Productspecificatie AHN 2000*. Tech. rept. MDTGM 2000.13. Rijkswaterstaat, Adviesdienst Geo-informatie en ICT, Delft.
- VAN RIJN, L. C. 1993. *Principles of sediment transport in rivers, estuaries and coastal seas*. Aqua Publications. 700 pp.
- VANNOTE, R. L., MINSHALL, G. W., CUMMINS, K. W., SEDELL, J. R., & CUSHING, C. E. 1980. The river continuum concept. *Canadian Journal of Fisheries and Aquatic Sciences*, **37**, 130–137.
- VENDITTI, J. G., NELSON, P. A., MINEAR, J. T., WOOSTER, J., & DIETRICH, W. E. 2012. Alternate bar response to sediment supply termination. *Journal of Geophysical Research*, **117**, F02039.
- VERDONSCHOT, P. F. M., & NIJBOER, R. C. 2002. Towards a decision support system for stream restoration in the Netherlands: An overview of restoration projects and future needs. *Hydrobiologia*, **478**, 131–148.
- VERDONSCHOT, P. F. M., DRIESSEN, O., VAN DER HOEK, W., DE KLEIN, J., PAARLBERG, A., SCHMIDT, G., SCHOT, J., & DE VRIES, D. 1995. *Beken stromen: Leidraad voor ecologisch beekherstel*. Tech. rept. STOWA, Utrecht.
- VIVASH, R., OTTOSEN, O., JANES, M., & SØRENSEN, H. V. 1998. Restoration of the rivers Brede, Cole and Skerne: a joint Danish and British EU-LIFE demonstration project, II - The river restoration works and other related practical aspects. *Aquatic Conservation: Marine and Freshwater Ecosystems*, **8**, 197–208.
- WARBURTON, J., DANKS, M., & WISHART, D. 2002. Stability of an upland gravel-bed stream, Swinhope Burn, Northern England. *Catena*, **49**, 309–329.
- WARD, J. V. 1989. The four-dimensional nature of lotic ecosystems. *Journal of the North American Benthological Society*, **8**, 2–8.
- WARD, J. V., TOCKNER, K., ARSCOTT, D. B., & CLARET, C. 2002. Riverine landscape diversity. *Freshwater Biology*, **47**, 517–539.
- WELFORD, M. R. 1994. A field test of Tubino's (1991) model of alternate bar formation. *Earth Surface Processes and Landforms*, **19**, 287–297.
- WHEATON, J. M., BRASINGTON, J., DARBY, S. E., & SEAR, D. A. 2010a. Accounting for uncertainty in DEMs from repeat topographic surveys: Improved sediment budgets. *Earth Surface Processes and Landforms*, **35**, 136–156.
- WHEATON, J. M., BRASINGTON, J., DARBY, S. E., MERZ, J., PASTERNAK, G. B., SEAR, D., & VERICAT, D. 2010b. Linking geomorphic changes to salmonid habitat at a scale relevant to fish. *River Research and Applications*, **26**, 469–486.
- WHEATON, J. M., BRASINGTON, J., DARBY, S. E., KASPRAK, A., SEAR, D., & VERICAT, D. 2013. Morphodynamic signatures of braiding mechanisms as expressed through change in sediment storage in a gravel-bed river. *Journal of Geophysical Research*, **118**, 759–779.
- WILSON, G. V., PERIKETI, R. K., FOX, G. A., DABNEY, S. M., SHIELDS, F. D., & CULLUM, R. F. 2007. Soil properties controlling seepage erosion contributions to streambank failure. *Earth Surface Processes and Landforms*, **32**, 447–459.

- WOHL, E., ANGERMEIER, P. L., BLEDSOE, B., KONDOLF, G. M., MACDONNELL, L., MERRITT, D. M., PALMER, M. A., POFF, N. L., & TARBOTON, D. 2005. River restoration. *Water Resources Research*, **41**, W10301.
- WOLFERT, H. P. 2001. *Geomorphological change and river rehabilitation: case studies on lowland fluvial systems in The Netherlands*. Ph.D. thesis, Utrecht University, The Netherlands. Alterra Scientific Contributions 6. 200 pp.
- WOLFERT, H. P., & DE LANGE, G. W. 1990. *Toelichting op kaartblad 52 Venlo; Geomorfologische kaart van Nederland 1:50 000*. Tech. rept. Staring Centrum, Wageningen/Rijks Geologische Dienst, Haarlem.
- WYNN, T. M., MOSTAGHIMI, S., BURGER, J. A., HARPOLD, A. A., HENDERSON, M. B., & HENRY, L. A. 2004. Variation in Root Density along Stream Banks. *Journal of Environmental Quality*, **33**, 2030–2039.
- ZINGER, J. A., RHOADS, B. L., & BEST, J. L. 2011. Extreme sediment pulses generated by bend cutoffs along a large meandering river. *Nature Geoscience*, **4**, 675–678.
- ZINGER, J. A., RHOADS, B. L., BEST, J. L., & JOHNSON, K. K. 2013. Flow structure and channel morphodynamics of meander bend chute cutoffs: A case study of the Wabash River, USA. *Journal of Geophysical Research - Earth Surface*, **118**, 2468–2487.
- ZOLEZZI, G., & SEMINARA, G. 2001. Downstream and upstream influence in river meandering. Part 1. General theory and application to overdeepening. *Journal of Fluid Mechanics*, **438**, 183–211.



# Summary

Halfway the 20th century, groundwater management in agricultural areas led to channelisation of the majority of lowland streams in the Netherlands. This has led to degradation of the aquatic and terrestrial ecosystems, characteristic for lowland streams. Over the past 25 years, water authorities in the Netherlands have aimed at restoring these degraded streams. Historical maps show that many lowland streams consist of a meandering planform. Re-meandering is the common practice regarding stream restoration in the Netherlands. Little is known about the morphological processes following the completion of such stream restoration projects. The aim of this thesis is to characterize the morphodynamic developments of restored lowland streams, with a focus on meander processes.

Three traditional stream restoration projects (Hagmolenbeek, Lunterse beek and Tungelroyse beek) were monitored during the initial two years after construction of the new channel. In these projects, the former straightened channel was replaced by a re-meandered channel. A standardized monitoring plan was implemented, which included three morphological surveys (cross-sections, with a one-year interval), sediment sampling (from the initial and final channel bed), habitat pattern surveys (three times per year) and continuous discharge and water level measurements. The morphological measurements revealed that morphodynamic developments are mainly concentrated in the first year following construction. Adjustment of the longitudinal bed profile was the main morphological response. Structures (e.g. bridges and weirs), channel width variation and heterogeneity of the channel substrate caused channel bed incision and aggradation, and hence, channel slope adjustment. Lateral development was observed only in a limited number of channel bends, and was mainly related to floodplain heterogeneity. The habitat surveys showed the occurrence of gravel, silt, vegetation and algae on the channel bed. Morphological developments at the scale of the channel cross-section were exceptional, despite the fine sediment characteristics (median grain size 125-250 µm). Due to these channel bed characteristics, sediment is transported during the entire year.

Water authorities are constantly looking for more cost-effective alternatives for

re-meandering. One such method is to remove bank protection and allow autogenous processes to develop a sinuous planform. To study these processes, a large-scale field experiment was performed in a 600 m long straight channel reach (Hooge Raam). Over a period of almost three years, the channel was allowed to evolve autogenously from initially flat-bed conditions, in response to a variable discharge. Alternate bars developed within eight months after the start of the experiment. The initial stages of bar development included bar growth, both in wavelength and in amplitude, and limited bar migration. Towards the end of the experiment, the alternate bar pattern became increasingly irregular and bar amplitudes started to decrease. During the experiment, the channel slope declined from  $1.8 \text{ m km}^{-1}$  to  $0.9 \text{ m km}^{-1}$ . Two bar theories were applied to establish their predictive capacity. Both bar theories predicted the development of alternate bars under the constructed channel conditions and a decreasing likelihood for the development of alternate bars in response to the declining channel slope. This study shows that it is unlikely that the typical sinuous planform in lowland streams, as observed from historical maps, is the result from autogenous processes alone. Exogenous processes, such as a local seepage or floodplain heterogeneity, may be needed to achieve channel sinuosity.

Processes of meander initiation were studied focussing on a man-made canal (Gelderns-Nierskanaal). The canal was constructed near the end of the 18th century, as a straight channel between the river Niers (Germany) and the river Meuse (The Netherlands). The banks on the Dutch part of the channel were left unprotected and developed into an active meandering channel, featuring meander development and valley incision. These processes were analysed using historical topographic maps and recent airborne LiDAR data. Meandering initiated in three sections of the channel, where the channel sinuosity developed asynchronously over time. Sedimentary successions in the study area show layers of iron oxide, indicating groundwater seepage from nearby located higher elevated terrains. Only at the spots where meandering had initiated, iron oxide was found close to the surface level. This provides a clue that seepage triggered bank erosion by increasing the moisture content of the banks. The spatial variation in meandering behaviour, as observed in this channel, justifies efforts to implement the influence of floodplain heterogeneity and the effect of seepage on bank erosion in meander models.

Backwater effects played a substantial role in the development of a chute cutoff, which occurred after the realization of a stream restoration project in the Lunterse beek. In this stream restoration project, additional measurements were performed, next to the standardized monitoring plan. Over a period of almost 2 years, the additional monitoring included fourteen high-resolution morphological surveys and

riparian vegetation mapping. Prior to the cutoff, a plug bar was deposited in the bend to be cutoff. Hydrodynamic model results were used to infer that the plug bar was related to a backwater effect, causing a drop of sediment transport capacity. Upstream from the plug bar, an embayment formed in the floodplain at a location where the former channel was located. The former channel was filled with sediment prior to channel construction, resulting in a less consolidated area of the floodplain. Consequently, it was prone to erosion. The chute channel continued to incise and widen into the floodplain and, after 6 months, acted as the main channel. These results show how upstream sediment supply and backwater effects are involved in the processes that lead to the occurrence of a chute cutoff.

The chute cutoff and several additional morphological adjustments occurred in a period without riparian vegetation in the Lunterse beek. Herbaceous vegetation started to develop approximately 7 months after construction, with a maximum coverage by the end of the summer period. Detailed morphological and hydrological data show a marked difference in morphological behaviour between the pre-vegetation and post-vegetation stage. A linear regression procedure was applied to relate morphological activity to time-averaged Shields stress. In the initial stage after construction, with negligible riparian vegetation, channel morphology adjusted with a weak response to the discharge hydrograph. In the subsequent period, morphological activity in the showed a clear relation to discharge variation. The two stages of morphological response to the restoration measures may be caused by riparian vegetation development, although additional field measurements are needed to substantiate these findings.

Lowland streams are small rivers, consisting of a sinuous channel pattern, a sandy channel bed and a gentle slope ( $<1 \text{ m km}^{-1}$ ). It is likely that the sinuous planform observed on historical maps is a result from exogenous influences, rather than autogenous processes. In general, the studied lowland streams show little morphological activity. The observed morphodynamics occurred mainly in the first year after construction and were caused by backwater effects and floodplain heterogeneity. After initial morphological adjustments, the channel planform remained stable. The rapid establishment towards an equilibrium state of the channel planform is at odds with the view on lowland streams as small rivers migrating actively in their own deposits. The term re-meandering may be misleading, because of the connotation with channel meandering in time. The steadiness of the channel planforms has not been extensively demonstrated over geological time scales. This study has focused on short-term observations, since engineering time scales are more relevant for stream restoration practitioners.



# Samenvatting

In de eerste helft van de 20<sup>ste</sup> eeuw zijn veel laaglandbeken in Nederland gekanaliseerd. De intensivering van de landbouw en de daaraan gekoppelde grondwaterbehoefte liggen ten grondslag aan deze grootschalige kanalisatie. Dit heeft geleid tot een degradatie van het karakteristieke laaglandecosysteem. In de afgelopen 25 jaar zijn de Nederlandse waterschappen begonnen met het herstellen van een groot deel van de laaglandbeken. Op historische kaarten is te zien dat laaglandbeken in het verleden een meanderend karakter hadden. Verder worden laaglandbeken getypeerd door een bodemverhang kleiner dan  $\sim 1 \text{ m km}^{-1}$ , een breedte kleiner dan  $\sim 20 \text{ m}$  en een zandige bodem. Het hermeanderen van laaglandbeken is een vaak gebruikte techniek om laaglandbeken te herstellen. Tot nu toe is er weinig onderzoek gedaan naar de morfologische processen na aanleg van beekherstelpunten. Het doel van dit proefschrift is het karakteriseren van de morfologische processen in herstelde laaglandbeken, met een focus op meanderprocessen.

In drie laaglandbeken waar traditionele hermeandering is toegepast (Hagmolenbeek, Lunterse beek en Tungelroyse beek), is gedurende de eerste twee jaar na aanleg een standaard monitoringsprogramma geïmplementeerd. Het monitoringsprogramma omvatte morfologische metingen (in dwarsprofielen, één keer per jaar), sedimentbemonstering (bij aanleg en na twee jaar), habitatopnames (drie keer per jaar) en continue afvoer- en waterstandsmetingen. De meeste morfologische veranderingen vonden in het eerste jaar na aanleg plaats, waarbij de meest dominante morfologische veranderingen in het lengteprofiel plaatsvonden. Constructies (bv. bruggen en stuwen), variatie in de breedte en heterogeniteit van de beekbodem waren de belangrijkste oorzaken van deze veranderingen. In twee beken heeft dit tot een afname van het bodemverhang geleid. Laterale aanpassingen zijn slechts op kleine schaal waargenomen, met name in bochten en gerelateerd aan de heterogeniteit van de ondergrond. Gedurende de twee jaar na aanleg zijn verschillende habitattypen waargenomen, zoals een grindbank, een slibbank, macrofyten en algen. Hoewel de morfologische aanpassingen gering waren, wordt er gedurende het hele jaar sediment getransporteerd. De fijne zandkarakteristieken (mediane

korrelgrootte 125-250  $\mu\text{m}$ ) spelen hierin een bepalende rol.

Waterschappen in Nederland zijn constant op zoek naar kostenefficiënte alternatieven voor beekherstel. Eén van deze methoden is het verwijderen van oeversbeschouwing, vervolgens zouden autogene morfologische processen een kronkelende loop moeten vormen. In een grootschalig veldexperiment zijn deze morfologische processen onderzocht. In de Hooge Raam is over een lengte van 600 m een rechte waterloop aangelegd. Gedurende een periode van bijna drie jaar is de morfologische ontwikkeling gevolgd. Binnen acht maanden na aanleg is een regelmatig alternerend bankenpatroon ontstaan, met een kronkelende stroomdraad. In de daaropvolgende periode namen de banklengte en bankamplitude toe en heeft bankmigratie plaatsgevonden. Halverwege het veldexperiment verdween de regelmaat in het bankenpatroon. Ook is een afname van de bankamplitude waargenomen. Gedurende het veldexperiment is het aangelegde bodemverhang gehalveerd, van  $1.8 \text{ m km}^{-1}$  tot  $0.9 \text{ m km}^{-1}$ . Het afnemen van het bodemverhang is gerelateerd aan stuweffecten. De stuweffecten zijn veroorzaakt door een ver nauwing van de beekbreedte benedenstroms van het experimentele traject. Op basis van de meetgegevens uit het veldexperiment is de voorspelkracht van twee banktheoriën getest. Beide theoriën voorspellen het ontstaan van alternerende banken onder de initiële veldcondities. Ook voorspellen de twee theoriën een afnemende waarschijnlijkheid van het ontstaan van alternerende banken als gevolg van het afnemen van het bodemverhang. Het regelmatige alternerende bankenpatroon verdween nadat het bodemverhang afnam tot een waarde die tegen de bovengrens ligt van typische waarden voor laaglandbekken. Het is daarom onwaarschijnlijk dat het typische kronkelende meanderpatroon, zoals te zien op historisch kaartmateriaal, veroorzaakt is door louter autogene morfologische processen. Het is aannemelijk dat in het verleden exogene invloeden, zoals lokale kwel en de heterogeniteit van de ondergrond, hebben bijgedragen aan het ontstaan van de kronkelende waterlopen in laaglandgebieden.

De invloed van exogene processen op de initiatie van meandering zijn in detail bestudeerd in het Gelderns-Nierskanaal. Aan het eind van de 18<sup>de</sup> eeuw is het kanaal aangelegd vanaf de Niers (Duitsland) naar de Maas (Nederland), met als doel het tegengaan van piekafvoeren op de Niers. De oevers van het Nederlandse deel van het kanaal zijn grotendeels onaangeroerd gelaten en er is in ruim 200 jaar een actief meanderende waterloop ontstaan, inclusief bocht afsnijdingen en insnijding in het aanwezige Maastrichtsche Bassin. De meanderprocessen zijn geanalyseerd op basis van historisch kaartmateriaal, een gedetailleerde hoogtekaart (Algemeen Hoogtebestand Nederland) en veldmetingen. Meandering is in drie onafhankelijke secties van het kanaal geïnitieerd. Op basis van grondboringen is aangetoond dat

ijzeroxide voorkomt in verschillende lagen in de ondergrond. IJzeroxide is een indicatie voor (lokale) kwel. Juist op de drie lokaties waar meandering is geïnitieerd zijn de ijzeroxidelagen dicht aan het maaiveld gevonden. De kwel heeft mogelijk lokaal voor een toename van het vochtgehalte van de oevers gezorgd, dit maakte de oevers vatbaar voor erosie en heeft het meanderproces op gang gebracht. De ruimtelijke variatie van het meanderpatroon, zoals in het Gelderns-Nierskanaal is waargenomen, rechtvaardigt de huidige inspanningen om exogene invloeden, zoals kwel en de heterogeniteit van de ondergrond, op te nemen in meandermodellen.

In de Lunterse beek speelden stuweffecten een substantiële rol in de morfologische ontwikkelingen die uiteindelijk tot een bochtafsnijding hebben geleid. Naast het gestandaardiseerde monitoringsplan zijn aanvullende morfologische metingen verricht, met een verhoogde ruimtelijke en temporele resolutie. Naast de morfologische metingen met een hoge resolutie is gedurende een periode van bijna twee jaar de vegetatieontwikkeling gevolgd. Binnen drie maanden na aanleg van de nieuwe beek heeft een bochtafsnijding plaatsgevonden, wat een morfologische aanpassing is die eerder nog maar weinig in detail is geobserveerd. In de periode voordat de bochtafsnijding plaatsvond is een rivierbank afgezet. Door middel van een 3D-stromingsmodel is aangetoond dat het ontstaan van de rivierbank gerelateerd is aan benedenstroomse stuweffecten. Daarnaast laten ingemeten lengteprofielen zien dat bovenstroms van het onderzoeksgebiedinsnijding heeft plaatsgevonden en sediment in benedenstroomse richting is getransporteerd. De combinatie van de bovenstroomse sedimenttoevoer en benedenstroomse stuweffecten hebben tot de vorming van de rivierbank geleid. Vervolgens is in de inundatiezone een nieuwe waterloop ontstaan, bovenstroms van de rivierbank. De initiële insnijding in de inundatiezone vond plaats op een lokatie waar de voormalige gekanaliseerde loop was gelegen. Nadat de nieuwe kronkelende beekloop was gegraven is de voormalige gekanaliseerde loop gedempt met zand dat vrij was gekomen bij de graafwerkzaamheden. Het is aannemelijk dat de oevers waar het zand was gedumpt een zwakkere pakking had dan rest van onderzoeksgebied, wat de oever vatbaar voor erosie maakte. De nieuwe waterloop heeft zich vervolgens verder ingesneden in de inundatiezone, zowel in de breedte als in de diepte. Na zes maanden was de bochtafsnijding voltooid en functioneerde de nieuwe waterloop als hoofdwaterloop. De resultaten van dit onderzoek laten zien hoe bovenstroomse sedimenttoevoer en benedenstroomse opstuwing een belangrijke rol kunnen spelen in de vorming van een bochtafsnijding.

De bochtafsnijding en daaropvolgende bochtmigratie vonden met name plaats in een periode waarin terrestrische vegetatie nog niet was ontwikkeld. Kruidige vegetatie begon zich ongeveer zeven maanden na aanleg van het hermeanderingspro-

ject te ontwikkelen. Aan het eind van de eerste zomer is een maximum in biomassa waargenomen. Gedetailleerde morfologische en hydrologische meetgegevens laten zien dat er een merkbaar verschil is tussen de initiële periode zonder vegetatie en de periode met vegetatie. Er is een lineair verband afgeleid tussen de morfologische ontwikkeling en de tijdgemiddelde Shields parameter. De Shields parameter geeft informatie over de schuifspanning die het water uitoefent op de beekbodem. Het lineaire verband laat zien dat de morfologische ontwikkeling in de initiële periode wordt getypeerd door een gebrekkige relatie met de Shields parameter. Zelfs bij lage afvoeren zijn veel morfologische veranderingen waargenomen. In de daarop volgende periode is de respons sterker aanwezig, waarbij grote morfologische veranderingen optradën in perioden met een hoge afvoer en vice versa. Het verschil tussen de initiële periode zonder vegetatie en de periode met vegetatie is mogelijk gerelateerd aan de bovenstroomse aanvoer van sediment, die tot het afzetten van de rivierbank heeft geleid. Het is in deze studie dan ook niet eenduidig vastgesteld of de oevervegetatie heeft bijgedragen aan de verandering van de morfologische respons. Vervolgonderzoek is nodig om de rol van vegetatieontwikkeling op morfologische processen binnen beekherstelprojecten duidelijker vast te stellen.

Het is aannemelijk dat het kronkelende bovenaanzicht van laaglandbekken in Nederland, dat op veel historisch kaartmateriaal is te zien, veroorzaakt is door exogene invloeden, in plaats van door autogene processen. Over het algemeen vindt er geen actieve oevermigratie plaats op de schaal van de beek als geheel. Lokale veranderingen concentreren zich in het eerste jaar na aanleg, waarbij opstuwing en de heterogeniteit van de ondergrond een belangrijke rol spelen. Na de initiële aanpassingsperiode ontstaat een stabiel bovenaanzicht. De kortstondige morfologische aanpassing staat haaks op het beeld dat laaglandbekken morfologisch actieve riviertjes zijn. De term '*hermeandering*' is misleidend, vanwege de suggestie dat laaglandbekken de kenmerken zouden hebben van actief meanderende rivieren. Dit onderzoek heeft zich met name gericht op korte morfologische tijdschalen vanwege de relevantie voor het Nederlandse waterbeheer. Dit heeft inzichten verschafft in de meest relevante morfologische processen voor de beekherstelpraktijk.

# Dankwoord

Een promotieonderzoek doe je natuurlijk niet alleen. In de afgelopen 5 jaar heb ik veel hulp gehad, niet alleen van mijn begeleiders, maar van veel meer mensen die op enigerlei wijze betrokken waren bij dit proefschrift. Ik wil iedereen op deze manier bedanken voor hun hulp.

In tegenstelling tot veel andere aio's ben ik niet zomaar in een promotietraject gerold. Op 7 april 2009 had ik mijn sollicitatiegesprek met m'n dagelijkse begeleider Ton Hoitink. Ik kan me nog goed herinneren dat mij tijdens het sollicitatiegesprek gevraagd werd waarom ik het woord 'beek' niet in mijn sollicitatiebrief had opgenomen. Ik wist destijds eerlijk gezegd ook niet echt wat een beek was (klein riviertje toch?), maar gezien dit boekje heb ik Ton tijdens dat gesprek kunnen overtuigen. Ton, ik wil je graag bedanken voor je toeloze enthousiasme dat je in mijn werk hebt gestopt. Je hebt me gestimuleerd om het uiterste uit dit onderzoek te halen en het heeft naast dit proefschrift geresulteerd in een rapport én verschillende Engels- en Nederlandstalige artikelen. Ik ben daar erg trots op en zonder jouw steun was dit niet tot stand gekomen. Ook wil ik je bedanken voor het feit dat je me zonder problemen naar Murcia op-en-neer hebt laten vliegen.

Ook wil ik mijn promotor, Remko Uijlenhoet, bedanken. Remko, ook al heb je het verloop van mijn promotie meer vanaf de zijlijn gevolgd, toch heb je een grote bijdrage geleverd aan de totstandkoming. Gedurende de eerste vier jaar was dat met name het volgen van de vooruitgang, wat mij ertoe dwong om bij tijd en wijle een planning te maken. In de laatste periode heb je veel tijd gestoken in het verbeteren van de tekst. Gezien het tijdstip waarop je de meeste mailtjes stuurde, heb je vaak tot in de kleine uurtjes doorgewerkt om alles op tijd af te krijgen. Het heeft mij positief verrast dat je als hoogleraar de gezelligheid erin probeert te houden (borrels op vrijdagmiddag, het HWM-weekend...). Erg bedankt voor je hulp bij het schrijven van mijn proefschrift en de gezelligheid op de leerstoelgroep! Gaandeweg is mijn tweede promotor, Piet Verdonschot, ook steeds meer betrokken geraakt bij mijn promotie. Eerst als projectleider van *Beekdalbreed Hermeanderen* en als grote vraagbaak voor beekherstel, maar ook bij de totstandkoming van de laatste

## Dankwoord

hoofdstukken van dit proefschrift en het rapport. Met name de interpretatie van mijn resultaten in het licht van beekherstel had niet kunnen plaatsvinden zonder zijn inbreng. Het proefschrift heeft hierdoor een échte toegevoegde waarde voor de praktijk gekregen. Heel erg dank daarvoor.

Een groot deel van mijn eerste jaar heb ik besteed aan het zoeken naar interessante beekherstelprojecten om het onderzoek te kunnen uitvoeren. Totdat het project *Beekdalbreed Hermeanderen* begon, had ik nog geen geschikte beekherstel-projecten gevonden. Het project, dat gefinancierd werd door Agentschap NL, begon een jaar nadat ik met mijn promotie was begonnen. Er waren verschillende waterschappen bij dit project betrokken, die allemaal een beekherstelproject inbracht. Jan de Brouwer (Alterra) en Rob Fraaije (Universiteit Utrecht) waren binnen dit project de aio's die onderzoek gingen doen naar het effect van beekherstel op de aquatische en terrestrische ecologie. Vanaf het begin hadden we regelmatig contact over de verschillende beekherstelprojecten. We bezochten alle waterschappen en gingen gedrieën het veld in om *stilling wells* te installeren en grondwaterbuizen te slaan. Na een geslaagd congres in Clermond-Ferrand besloten we een tripje naar Polen op te zetten, met als doel het karakteriseren van "natuurlijke" laaglandbekken. Ik denk, dat we in die drie weken veel van elkaar én van elkaars onderzoek hebben geleerd. Helaas bleek het lastiger dan gedacht om ons onderzoek in Nederland helemaal op elkaar af te stemmen. Toch hebben jullie allebei een grote bijdrage geleverd aan twee hoofdstukken in dit proefschrift. Heel erg bedankt voor deze bijdrage en voor de goede samenwerking. Ook wil ik Erik Mosselman (Deltares) en Bart Makaske (Alterra en Wageningen Universiteit) bedanken voor hun bijdrage aan de hoofdstukken over de Hooge Raam en het Gelderns-Nierskanaal. En ik wil Eddy Langendoen (USDA-ARS, USA) bedanken voor de vruchtbare discussies bij zijn bezoek aan Wageningen en Ithaca.

In de periode dat ik bij de leerstoelgroep HWM werkzaam was, heb ik verschillende kamergenoten versleten. Met name de eerste drie jaar met Pieter zijn mij uitermate bevallen. In die drie jaar is een goede vriendschap ontstaan. We waren goed op elkaar ingespeeld met af en toe een muziekje, een filmpje en een vrijmbo'tje. Maar ook buiten het werk om hebben we elkaar veel gezien. Pieter, bedankt voor de mooie tijd! Toen we met de leerstoelgroep, maar zonder Pieter, naar Lumen verhuisden werden Olda en Lieke mijn nieuwe kamergenoten. Olda, in the period we shared a room we were dealing with the same issues, mainly related to finishing our PhD theses. Olda, thanks for all your help! In het laatste jaar was Lieke mijn kamergenoot, dat bleek al snel erg gezellig. Lieke begon in die periode aan haar promotieonderzoek en ik herkende veel van haar ervaringen uit mijn eerste jaar. Lieke, ik vond het erg leuk om jouw als kamergenoot te hebben.

Ook de rest van mijn collega's wil ik graag bedanken voor hun, vaak hydrologische, advies, de lunches en de gezellige borrels op de vrijdagmiddag. Daarnaast wil ik graag alle technici bedanken, die een bijdrage geleverd hebben aan mijn veldwerkzaamheden: Matthijs Boersema, Pieter Hazenberg, Johan Römelings, Henny Gertsen, Dorine Dekkers en Philip Wenting. Met name wil ik Philip bedanken voor het beschikbaar stellen van de GNSS(!)-apparatuur en de leuke discussies in zijn werkplaats. In totaal heb ik vijf studenten begeleid bij hun Bachelor en Master theses. De resultaten zijn helaas niet direct naar het proefschrift gevloeid, maar hebben wel bijgedragen aan het onderzoek naar laaglandbekken en hebben verschillende interessante inzichten opgeleverd. Iris, Wieneke, Tjitske, Marjan en Serge: bedankt voor jullie hulp!

Dit proefschrift zou nooit geschreven kunnen worden zonder de financiële steun van de STOWA (Stichting Toegepast Onderzoek WAterbeheer). Ik wil met name Michelle Talsma bedanken voor haar enthousiasme en haar drive om de opgedane kennis beschikbaar te maken voor de Nederlandse waterschappen. Dit heeft zich geuit in het rapport *Morfodynamiek van Nederlandse laaglandbekken* en drie Nederlandstalige artikelen, waarin Michelle een grote bijdrage heeft geleverd. Ook wil ik graag de leden en het kernteam van de Community of Practice Hermeandering bedanken voor de initiële ideeën die hebben geleid tot het opzetten van dit promotieonderzoek en, in het laatste half jaar, de vertaling naar de praktijk. Een belangrijke rol was hierin weggelegd voor Wim Zeeman (voormalig DLG), die zelfs in de periode na zijn pensionering nog druk in de weer is geweest met deze vertaalslag. Ook wil ik de betrokken waterschappen bedanken voor hun bijdrage bij het verzamelen van meetgegevens: Waterschap Aa & Maas, Waterschap Peel & Maasvallei, Waterschap Vallei & Veluwe en Waterschap Vechtstromen. In het bijzonder wil ik Mirja Kits (Waterschap Aa & Maas) bedanken voor haar enthousiasme in het Hooge Raam project en haar toewijding in het beekherstel.

Werk is één ding, maar mijn sociale leven is minstens zo belangrijk. Een paar weken nadat ik met mijn promotie was begonnen, leerde ik Anton kennen. Samen met Pieter waren we in het weekend vaak in de Doctor te vinden. Dit was niet alleen gezellig, maar hielp ook in het relativeren van mijn onderzoek. Anton, bedankt voor de mooie tijd in Wageningen! Na een paar maanden introduceerde Anton mij bij VV Wageningen, alwaar ik de onnavolgbare linkermiddenvelder werd waar ik altijd al van droomde, helaas uitte zich dat met name in de derde helft... Mannen van Wageningen 4, bedankt voor de gezellige tijd! Aangezien ik niet echt honkvast ben, is het lastig om vriendschappen te onderhouden. Ik ben blij dat het met Bas, Louis, Bjorn, Ard en Marit wel gelukt is. Ik hoop dat jullie nu eindelijk weten wat mijn promotie inhoudt en ik wil jullie graag bedanken voor de gezellige stapavonden die

## Dankwoord

we in de afgelopen vijf jaar hebben gehad. Ik wil graag mijn ouders bedanken voor hun volwaardige steun in de afgelopen vijf jaar. Na de verhuizing vanuit Enschede en de verbouwing van mijn appartement in Wageningen, was er de verhuizing naar Murcia. Ik wil jullie heel erg bedanken voor wat jullie voor mij hebben gedaan de afgelopen 5 jaar, ik waardeer het zeer. Ook wil ik mijn broer Bastiaan en zijn gezin (Karin, Noa en Mick) bedanken voor de steun die ik de afgelopen vijf jaar heb gekregen.

Mari Luz, you are the best thing that happenend in my life. The three years of flying back-and-forth were very long, that's why I'm very happy now to finally be with you. In the final year you encouraged me to finish my PhD thesis and to follow in research. I just want to say this: iMe encantas!

Joris Eekhout

Murcia, 25 maart 2014

# Publications

## Journal articles

EEKHOUT, J. P. C., HOITINK, A. J. F., & MAKASKE, B. 2013. Historical analysis indicates seepage control on initiation of meandering. *Earth Surface Processes and Landforms*, **38**, 888-897.

EEKHOUT, J. P. C., HOITINK, A. J. F., & MOSSELMAN, E. 2013. Field experiment on alternate bar development in a straight sand-bed stream. *Water Resources Research*, **49**, 8357-8369.

EEKHOUT, J. P. C., FRAAIJE, R. G. A., & HOITINK, A. J. F. (*under review*). Morphodynamic regime change in a restored lowland stream. Submitted to *Earth Surface Dynamics*.

EEKHOUT, J. P. C., & HOITINK, A. J. F. (*under review*). Importance of backwater effects to the occurrence of a chute cutoff. Submitted to *Journal of Geophysical Research - Earth Surface*.

EEKHOUT, J. P. C., HOITINK, A. J. F., DE BROUWER, J. H. F., & VERDONSCHOT, P. F. M. (*submitted*). Morphological assessment of reconstructed lowland streams in the Netherlands. Submitted to *Advances in Water Resources*.

DE BROUWER, J. H. F., EEKHOUT, J. P. C., HOITINK, A. J. F., BESSELLOTOTSKAYA, A., & VERDONSCHOT, P. F. M. (*in preparation*). Quantified flow conditions for leaf transport in streams.

## Conference proceedings

EEKHOUT, J. P. C., & HOITINK, A. J. F. 2011. Field-scale experiment of migrating bar behavior: preliminary analysis. In: *EUROMECH Colloquium 523, Ecohydraulics: linkages between hydraulics, morphodynamics and ecological processes in rivers, Clermont-Ferrand, France, June 15-17*, 207-211.

EEKHOUT, J. P. C., & HOITINK, A. J. F. 2012. Field-scale experiment on migrating bar dynamics: preliminary analysis. In: *River Flow 2012: Proceedings of the 6th edition of the international conference on fluvial hydraulics, San Jose, Costa Rica, September 5-7*, 623-627.

## Professional publications

- EEKHOUT, J. P. C., HOITINK, A. J. F., MAKASKE, B., & TALSMA, M. 2013. Het Geldernsch-Nierskanaal: hoe een recht kanaal gaat meanderen als gevolg van kwel. *H<sub>2</sub>O* (online).
- EEKHOUT, J. P. C., HOITINK, A. J. F., HUISING, G., & TALSMA, M. 2014. Morfologische aanpassing na beekherstel - casestudie Lunterse Beek. *H<sub>2</sub>O* (online).
- EEKHOUT, J. P. C., & HOITINK, A. J. F. 2014. Morfodynamiek van Nederlandse laaglandbekken. Tech. rept. 2014-15. STOWA, Amersfoort, *in press*.
- EEKHOUT, J. P. C., HOITINK, A. J. F., MOSELMAN, E., KITS, M., & TALSMA, M. 2014. Veldexperiment in de Hooge Raam: winst voor beekherstel én wetenschap. *Stromingen*, *in press*.

# About the Author

Joris Eekhout (April 6, 1981), was born and raised in Nijmegen, the Netherlands. During his childhood, he was always fascinated by the River Waal, which borders the city of Nijmegen. In 2000 he finished high school (Canisius College), where he got interested in mathematics. He started studying *Applied Mathematics* at Twente University in Enschede, but soon after he realised that he missed the practical applicability of the knowledge he was obtaining. After half a year he switched to *Civil Engineering and Management* and got more and more interested in the subjects related to hydraulics and morphodynamics. In 2006 he spent an internship at Royal Haskoning (Nijmegen), where he developed a numerical model on the morphodynamics of the Oosterschelde (Eastern Scheldt) in response to the construction of the storm surge barrier. His findings were included in the report '*Plaat – Geul interactie in de Oosterschelde*'. In 2007 he assisted Dr. Jolanthe Schretlen during her large-scale wave experiments at the GWK-flume in Hannover (Germany). Data from these experiments he used for his MSc thesis, supervised by Dr. Jan Ribberink. He obtained his master degree with the MSc-thesis '*Measurements and modeling of cross-shore morphodynamics*', which focussed on the interaction of full-scale waves on cross-shore morphodynamics in coastal areas. In May 2009, Joris started as a PhD-candidate at the *Hydrology and Quantitative Water Management Group* of Wageningen University (Wageningen), under supervision of Dr. Ton Hoitink. During his PhD research his focus switched from coastal to fluvial morphodynamics. In 2010 he joined the multi-disciplinary research project *Beekdalbreed Hermeanderen* (*Valley-wide stream restoration*), coordinated by Prof. Piet Verdonschot (Alterra and the University of Amsterdam). During his period as a PhD-candidate, he spent one month at the *Department of Biological and Environmental Engineering* of Cornell University (Ithaca, USA) and six months at the *Soil Erosion and Conservation Group* of CEBAS-CSIC (Murcia, Spain).





Netherlands Research School for the  
Socio-Economic and Natural Sciences of the Environment

# C E R T I F I C A T E

The Netherlands Research School for the  
Socio-Economic and Natural Sciences of the Environment  
(SENSE), declares that

*Joris Eekhout*

born on 6 April 1981 in Nijmegen, The Netherlands

has successfully fulfilled all requirements of the  
Educational Programme of SENSE.

Wageningen, 9 May 2014

the Chairman of the SENSE board

Prof.dr.ir. Huub Rijnaarts

the SENSE Director of Education

Dr. Ad van Dommelen

The SENSE Research School has been accredited by the Royal Netherlands Academy of Arts and Sciences (KNAW)



K O N I N K L I J K E   N E D E R L A N D S E  
A K A D E M I E   V A N   W E T E N S C H A P P E N



The SENSE Research School declares that Mr. Eekhout has successfully fulfilled all requirements of the Educational PhD Programme of SENSE with a work load of 38.6 EC, including the following activities:

**SENSE PhD Courses**

- o Environmental Research in Context (2010)
- o Research Context Activity: Co-organizing SENSE Symposium on Land-Water-Atmosphere Interactions (Wageningen, 9 March 2010)

**Other PhD and Advanced MSc Courses**

- o River Restoration: Fluvial Geomorphic & Ecological Tools (2010)
- o Techniques for Writing a Scientific Paper (2011)
- o Workshop I-RIC (2011)
- o Sediment Transport and Associated Fluvial Processes (2012)
- o Career Assessment (2013)

**Management and Didactic Skills Training**

- o Supervision of 2 MSc and 2 BSc theses (2009-2013)

**Oral Presentations**

- o *Long-term evolution of a morphologically active man-made stream in the Netherlands.* SENSE Symposium 'Modelling and observing earth system compartments', 22 February 2011, Wageningen, The Netherlands
- o *Field-scale experiment of migrating bar behavior: preliminary analysis.* Ecohydraulics, 15-17 June 2011, Clermont-Ferrand, France
- o *Field experiment on alternate bar dynamics.* International Conference on Fluvial Hydraulics: River Flow 2012, 5-7 September 2012, San José, Costa Rica
- o *Stabiliteitsdiagram van laaglandbekken.* Community of Practice: Hermeandering, 15 November 2012, Wageningen, The Netherlands

SENSE Coordinator PhD Education



A handwritten signature in black ink, appearing to read "Monique Gulickx". It is written in a cursive, flowing style with a long horizontal stroke extending from the end of the first name.

Dr. ing. Monique Gulickx

The research described in this thesis was financially supported by STOWA (Foundation for Applied Water Research).